A report accepted by Working Group I of the Intergovernmental Panel on Climate Change but not approved in detail

"Acceptance" of IPCC Reports at a Session of the Working Group or Panel signifies that the material has not been subject to line-by-line discussion and agreement, but nevertheless presents a comprehensive, objective and balanced view of the subject matter.

Technical Summary

Coordinating Lead Authors:

Susan Solomon (USA), Dahe Qin (China), Martin Manning (USA, New Zealand)

Lead Authors:

Richard B. Alley (USA), Terje Berntsen (Norway), Nathaniel L. Bindoff (Australia), Zhenlin Chen (China), Amnat Chidthaisong (Thailand), Jonathan M. Gregory (UK), Gabriele C. Hegerl (USA, Germany), Martin Heimann (Germany, Switzerland), Bruce Hewitson (South Africa), Brian J. Hoskins (UK), Fortunat Joos (Switzerland), Jean Jouzel (France), Vladimir Kattsov (Russia), Ulrike Lohmann (Switzerland), Taroh Matsuno (Japan), Mario Molina (USA, Mexico), Neville Nicholls (Australia), Jonathan Overpeck (USA), Graciela Raga (Mexico, Argentina), Venkatachalam Ramaswamy (USA), Jiawen Ren (China), Matilde Rusticucci (Argentina), Richard Somerville (USA), Thomas F. Stocker (Switzerland), Ronald J. Stouffer (USA), Penny Whetton (Australia), Richard A. Wood (UK), David Wratt (New Zealand)

Contributing Authors:

J. Arblaster (USA, Australia), G. Brasseur (USA, Germany), J.H. Christensen (Denmark), K.L. Denman (Canada), D.W. Fahey (USA), P. Forster (UK), J. Haywood (UK), E. Jansen (Norway), P.D. Jones (UK), R. Knutti (Switzerland), H. Le Treut (France), P. Lemke (Germany), G. Meehl (USA), D. Randall (USA), D.A. Stone (UK, Canada), K.E. Trenberth (USA), J. Willebrand (Germany), F. Zwiers (Canada)

Review Editors:

Kansri Boonpragob (Thailand), Filippo Giorgi (Italy), Bubu Pateh Jallow (The Gambia)

Table of Contents

TS.1   Introduction

In the six years since the IPCC's Third Assessment Report (TAR), significant progress has been made in understanding past and recent climate change and in projecting future changes. These advances have arisen from large amounts of new data, more sophisticated analyses of data, improvements in the understanding and simulation of physical processes in climate models and more extensive exploration of uncertainty ranges in model results. The increased confidence in climate science provided by these developments is evident in this Working Group I contribution to the IPCC's Fourth Assessment Report.

While this report provides new and important policy-relevant information on the scientific understanding of climate change, the complexity of the climate system and the multiple interactions that determine its behaviour impose limitations on our ability to understand fully the future course of Earth's global climate. There is still an incomplete physical understanding of many components of the climate system and their role in climate change. Key uncertainties include aspects of the roles played by clouds, the cryosphere, the oceans, land use and couplings between climate and biogeochemical cycles. The areas of science covered in this report continue to undergo rapid progress and it should be recognised that the present assessment reflects scientific understanding based on the peer-reviewed literature available in mid-2006.

The key findings of the IPCC Working Group I assessment are presented in the Summary for Policymakers. This Technical Summary provides a more detailed overview of the scientific basis for those findings and provides a road map to the chapters of the underlying report. It focuses on key findings, highlighting what is new since the TAR. The structure of the Technical Summary is as follows:

- Section 2: an overview of current scientific understanding of the natural and anthropogenic drivers of changes in climate;
- Section 3: an overview of observed changes in the climate system (including the atmosphere, oceans and cryosphere) and their relationships to physical processes;
- Section 4: an overview of explanations of observed climate changes based on climate models and physical understanding, the extent to which climate change can be attributed to specific causes and a new evaluation of climate sensitivity to greenhouse gas increases;
- Section 5: an overview of projections for both near- and far-term climate changes including the time scales of responses to changes in forcing, and probabilistic information about future climate change; and
- Section 6: a summary of the most robust findings and the key uncertainties in current understanding of physical climate change science.

Each paragraph in the Technical Summary reporting substantive results is followed by a reference in curly brackets to the corresponding chapter section(s) of the underlying report where the detailed assessment of the scientific literature and additional information can be found.

TS.2 Changes in Human and Natural Drivers of Climate

The Earth's global mean climate is determined by incoming energy from the Sun and by the properties of the Earth and its atmosphere, namely the reflection, absorption and emission of energy within the atmosphere and at the surface. Although changes in received solar energy (e.g., caused by variations in the Earth's orbit around the Sun) inevitably affect the Earth's energy budget, the properties of the atmosphere and surface are also important and these may be affected by climate feedbacks. The importance of climate feedbacks is evident in the nature of past climate changes as recorded in ice cores up to 650,000 years old.

Changes have occurred in several aspects of the atmosphere and surface that alter the global energy budget of the Earth and can therefore cause the climate to change. Among these are increases in greenhouse gas concentrations that act primarily to increase the atmospheric absorption of outgoing radiation, and increases in aerosols (microscopic airborne particles or droplets) that act to reflect and absorb incoming solar radiation and change cloud radiative properties. Such changes cause a radiative forcing of the climate system.[1] Forcing agents can differ considerably from one another in terms of the magnitudes of forcing, as well as spatial and temporal features. Positive and negative radiative forcings contribute to increases and decreases, respectively, in

---

[1] 'Radiative forcing' is a measure of the influence a factor has in altering the balance of incoming and outgoing energy in the Earth-atmosphere system and is an index of the importance of the factor as a potential climate change mechanism. Positive forcing tends to warm the surface while negative forcing tends to cool it. In this report, radiative forcing values are for changes relative to a pre-industrial background at 1750, are expressed in Watts per square metre (W m^{-2}) and, unless otherwise noted, refer to a global and annual average value. See Glossary for further details.

Box TS.1: Treatment of Uncertainties in the Working Group I Assessment

The importance of consistent and transparent treatment of uncertainties is clearly recognised by the IPCC in preparing its assessments of climate change. The increasing attention given to formal treatments of uncertainty in previous assessments is addressed in Section 1.6. To promote consistency in the general treatment of uncertainty across all three Working Groups, authors of the Fourth Assessment Report have been asked to follow a brief set of guidance notes on determining and describing uncertainties in the context of an assessment.[2] This box summarises the way that Working Group I has applied those guidelines and covers some aspects of the treatment of uncertainty specific to material assessed here.

Uncertainties can be classified in several different ways according to their origin. Two primary types are 'value uncertainties' and 'structural uncertainties'. Value uncertainties arise from the incomplete determination of particular values or results, for example, when data are inaccurate or not fully representative of the phenomenon of interest. Structural uncertainties arise from an incomplete understanding of the processes that control particular values or results, for example, when the conceptual framework or model used for analysis does not include all the relevant processes or relationships. Value uncertainties are generally estimated using statistical techniques and expressed probabilistically. Structural uncertainties are generally described by giving the authors' collective judgment of their confidence in the correctness of a result. In both cases, estimating uncertainties is intrinsically about describing the limits to knowledge and for this reason involves expert judgment about the state of that knowledge. A different type of uncertainty arises in systems that are either chaotic or not fully deterministic in nature and this also limits our ability to project all aspects of climate change.

The scientific literature assessed here uses a variety of other generic ways of categorising uncertainties. Uncertainties associated with 'random errors' have the characteristic of decreasing as additional measurements are accumulated, whereas those associated with 'systematic errors' do not. In dealing with climate records, considerable attention has been given to the identification of systematic errors or unintended biases arising from data sampling issues and methods of analysing and combining data. Specialised statistical methods based on quantitative analysis have been developed for the detection and attribution of climate change and for producing probabilistic projections of future climate parameters. These are summarised in the relevant chapters.

The uncertainty guidance provided for the Fourth Assessment Report draws, for the first time, a careful distinction between levels of confidence in scientific understanding and the likelihoods of specific results. This allows authors to express high confidence that an event is extremely unlikely (e.g., rolling a dice twice and getting a six both times), as well as high confidence that an event is about as likely as not (e.g., a tossed coin coming up heads). Confidence and likelihood as used here are distinct concepts but are often linked in practice.

The standard terms used to define levels of confidence in this report are as given in the IPCC Uncertainty Guidance Note, namely:

Confidence Terminology	Degree of confidence in being correct
Very high confidence	At least 9 out of 10 chance
High confidence	About 8 out of 10 chance
Medium confidence	About 5 out of 10 chance
Low confidence	About 2 out of 10 chance
Very low confidence	Less than 1 out of 10 chance

Note that 'low confidence' and 'very low confidence' are only used for areas of major concern and where a risk-based perspective is justified.

Chapter 2 of this report uses a related term 'level of scientific understanding' when describing uncertainties in different contributions to radiative forcing. This terminology is used for consistency with the Third Assessment Report, and the basis on which the authors have determined particular levels of scientific understanding uses a combination of approaches consistent with the uncertainty guidance note as explained in detail in Section 2.9.2 and Table 2.11.

(continued)

---

[2] The IPCC Uncertainty Guidance Note is included in Supplementary Material for this report.

The standard terms used in this report to define the likelihood of an outcome or result where this can be estimated probabilistically are:

Likelihood Terminology	Likelihood of the occurrence/ outcome
Virtually certain	> 99% probability
Extremely likely	> 95% probability
Very likely	> 90% probability
Likely	> 66% probability
More likely than not	> 50% probability
About as likely as not	33 to 66% probability
Unlikely	< 33% probability
Very unlikely	< 10% probability
Extremely unlikely	< 5% probability
Exceptionally unlikely	< 1% probability

The terms 'extremely likely', 'extremely unlikely' and 'more likely than not' as defined above have been added to those given in the IPCC Uncertainty Guidance Note in order to provide a more specific assessment of aspects including attribution and radiative forcing.

Unless noted otherwise, values given in this report are assessed best estimates and their uncertainty ranges are 90% confidence intervals (i.e., there is an estimated 5% likelihood of the value being below the lower end of the range or above the upper end of the range). Note that in some cases the nature of the constraints on a value, or other information available, may indicate an asymmetric distribution of the uncertainty range around a best estimate. In such cases, the uncertainty range is given in square brackets following the best estimate.

global average surface temperature. This section updates the understanding of estimated anthropogenic and natural radiative forcings.

The overall response of global climate to radiative forcing is complex due to a number of positive and negative feedbacks that can have a strong influence on the climate system (see e.g., Sections 4.5 and 5.4). Although water vapour is a strong greenhouse gas, its concentration in the atmosphere changes in response to changes in surface climate and this must be treated as a feedback effect and not as a radiative forcing. This section also summarises changes in the surface energy budget and its links to the hydrological cycle. Insights into the effects of agents such as aerosols on precipitation are also noted.

TS.2.1   Greenhouse Gases

The dominant factor in the radiative forcing of climate in the industrial era is the increasing concentration of various greenhouse gases in the atmosphere. Several of the major greenhouse gases occur naturally but increases in their atmospheric concentrations over the last 250 years are due largely to human activities. Other greenhouse gases are entirely the result of human activities. The contribution of each greenhouse gas to radiative forcing

over a particular period of time is determined by the change in its concentration in the atmosphere over that period and the effectiveness of the gas in perturbing the radiative balance. Current atmospheric concentrations of the different greenhouse gases considered in this report vary by more than eight orders of magnitude (factor of 10^8), and their radiative efficiencies vary by more than four orders of magnitude (factor of 10^4), reflecting the enormous diversity in their properties and origins.

The current concentration of a greenhouse gas in the atmosphere is the net result of the history of its past emissions and removals from the atmosphere. The gases and aerosols considered here are emitted to the atmosphere by human activities or are formed from precursor species emitted to the atmosphere. These emissions are offset by chemical and physical removal processes. With the important exception of carbon dioxide (CO_2), it is generally the case that these processes remove a specific fraction of the amount of a gas in the atmosphere each year and the inverse of this removal rate gives the mean lifetime for that gas. In some cases, the removal rate may vary with gas concentration or other atmospheric properties (e.g., temperature or background chemical conditions).

Long-lived greenhouse gases (LLGHGs), for example, CO_2, methane (CH_4) and nitrous oxide (N_2O), are

chemically stable and persist in the atmosphere over time scales of a decade to centuries or longer, so that their emission has a long-term influence on climate. Because these gases are long lived, they become well mixed throughout the atmosphere much faster than they are removed and their global concentrations can be accurately estimated from data at a few locations. Carbon dioxide does not have a specific lifetime because it is continuously cycled between the atmosphere, oceans and land biosphere and its net removal from the atmosphere involves a range of processes with different time scales.

Short-lived gases (e.g., sulphur dioxide and carbon monoxide) are chemically reactive and generally removed by natural oxidation processes in the atmosphere, by removal at the surface or by washout in precipitation; their concentrations are hence highly variable. Ozone is a significant greenhouse gas that is formed and destroyed by chemical reactions involving other species in the atmosphere. In the troposphere, the human influence on ozone occurs primarily through changes in precursor gases that lead to its formation, whereas in the stratosphere, the human influence has been primarily through changes in ozone removal rates caused by chlorofluorocarbons (CFCs) and other ozone-depleting substances.

TS.2.1.1 Changes in Atmospheric Carbon Dioxide, Methane and Nitrous Oxide

Current concentrations of atmospheric CO_2 and CH_4 far exceed pre-industrial values found in polar ice core records of atmospheric composition dating back 650,000 years. Multiple lines of evidence confirm that the post-industrial rise in these gases does not stem from natural mechanisms (see Figure TS.1 and Figure TS.2). {2.3, 6.3–6.5, FAQ 7.1}

The total radiative forcing of the Earth's climate due to increases in the concentrations of the LLGHGs CO_2, CH_4 and N_2O, and *very likely* the rate of increase in the total forcing due to these gases over the period since 1750, are unprecedented in more than 10,000 years (Figure TS.2). It is *very likely* that the sustained rate of increase in the combined radiative forcing from these greenhouse gases of about +1 W m^{-2} over the past four decades is at least six times faster than at any time during the two millennia before the Industrial Era, the period for which ice core data have the required temporal resolution. The radiative forcing due to these LLGHGs has the highest level of confidence of any forcing agent. {2.3, 6.4}

GLACIAL-INTERGLACIAL ICE CORE DATA
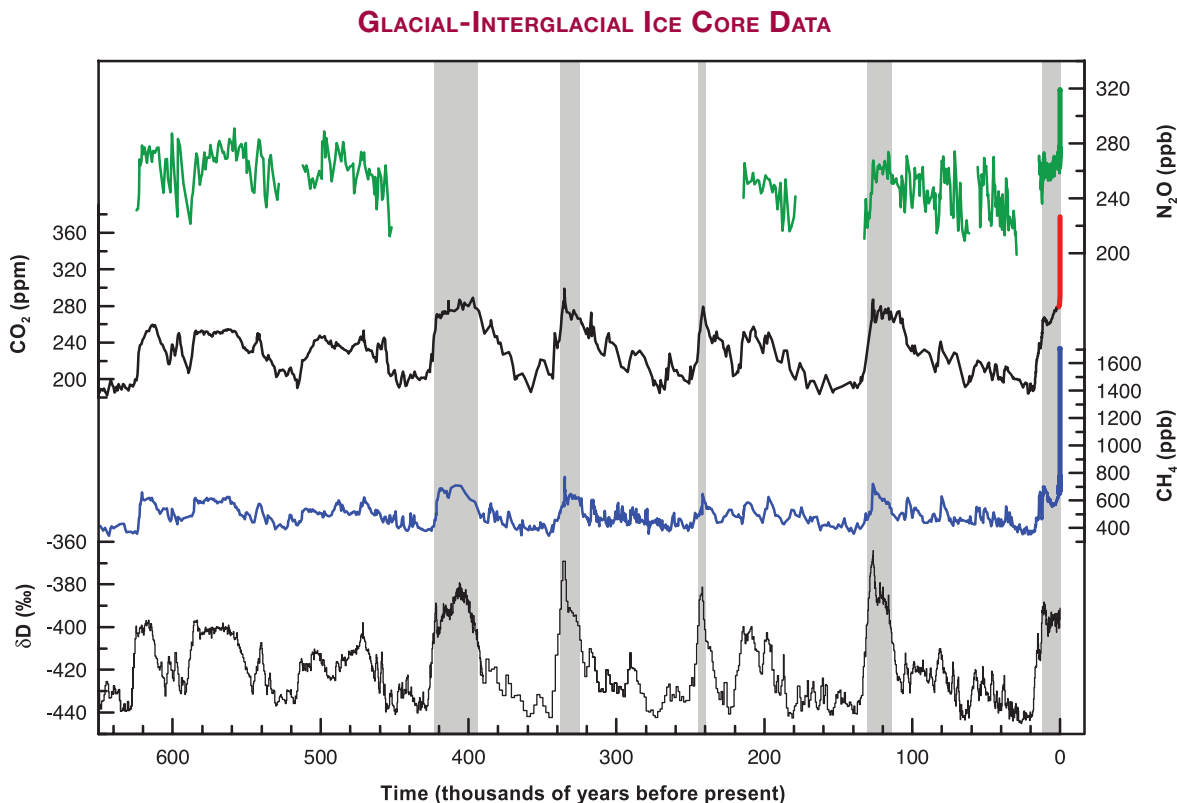
Figure TS.1. *Variations of deuterium (δD) in antarctic ice, which is a proxy for local temperature, and the atmospheric concentrations of the greenhouse gases carbon dioxide (CO_2), methane (CH_4), and nitrous oxide (N_2O) in air trapped within the ice cores and from recent atmospheric measurements. Data cover 650,000 years and the shaded bands indicate current and previous interglacial warm periods. {Adapted from Figure 6.3}*

Changes in Greenhouse Gases from Ice Core and Modern Data
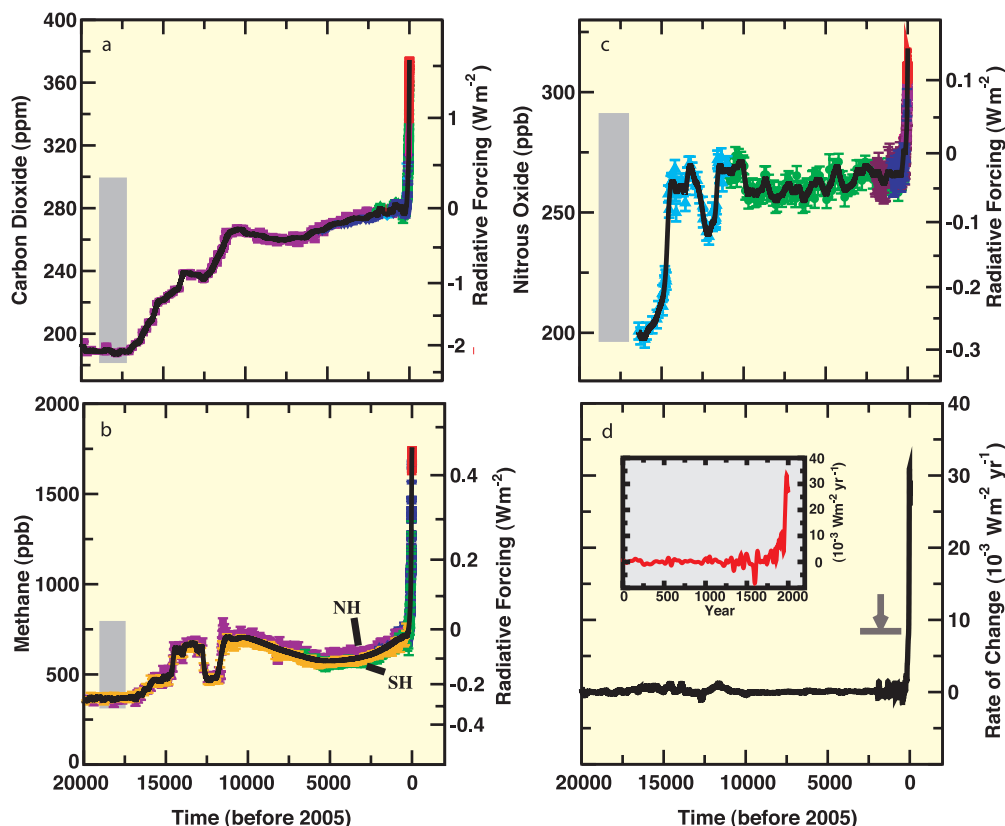
Figure TS.2. *The concentrations and radiative forcing by (a) carbon dioxide (CO$_2$), (b) methane (CH$_4$), (c) nitrous oxide (N$_2$O) and (d) the rate of change in their combined radiative forcing over the last 20,000 years reconstructed from antarctic and Greenland ice and firn data (symbols) and direct atmospheric measurements (panels a,b,c, red lines). The grey bars show the reconstructed ranges of natural variability for the past 650,000 years. The rate of change in radiative forcing (panel d, black line) has been computed from spline fits to the concentration data. The width of the age spread in the ice data varies from about 20 years for sites with a high accumulation of snow such as Law Dome, Antarctica, to about 200 years for low-accumulation sites such as Dome C, Antarctica. The arrow shows the peak in the rate of change in radiative forcing that would result if the anthropogenic signals of CO$_2$, CH$_4$, and N$_2$O had been smoothed corresponding to conditions at the low-accumulation Dome C site. The negative rate of change in forcing around 1600 shown in the higher-resolution inset in panel d results from a CO$_2$ decrease of about 10 ppm in the Law Dome record. {Figure 6.4}*

The concentration of atmospheric CO$_2$ has increased from a pre-industrial value of about 280 ppm to 379 ppm in 2005. Atmospheric CO$_2$ concentration increased by only 20 ppm over the 8000 years prior to industrialisation; multi-decadal to centennial-scale variations were less than 10 ppm and *likely* due mostly to natural processes. However, since 1750, the CO$_2$ concentration has risen by nearly 100 ppm. The annual CO$_2$ growth rate was larger during the last 10 years (1995–2005 average: 1.9 ppm yr^{-1}) than it has been since continuous direct atmospheric measurements began (1960–2005 average: 1.4 ppm yr^{-1}). {2.3, 6.4, 6.5}

Increases in atmospheric CO$_2$ since pre-industrial times are responsible for a radiative forcing of +1.66 ± 0.17 W m^{-2}; a contribution which dominates all other radiative forcing agents considered in this report. For the decade from 1995 to 2005, the growth rate of CO$_2$

in the atmosphere led to a 20% increase in its radiative forcing. {2.3, 6.4, 6.5}

Emissions of CO$_2$ from fossil fuel use and from the effects of land use change on plant and soil carbon are the primary sources of increased atmospheric CO$_2$. Since 1750, it is estimated that about 2/3rds of anthropogenic CO$_2$ emissions have come from fossil fuel burning and about 1/3rd from land use change. About 45% of this CO$_2$ has remained in the atmosphere, while about 30% has been taken up by the oceans and the remainder has been taken up by the terrestrial biosphere. About half of a CO$_2$ pulse to the atmosphere is removed over a time scale of 30 years; a further 30% is removed within a few centuries; and the remaining 20% will typically stay in the atmosphere for many thousands of years. {7.3}

In recent decades, emissions of CO$_2$ have continued to increase (see Figure TS.3). Global annual fossil

CO_2 emissions[3] increased from an average of 6.4 ± 0.4 GtC yr^{-1} in the 1990s to 7.2 ± 0.3 GtC yr^{-1} in the period 2000 to 2005. Estimated CO_2 emissions associated with land use change, averaged over the 1990s, were[4] 0.5 to 2.7 GtC yr^{-1}, with a central estimate of 1.6 Gt yr^{-1}. Table TS.1 shows the estimated budgets of CO_2 in recent decades. {2.3, 6.4, 7.3, FAQ 7.1}

Since the 1980s, natural processes of CO_2 uptake by the terrestrial biosphere (i.e., the residual land sink in Table TS.1) and by the oceans have removed about 50% of anthropogenic emissions (i.e., fossil CO_2 emissions and land use change flux in Table TS.1). These removal processes are influenced by the atmospheric CO_2 concentration and by changes in climate. Uptake by the oceans and the terrestrial biosphere have been similar in magnitude but the terrestrial biosphere uptake is more variable and was higher in the 1990s than in the 1980s by about 1 GtC yr^{-1}. Observations demonstrate that dissolved CO_2 concentrations in the surface ocean (pCO_2) have been increasing nearly everywhere, roughly following the atmospheric CO_2 increase but with large regional and temporal variability. {5.4, 7.3}

Carbon uptake and storage in the terrestrial biosphere arise from the net difference between uptake due to vegetation growth, changes in reforestation and sequestration, and emissions due to heterotrophic respiration, harvest, deforestation, fire, damage by pollution and other disturbance factors affecting biomass and soils. Increases and decreases in fire frequency in different regions have affected net carbon uptake, and in boreal regions, emissions due to fires appear to have increased over recent decades. Estimates of net CO_2 surface fluxes from inverse studies using networks of atmospheric data demonstrate significant land uptake in the mid-latitudes of the Northern Hemisphere (NH) and near-zero land-atmosphere fluxes in the tropics, implying that tropical deforestation is approximately balanced by regrowth. {7.3}

Short-term (interannual) variations observed in the atmospheric CO_2 growth rate are primarily controlled by changes in the flux of CO_2 between the atmosphere and the terrestrial biosphere, with a smaller but significant fraction due to variability in ocean fluxes (see Figure TS.3). Variability in the terrestrial biosphere flux is driven by climatic fluctuations, which affect the uptake of CO_2 by plant growth and the return of CO_2 to the atmosphere by the decay of organic material through heterotrophic respiration and fires. El Niño-Southern Oscillation (ENSO) events are a major source of interannual variability in atmospheric CO_2 growth rate, due to their effects on fluxes through land and sea surface temperatures, precipitation and the incidence of fires. {7.3}

The direct effects of increasing atmospheric CO_2 on large-scale terrestrial carbon uptake cannot be quantified reliably at present. Plant growth can be stimulated by increased atmospheric CO_2 concentrations and by nutrient deposition (fertilization effects). However, most experiments and studies show that such responses appear to be relatively short lived and strongly coupled

Table TS.1. *Global carbon budget. By convention, positive values are CO_2 fluxes (GtC yr^{-1}) into the atmosphere and negative values represent uptake from the atmosphere (i.e., 'CO_2 sinks'). Fossil CO_2 emissions for 2004 and 2005 are based on interim estimates. Due to the limited number of available studies, for the net land-to-atmosphere flux and its components, uncertainty ranges are given as 65% confidence intervals and do not include interannual variability (see Section 7.3). NA indicates that data are not available.*

	1980s	1990s	2000–2005
Atmospheric increase	3.3 ± 0.1	3.2 ± 0.1	4.1 ± 0.1
Fossil carbon dioxide emissions	5.4 ± 0.3	6.4 ± 0.4	7.2 ± 0.3
Net ocean-to-atmosphere flux	-1.8 ± 0.8	-2.2 ± 0.4	-2.2 ± 0.5
Net land-to-atmosphere flux	-0.3 ± 0.9	-1.0 ± 0.6	-0.9 ± 0.6
Partitioned as follows			
Land use change flux	1.4 (0.4 to 2.3)	1.6 (0.5 to 2.7)	NA
Residual land sink	−1.7 (−3.4 to 0.2)	−2.6 (−4.3 to −0.9)	NA

---

[3] Fossil CO_2 emissions include those from the production, distribution and consumption of fossil fuels and from cement production. Emission of 1 GtC corresponds to 3.67 $GtCO_2$.

[4] As explained in Section 7.3, uncertainty ranges for land use change emissions, and hence for the full carbon cycle budget, can only be given as 65% confidence intervals.

CO₂ EMISSIONS AND INCREASES
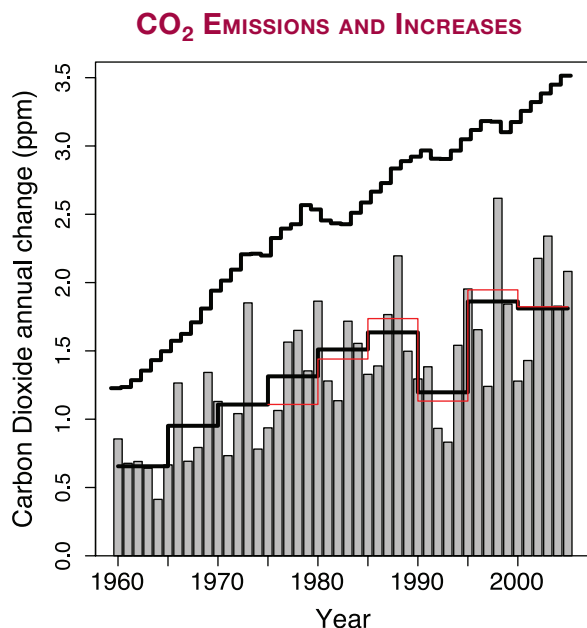
Figure TS.3. *Annual changes in global mean CO₂ concentration (grey bars) and their five-year means from two different measurement networks (red and lower black stepped lines). The five-year means smooth out short-term perturbations associated with strong ENSO events in 1972, 1982, 1987 and 1997. Uncertainties in the five-year means are indicated by the difference between the red and lower black lines and are of order 0.15 ppm. The upper stepped line shows the annual increases that would occur if all fossil fuel emissions stayed in the atmosphere and there were no other emissions. {Figure 7.4}*

to other effects such as availability of water and nutrients. Likewise, experiments and studies of the effects of climate (temperature and moisture) on heterotrophic respiration of litter and soils are equivocal. Note that the effect of climate change on carbon uptake is addressed separately in section TS.5.4. {7.3}

The CH₄ abundance in 2005 of about 1774 ppb is more than double its pre-industrial value. Atmospheric CH₄ concentrations varied slowly between 580 and 730 ppb over the last 10,000 years, but increased by about 1000 ppb in the last two centuries, representing the fastest changes in this gas over at least the last 80,000 years. In the late 1970s and early 1980s, CH₄ growth rates displayed maxima above 1% yr⁻¹, but since the early 1990s have decreased significantly and were close to zero for the six-year period from 1999 to 2005. Increases in CH₄ abundance occur when emissions exceed removals. The recent decline in growth rates implies that emissions now approximately match removals, which are due primarily to oxidation by the hydroxyl radical (OH). Since the TAR, new studies using two independent tracers (methyl chloroform and ¹⁴CO) suggest no significant long-term change in the global abundance of OH. Thus,

the slowdown in the atmospheric CH₄ growth rate since about 1993 is *likely* due to the atmosphere approaching an equilibrium during a period of near-constant total emissions. {2.3, 7.4, FAQ 7.1}

Increases in atmospheric CH₄ concentrations since pre-industrial times have contributed a radiative forcing of +0.48 ± 0.05 W m⁻². Among greenhouse gases, this forcing remains second only to that of CO₂ in magnitude. {2.3}

Current atmospheric CH₄ levels are due to continuing anthropogenic emissions of CH₄, which are greater than natural emissions. Total CH₄ emissions can be well determined from observed concentrations and independent estimates of removal rates. Emissions from individual sources of CH₄ are not as well quantified as the total emissions but are mostly biogenic and include emissions from wetlands, ruminant animals, rice agriculture and biomass burning, with smaller contributions from industrial sources including fossil fuel-related emissions. This knowledge of CH₄ sources, combined with the small natural range of CH₄ concentrations over the past 650,000 years (Figure TS.1) and their dramatic increase since 1750 (Figure TS.2), make it *very likely* that the observed long-term changes in CH₄ are due to anthropogenic activity. {2.3, 6.4, 7.4}

In addition to its slowdown over the last 15 years, the growth rate of atmospheric CH₄ has shown high interannual variability, which is not yet fully explained. The largest contributions to interannual variability during the 1996 to 2001 period appear to be variations in emissions from wetlands and biomass burning. Several studies indicate that wetland CH₄ emissions are highly sensitive to temperature and are also affected by hydrological changes. Available model estimates all indicate increases in wetland emissions due to future climate change but vary widely in the magnitude of such a positive feedback effect. {7.4}

The N₂O concentration in 2005 was 319 ppb, about 18% higher than its pre-industrial value. Nitrous oxide increased approximately linearly by about 0.8 ppb yr⁻¹ over the past few decades. Ice core data show that the atmospheric concentration of N₂O varied by less than about 10 ppb for 11,500 years before the onset of the industrial period. {2.3, 6.4, 6.5}

The increase in N₂O since the pre-industrial era now contributes a radiative forcing of +0.16 ± 0.02 W m⁻² and is due primarily to human activities, particularly agriculture and associated land use change. Current estimates are that about 40% of total N₂O emissions are anthropogenic but individual source estimates remain subject to significant uncertainties. {2.3, 7.4}

TS.2.1.3 Changes in Atmospheric Halocarbons, Stratospheric Ozone, Tropospheric Ozone and Other Gases

CFCs and hydrochlorofluorocarbons (HCFCs) are greenhouse gases that are purely anthropogenic in origin and used in a wide variety of applications. Emissions of these gases have decreased due to their phase-out under the Montreal Protocol, and the atmospheric concentrations of CFC-11 and CFC-113 are now decreasing due to natural removal processes. Observations in polar firn cores since the TAR have now extended the available time series information for some of these greenhouse gases. Ice core and *in situ* data confirm that industrial sources are the cause of observed atmospheric increases in CFCs and HCFCs. {2.3}

The Montreal Protocol gases contributed +0.32 ± 0.03 W m^{-2} to direct radiative forcing in 2005, with CFC-12 continuing to be the third most important long-lived radiative forcing agent. These gases as a group contribute about 12% of the total forcing due to LLGHGs. {2.3}

The concentrations of industrial fluorinated gases covered by the Kyoto Protocol (hydrofluorocarbons (HFCs), perfluorocarbons (PFCs), sulphur hexafluoride (SF$_6$)) are relatively small but are increasing rapidly. Their total radiative forcing in 2005 was +0.017 W m^{-2}. {2.3}

Tropospheric ozone is a short-lived greenhouse gas produced by chemical reactions of precursor species in the atmosphere and with large spatial and temporal variability. Improved measurements and modelling have advanced the understanding of chemical precursors that lead to the formation of tropospheric ozone, mainly carbon monoxide, nitrogen oxides (including sources and possible long-term trends in lightning) and formaldehyde. Overall, current models are successful in describing the principal features of the present global tropospheric ozone distribution on the basis of underlying processes. New satellite and *in situ* measurements provide important global constraints for these models; however, there is less confidence in their ability to reproduce the changes in ozone associated with large changes in emissions or climate, and in the simulation of observed long-term trends in ozone concentrations over the 20th century. {7.4}

Tropospheric ozone radiative forcing is estimated to be +0.35 [+0.25 to +0.65] W m^{-2} with a *medium* level of scientific understanding. The best estimate of this radiative forcing has not changed since the TAR. Observations show that trends in tropospheric ozone during the last few decades vary in sign and magnitude at many locations, but there are indications of significant upward trends at low latitudes. Model studies of the radiative forcing due to the increase in tropospheric ozone since pre-industrial times have increased in complexity and comprehensiveness compared with models used in the TAR. {2.3, 7.4}

Changes in tropospheric ozone are linked to air quality and climate change. A number of studies have shown that summer daytime ozone concentrations correlate strongly with temperature. This correlation appears to reflect contributions from temperature-dependent biogenic volatile organic carbon emissions, thermal decomposition of peroxyacetylnitrate, which acts as a reservoir for nitrogen oxides (NO$_x$), and association of high temperatures with regional stagnation. Anomalously hot and stagnant conditions during the summer of 1988 were responsible for the highest surface-level ozone year on record in the north-eastern USA. The summer heat wave in Europe in 2003 was also associated with exceptionally high local ozone at the surface. {Box 7.4}

The radiative forcing due to the destruction of stratospheric ozone is caused by the Montreal Protocol gases and is re-evaluated to be −0.05 ± 0.10 W m^{-2}, weaker than in the TAR, with a medium level of scientific understanding. The trend of greater and greater depletion of global stratospheric ozone observed during the 1980s and 1990s is no longer occurring; however, global stratospheric ozone is still about 4% below pre-1980 values and it is not yet clear whether ozone recovery has begun. In addition to the chemical destruction of ozone, dynamical changes may have contributed to NH mid-latitude ozone reduction. {2.3}

Direct emission of water vapour by human activities makes a negligible contribution to radiative forcing. However, as global mean temperatures increase, tropospheric water vapour concentrations increase and this represents a key feedback but not a forcing of climate change. Direct emission of water to the atmosphere by anthropogenic activities, mainly irrigation, is a possible forcing factor but corresponds to less than 1% of the natural sources of atmospheric water vapour. The direct injection of water vapour into the atmosphere from fossil fuel combustion is significantly lower than that from agricultural activity. {2.5}

Based on chemical transport model studies, the radiative forcing from increases in stratospheric water vapour due to oxidation of CH$_4$ is estimated to be +0.07 ± 0.05 W m^{-2}. The level of scientific understanding is low because the contribution of CH$_4$ to the corresponding vertical structure of the water vapour change near the tropopause is uncertain. Other potential human causes of stratospheric water vapour increases that could contribute to radiative forcing are poorly understood. {2.3}

TS.2.2   Aerosols

Direct aerosol radiative forcing is now considerably better quantified than previously and represents a major advance in understanding since the time of the TAR, when several components had a very low level of scientific understanding. A total direct aerosol radiative forcing combined across all aerosol types can now be given for the first time as –0.5 ± 0.4 W m^{-2}, with a medium-low level of scientific understanding. Atmospheric models have improved and many now represent all aerosol components of significance. Aerosols vary considerably in their properties that affect the extent to which they absorb and scatter radiation, and thus different types may have a net cooling or warming effect. Industrial aerosol consisting mainly of a mixture of sulphates, organic and black carbon, nitrates and industrial dust is clearly discernible over many continental regions of the NH. Improved *in situ*, satellite and surface-based measurements (see Figure TS.4) have enabled verification of global aerosol model simulations. These improvements allow quantification of the total direct aerosol radiative forcing for the first time, representing an important advance since the TAR. The direct radiative forcing for individual species remains less certain and is estimated from models to be –0.4 ± 0.2 W m^{-2} for sulphate, –0.05 ± 0.05 W m^{-2} for fossil fuel organic carbon, +0.2 ± 0.15 W m^{-2} for fossil fuel black carbon, +0.03 ± 0.12 W m^{-2} for biomass burning, –0.1 ± 0.1 W m^{-2} for nitrate and –0.1 ± 0.2 W m^{-2} for mineral dust. Two recent emission inventory studies support data from ice cores and suggest that global anthropogenic sulphate emissions decreased over the 1980 to 2000 period and that the geographic distribution of sulphate forcing has also changed. {2.4, 6.6}

Significant changes in the estimates of the direct radiative forcing due to biomass-burning, nitrate and mineral dust aerosols have occurred since the TAR. For biomass-burning aerosol, the estimated direct radiative forcing is now revised from being negative to near zero due to the estimate being strongly influenced by the occurrence of these aerosols over clouds. For the first time, the radiative forcing due to nitrate aerosol is given. For mineral dust, the range in the direct radiative forcing is reduced due to a reduction in the estimate of its anthropogenic fraction. {2.4}

TOTAL AEROSOL OPTICAL DEPTH
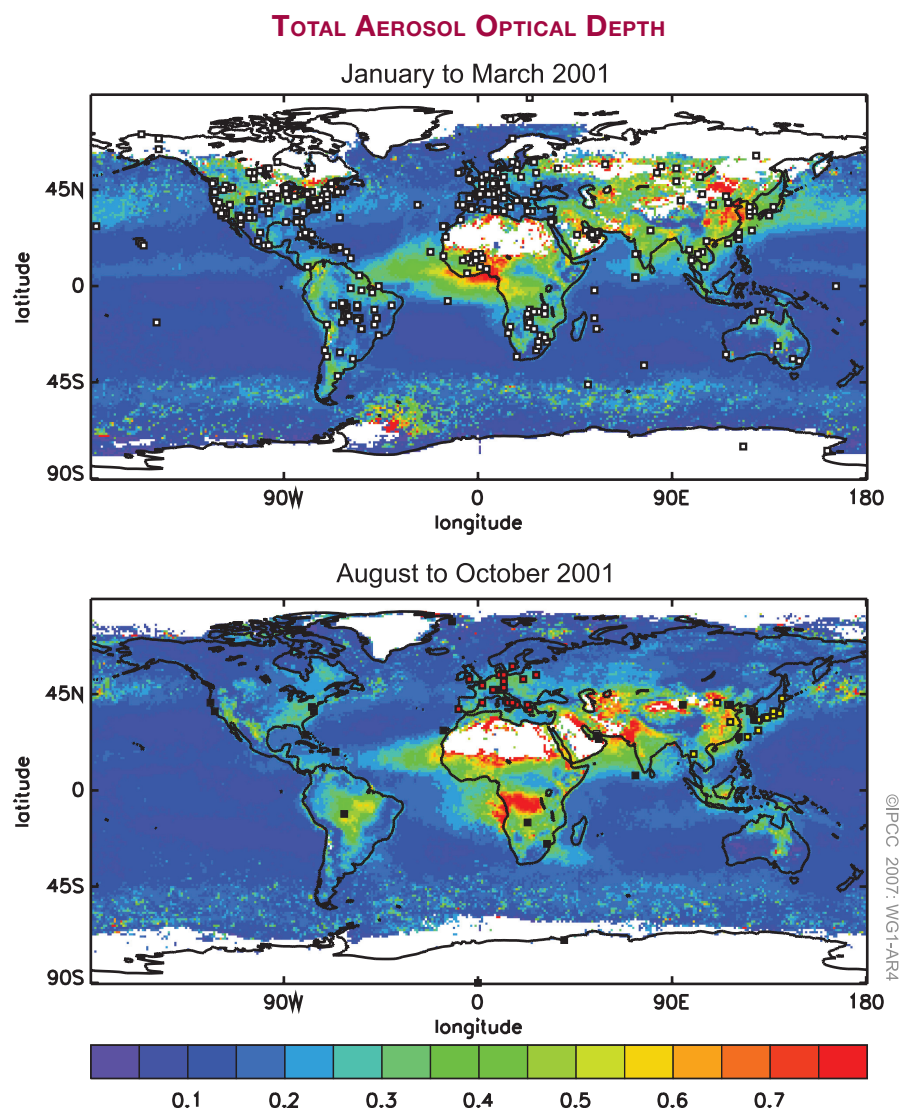
Figure TS.4. *(Top) The total aerosol optical depth (due to natural plus anthropogenic aerosols) at a mid-visible wavelength determined by satellite measurements for January to March 2001 and (bottom) August to October 2001, illustrating seasonal changes in industrial and biomass-burning aerosols. Data are from satellite measurements, complemented by two different kinds of ground-based measurements at locations shown in the two panels (see Section 2.4.2 for details). {Figure 2.11}*

©IPCC 2007: WG1-AR4

Anthropogenic aerosols effects on water clouds cause an indirect cloud albedo effect (referred to as the first indirect effect in the TAR), which has a best estimate for the first time of –0.7 [–0.3 to –1.8] W m^{-2}. The number of global model estimates of the albedo effect for liquid water clouds has increased substantially since the TAR, and the estimates have been evaluated in a more rigorous way. The estimate for this radiative forcing comes from multiple model studies incorporating more aerosol species and describing aerosol-cloud interaction processes in greater detail. Model studies including more aerosol species or constrained by satellite observations tend to yield a relatively weaker cloud albedo effect. Despite the advances and progress since the TAR and the reduction in the spread of the estimate of the forcing, there remain large uncertainties in both measurements and modelling of processes, leading to a low level of scientific understanding, which is an elevation from the very low rank in the TAR. {2.4, 7.5, 9.2}

Other effects of aerosol include a cloud lifetime effect, a semi-direct effect and aerosol-ice cloud interactions. These are considered to be part of the climate response rather than radiative forcings. {2.4, 7.5}

TS.2.3 Aviation Contrails and Cirrus, Land Use and Other Effects

Persistent linear contrails from global aviation contribute a small radiative forcing of +0.01 [+0.003 to +0.03] W m^{-2}, with a low level of scientific understanding. This best estimate is smaller than the estimate in the TAR. This difference results from new observations of contrail cover and reduced estimates of contrail optical depth. No best estimates are available for the net forcing from spreading contrails. Their effects on cirrus cloudiness and the global effect of aviation aerosol on background cloudiness remain unknown. {2.6}

Human-induced changes in land cover have increased the global surface albedo, leading to a radiative forcing of –0.2 ± 0.2 W m^{-2}, the same as in the TAR, with a medium-low level of scientific understanding. Black carbon aerosols deposited on snow reduce the surface albedo and are estimated to yield an associated radiative forcing of +0.1 ± 0.1 W m^{-2}, with a low level of scientific understanding. Since the TAR, a number of estimates of the forcing from land use changes have been made, using better techniques, exclusion of feedbacks in the evaluation and improved incorporation of large-scale observations. Uncertainties in the estimate include mapping and characterisation of present-day vegetation and historical state, parametrization of surface radiation processes and biases in models'

climate variables. The presence of soot particles in snow leads to a decrease in the albedo of snow and a positive forcing, and could affect snowmelt. Uncertainties are large regarding the manner in which soot is incorporated in snow and the resulting optical properties. {2.5}

The impacts of land use change on climate are expected to be locally significant in some regions, but are small at the global scale in comparison with greenhouse gas warming. Changes in the land surface (vegetation, soils, water) resulting from human activities can significantly affect local climate through shifts in radiation, cloudiness, surface roughness and surface temperatures. Changes in vegetation cover can also have a substantial effect on surface energy and water balance at the regional scale. These effects involve non-radiative processes (implying that they cannot be quantified by a radiative forcing) and have a very low level of scientific understanding. {2.5, 7.2, 9.3, Box 11.4}

The release of heat from anthropogenic energy production can be significant over urban areas but is not significant globally. {2.5}

TS.2.4 Radiative Forcing Due to Solar Activity and Volcanic Eruptions

Continuous monitoring of total solar irradiance now covers the last 28 years. The data show a well-established 11-year cycle in irradiance that varies by 0.08% from solar cycle minima to maxima, with no significant long-term trend. New data have more accurately quantified changes in solar spectral fluxes over a broad range of wavelengths in association with changing solar activity. Improved calibrations using high-quality overlapping measurements have also contributed to a better understanding. Current understanding of solar physics and the known sources of irradiance variability suggest comparable irradiance levels during the past two solar cycles, including at solar minima. The primary known cause of contemporary irradiance variability is the presence on the Sun's disk of sunspots (compact, dark features where radiation is locally depleted) and faculae (extended bright features where radiation is locally enhanced). {2.7}

The estimated direct radiative forcing due to changes in the solar output since 1750 is +0.12 [+0.06 to +0.3] W m^{-2}, which is less than half of the estimate given in the TAR, with a low level of scientific understanding. The reduced radiative forcing estimate comes from a re-evaluation of the long-term change in solar irradiance since 1610 (the Maunder Minimum) based upon: a new reconstruction using a model of solar magnetic flux variations that does not invoke geomagnetic,

cosmogenic or stellar proxies; improved understanding of recent solar variations and their relationship to physical processes; and re-evaluation of the variations of Sun-like stars. While this leads to an elevation in the level of scientific understanding from very low in the TAR to low in this assessment, uncertainties remain large because of the lack of direct observations and incomplete understanding of solar variability mechanisms over long time scales. {2.7, 6.6}

Empirical associations have been reported between solar-modulated cosmic ray ionization of the atmosphere and global average low-level cloud cover but evidence for a systematic indirect solar effect remains ambiguous. It has been suggested that galactic cosmic rays with sufficient energy to reach the troposphere could alter the population of cloud condensation nuclei and hence microphysical cloud properties (droplet number and concentration), inducing changes in cloud processes analogous to the indirect cloud albedo effect of tropospheric aerosols and thus causing an indirect solar forcing of climate. Studies have probed various correlations with clouds in particular regions or using limited cloud types or limited time periods; however, the cosmic ray time series does not appear to correspond to global total cloud cover after 1991 or to global low-level cloud cover after 1994. Together with the lack of a proven physical mechanism and the plausibility of other causal factors affecting changes in cloud cover, this makes the association between galactic cosmic ray-induced changes in aerosol and cloud formation controversial. {2.7}

Explosive volcanic eruptions greatly increase the concentration of stratospheric sulphate aerosols. A single eruption can thereby cool global mean climate for a few years. Volcanic aerosols perturb both the stratosphere and surface/troposphere radiative energy budgets and climate in an episodic manner, and many past events are evident in ice core observations of sulphate as well as temperature records. There have been no explosive volcanic events since the 1991 Mt. Pinatubo eruption capable of injecting significant material to the stratosphere. However, the potential exists for volcanic eruptions much larger than the 1991 Mt. Pinatubo eruption, which could produce larger radiative forcing and longer-term cooling of the climate system. {2.7, 6.4, 6.6, 9.2}

TS.2.5 Net Global Radiative Forcing, Global Warming Potentials and Patterns of Forcing
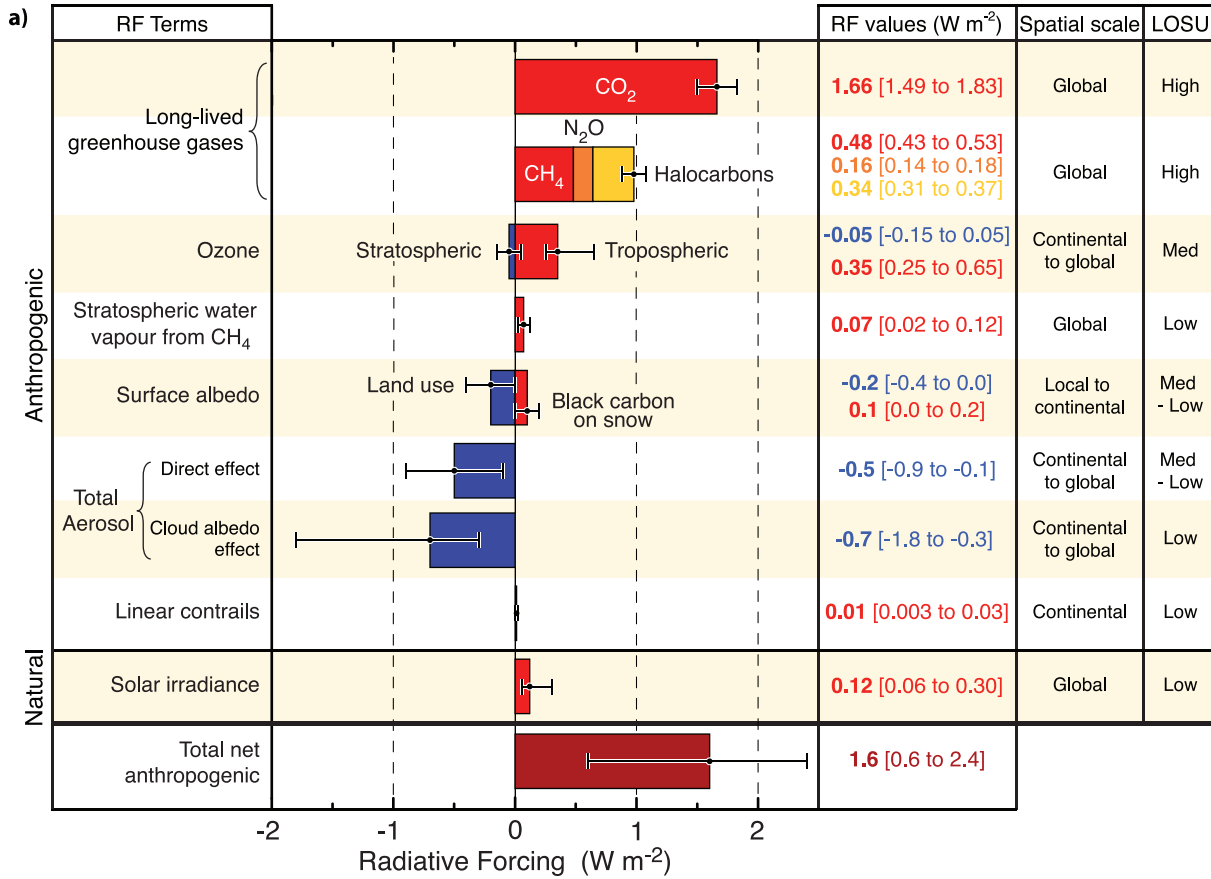
The understanding of anthropogenic warming and cooling influences on climate has improved since the TAR, leading to *very high confidence* that the effect of human activities since 1750 has been a net positive forcing of +1.6 [+0.6 to +2.4] W m^{-2}. Improved understanding and better quantification of the forcing mechanisms since the TAR make it possible to derive a combined net anthropogenic radiative forcing for the first time. Combining the component values for each forcing agent and their uncertainties yields the probability distribution of the combined anthropogenic radiative forcing estimate shown in Figure TS.5; the most likely value is about an order of magnitude larger than the estimated radiative forcing from changes in solar irradiance. Since the range in the estimate is +0.6 to +2.4 W m^{-2}, there is very high confidence in the net positive radiative forcing of the climate system due to human activity. The LLGHGs together contribute +2.63 ± 0.26 W m^{-2}, which is the dominant radiative forcing term and has the highest level of scientific understanding. In contrast, the total direct aerosol, cloud albedo and surface albedo effects that contribute negative forcings are less well understood and have larger uncertainties. The range in the net estimate is increased by the negative forcing terms, which have larger uncertainties than the positive terms. The nature of the uncertainty in the estimated cloud albedo effect introduces a noticeable asymmetry in the distribution. Uncertainties in the distribution include structural aspects (e.g., representation of extremes in the component values, absence of any weighting of the radiative forcing mechanisms, possibility of unaccounted for but as yet unquantified radiative forcings) and statistical aspects (e.g., assumptions about the types of distributions describing component uncertainties). {2.7, 2.9}

The Global Warming Potential (GWP) is a useful metric for comparing the potential climate impact of the emissions of different LLGHGs (see Table TS.2). Global Warming Potentials compare the integrated radiative forcing over a specified period (e.g., 100 years) from a unit mass pulse emission and are a way of comparing the potential climate change associated with emissions of different greenhouse gases. There are well-documented shortcomings of the GWP concept, particularly in using it to assess the impact of short-lived species. {2.10}

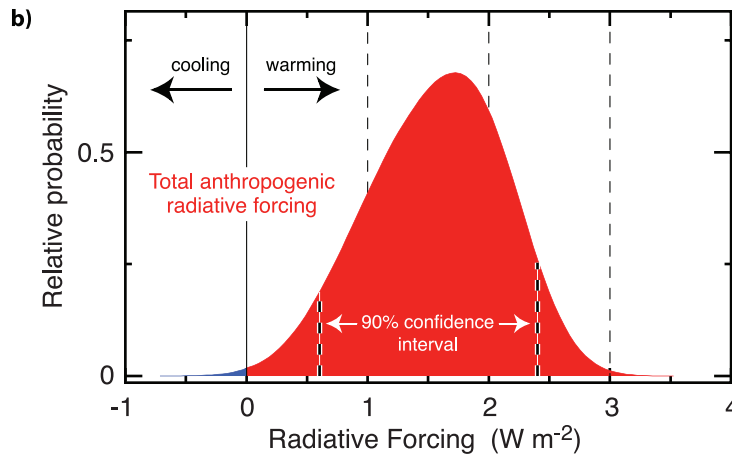**For the magnitude and range of realistic forcings considered, evidence suggests an approximately linear relationship between global mean radiative forcing and global mean surface temperature response. The spatial patterns of radiative forcing vary between different forcing agents. However, the spatial signature of the climate response is not generally expected to match that of the forcing.** Spatial patterns of climate response

GLOBAL MEAN RADIATIVE FORCINGS

a)

RF Terms		RF values (W m^{-2})	Spatial scale	LOSU
Anthropogenic Long-lived greenhouse gases	CO$_2$	**1.66** [1.49 to 1.83]	Global	High
	N$_2$O CH$_4$ Halocarbons	**0.48** [0.43 to 0.53] **0.16** [0.14 to 0.18] **0.34** [0.31 to 0.37]	Global	High
Ozone	Stratospheric Tropospheric	**-0.05** [-0.15 to 0.05] **0.35** [0.25 to 0.65]	Continental to global	Med
Stratospheric water vapour from CH$_4$		**0.07** [0.02 to 0.12]	Global	Low
Surface albedo	Land use Black carbon on snow	**-0.2** [-0.4 to 0.0] **0.1** [0.0 to 0.2]	Local to continental	Med - Low
Total Aerosol Direct effect		**-0.5** [-0.9 to -0.1]	Continental to global	Med - Low
Cloud albedo effect		**-0.7** [-1.8 to -0.3]	Continental to global	Low
Linear contrails		**0.01** [0.003 to 0.03]	Continental	Low
Natural Solar irradiance		**0.12** [0.06 to 0.30]	Global	Low
Total net anthropogenic		**1.6** [0.6 to 2.4]		

Radiative Forcing (W m^{-2})

©IPCC 2007: WG1-AR4

PROBABILITY DISTRIBUTION

b)

Relative probability

Radiative Forcing (W m^{-2})

cooling warming

Total anthropogenic radiative forcing

90% confidence interval

©IPCC 2007: WG1-AR4

Figure TS.5. *(a) Global mean radiative forcings (RF) and their 90% confidence intervals in 2005 for various agents and mechanisms. Columns on the right-hand side specify best estimates and confidence intervals (RF values); typical geographical extent of the forcing (Spatial scale); and level of scientific understanding (LOSU) indicating the scientific confidence level as explained in Section 2.9. Errors for CH$_4$, N$_2$O and halocarbons have been combined. The net anthropogenic radiative forcing and its range are also shown. Best estimates and uncertainty ranges can not be obtained by direct addition of individual terms due to the asymmetric uncertainty ranges for some factors; the values given here were obtained from a Monte Carlo technique as discussed in Section 2.9. Additional forcing factors not included here are considered to have a very low LOSU. Volcanic aerosols contribute an additional form of natural forcing but are not included due to their episodic nature. The range for linear contrails does not include other possible effects of aviation on cloudiness. (b) Probability distribution of the global mean combined radiative forcing from all anthropogenic agents shown in (a). The distribution is calculated by combining the best estimates and uncertainties of each component. The spread in the distribution is increased significantly by the negative forcing terms, which have larger uncertainties than the positive terms. {2.9.1, 2.9.2; Figure 2.20}*

Table TS.2. *Lifetimes, radiative efficiencies and direct (except for CH_4) global warming potentials (GWP) relative to CO_2.* {Table 2.14}

Industrial Designation or Common Name (years)	Chemical Formula	Lifetime (years)	Radiative Efficiency (W m^{-2} ppb^{-1})	Global Warming Potential for Given Time Horizon			
				SAR[‡] (100-yr)	20-yr	100-yr	500-yr
Carbon dioxide	CO_2	See below[a]	[b]1.4x10^{-5}	1	1	1	1
Methane[c]	CH_4	12[c]	3.7x10^{-4}	21	72	25	7.6
Nitrous oxide	N_2O	114	3.03x10^{-3}	310	289	298	153
Substances controlled by the Montreal Protocol							
CFC-11	CCl_3F	45	0.25	3,800	6,730	4,750	1,620
CFC-12	CCl_2F_2	100	0.32	8,100	11,000	10,900	5,200
CFC-13	$CClF_3$	640	0.25		10,800	14,400	16,400
CFC-113	CCl_2FCClF_2	85	0.3	4,800	6,540	6,130	2,700
CFC-114	$CClF_2CClF_2$	300	0.31		8,040	10,000	8,730
CFC-115	$CClF_2CF_3$	1,700	0.18		5,310	7,370	9,990
Halon-1301	$CBrF_3$	65	0.32	5,400	8,480	7,140	2,760
Halon-1211	$CBrClF_2$	16	0.3		4,750	1,890	575
Halon-2402	$CBrF_2CBrF_2$	20	0.33		3,680	1,640	503
Carbon tetrachloride	CCl_4	26	0.13	1,400	2,700	1,400	435
Methyl bromide	CH_3Br	0.7	0.01		17	5	1
Methyl chloroform	CH_3CCl_3	5	0.06		506	146	45
HCFC-22	$CHClF_2$	12	0.2	1,500	5,160	1,810	549
HCFC-123	$CHCl_2CF_3$	1.3	0.14	90	273	77	24
HCFC-124	$CHClFCF_3$	5.8	0.22	470	2,070	609	185
HCFC-141b	CH_3CCl_2F	9.3	0.14		2,250	725	220
HCFC-142b	CH_3CClF_2	17.9	0.2	1,800	5,490	2,310	705
HCFC-225ca	$CHCl_2CF_2CF_3$	1.9	0.2		429	122	37
HCFC-225cb	$CHClFCF_2CClF_2$	5.8	0.32		2,030	595	181
Hydrofluorocarbons							
HFC-23	CHF_3	270	0.19	11,700	12,000	14,800	12,200
HFC-32	CH_2F_2	4.9	0.11	650	2,330	675	205
HFC-125	CHF_2CF_3	29	0.23	2,800	6,350	3,500	1,100
HFC-134a	CH_2FCF_3	14	0.16	1,300	3,830	1,430	435
HFC-143a	CH_3CF_3	52	0.13	3,800	5,890	4,470	1,590
HFC-152a	CH_3CHF_2	1.4	0.09	140	437	124	38
HFC-227ea	CF_3CHFCF_3	34.2	0.26	2,900	5,310	3,220	1,040
HFC-236fa	$CF_3CH_2CF_3$	240	0.28	6,300	8,100	9,810	7,660
HFC-245fa	$CHF_2CH_2CF_3$	7.6	0.28		3,380	1030	314
HFC-365mfc	$CH_3CF_2CH_2CF_3$	8.6	0.21		2,520	794	241
HFC-43-10mee	$CF_3CHFCHFCF_2CF_3$	15.9	0.4	1,300	4,140	1,640	500
Perfluorinated compounds							
Sulphur hexafluoride	SF_6	3,200	0.52	23,900	16,300	22,800	32,600
Nitrogen trifluoride	NF_3	740	0.21		12,300	17,200	20,700
PFC-14	CF_4	50,000	0.10	6,500	5,210	7,390	11,200
PFC-116	C_2F_6	10,000	0.26	9,200	8,630	12,200	18,200

Table TS.2 (continued)

Industrial Designation or Common Name (years)	Chemical Formula	Lifetime (years)	Radiative Efficiency (W m^{-2} ppb^{-1})	Global Warming Potential for Given Time Horizon			
				SAR[‡] (100-yr)	20-yr	100-yr	500-yr
Perfluorinated compounds (continued)							
PFC-218	C_3F_8	2,600	0.26	7,000	6,310	8,830	12,500
PFC-318	$c\text{-}C_4F_8$	3,200	0.32	8,700	7,310	10,300	14,700
PFC-3-1-10	C_4F_{10}	2,600	0.33	7,000	6,330	8,860	12,500
PFC-4-1-12	C_5F_{12}	4,100	0.41		6,510	9,160	13,300
PFC-5-1-14	C_6F_{14}	3,200	0.49	7,400	6,600	9,300	13,300
PFC-9-1-18	$C_{10}F_{18}$	>1,000[d]	0.56		>5,500	>7,500	>9,500
trifluoromethyl sulphur pentafluoride	SF_5CF_3	800	0.57		13,200	17,700	21,200
Fluorinated ethers							
HFE-125	CHF_2OCF_3	136	0.44		13,800	14,900	8,490
HFE-134	CHF_2OCHF_2	26	0.45		12,200	6,320	1,960
HFE-143a	CH_3OCF_3	4.3	0.27		2,630	756	230
HCFE-235da2	$CHF_2OCHClCF_3$	2.6	0.38		1,230	350	106
HFE-245cb2	$CH_3OCF_2CHF_2$	5.1	0.32		2,440	708	215
HFE-245fa2	$CHF_2OCH_2CF_3$	4.9	0.31		2,280	659	200
HFE-254cb2	$CH_3OCF_2CHF_2$	2.6	0.28		1,260	359	109
HFE-347mcc3	$CH_3OCF_2CF_2CF_3$	5.2	0.34		1,980	575	175
HFE-347pcf2	$CHF_2CF_2OCH_2CF_3$	7.1	0.25		1,900	580	175
HFE-356pcc3	$CH_3OCF_2CF_2CHF_2$	0.33	0.93		386	110	33
HFE-449sl (HFE-7100)	$C_4F_9OCH_3$	3.8	0.31		1,040	297	90
HFE-569sf2 (HFE-7200)	$C_4F_9OC_2H_5$	0.77	0.3		207	59	18
HFE-43-10pccc124 (H-Galden 1040x)	$CHF_2OCF_2OC_2F_4OCHF_2$	6.3	1.37		6,320	1,870	569
HFE-236ca12 (HG-10)	$CHF_2OCF_2OCHF_2$	12.1	0.66		8,000	2,800	860
HFE-338pcc13 (HG-01)	$CHF_2OCF_2CF_2OCHF_2$	6.2	0.87		5,100	1,500	460
Perfluoropolyethers							
PFPMIE	$CF_3OCF(CF_3)CF_2OCF_2OCF_3$	800	0.65		7,620	10,300	12,400
Hydrocarbons and other compounds – Direct Effects							
Dimethylether	CH_3OCH_3	0.015	0.02		1	1	<<1
Methylene chloride	CH_2Cl_2	0.38	0.03		31	8.7	2.7
Methyl chloride	CH_3Cl	1.0	0.01		45	13	4

Notes:

[‡] SAR refers to the IPCC Second Assessment Report (1995) used for reporting under the UNFCCC.

[a] The CO_2 response function used in this report is based on the revised version of the Bern Carbon cycle model used in Chapter 10 of this report (Bern2.5CC; Joos et al. 2001) using a background CO_2 concentration value of 378 ppm. The decay of a pulse of CO_2 with time t is given by

$$a_0 + \sum_{i=1}^{3} a_i \cdot e^{-t/\tau_i}$$ where $a_0 = 0.217$, $a_1 = 0.259$, $a_2 = 0.338$, $a_3 = 0.186$, $\tau_1 = 172.9$ years, $\tau_2 = 18.51$ years, and $\tau_3 = 1.186$ years, for t < 1,000 years.

[b] The radiative efficiency of CO_2 is calculated using the IPCC (1990) simplified expression as revised in the TAR, with an updated background concentration value of 378 ppm and a perturbation of +1 ppm (see Section 2.10.2).

[c] The perturbation lifetime for CH_4 is 12 years as in the TAR (see also Section 7.4). The GWP for CH_4 includes indirect effects from enhancements of ozone and stratospheric water vapour (see Section 2.10) .

[d] The assumed lifetime of 1000 years is a lower limit.

are largely controlled by climate processes and feedbacks. For example, sea ice-albedo feedbacks tend to enhance the high-latitude response. Spatial patterns of response are also affected by differences in thermal inertia between land and sea areas. {2.8, 9.2}

The pattern of response to a radiative forcing can be altered substantially if its structure is favourable for affecting a particular aspect of the atmospheric structure or circulation. Modelling studies and data comparisons suggest that mid- to high-latitude circulation patterns are *likely* to be affected by some forcings such as volcanic eruptions, which have been linked to changes in the Northern Annular Mode (NAM) and North Atlantic Oscillation (NAO) (see Section 3.1 and Box TS.2). Simulations also suggest that absorbing aerosols, particularly black carbon, can reduce the solar radiation reaching the surface and can warm the atmosphere at regional scales, affecting the vertical temperature profile and the large-scale atmospheric circulation. {2.8, 7.5, 9.2}

The spatial patterns of radiative forcings for ozone, aerosol direct effects, aerosol-cloud interactions and land use have considerable uncertainties. This is in contrast to the relatively high confidence in the spatial pattern of radiative forcing for the LLGHGs. The net positive radiative forcing in the Southern Hemisphere (SH) *very likely* exceeds that in the NH because of smaller aerosol concentrations in the SH. {2.9}

TS 2.6 Surface Forcing and the Hydrologic Cycle

Observations and models indicate that changes in the radiative flux at the Earth's surface affect the surface heat and moisture budgets, thereby involving the hydrologic cycle. Recent studies indicate that some forcing agents can influence the hydrologic cycle differently than others through their interactions with clouds. In particular, changes in aerosols may have affected precipitation and other aspects of the hydrologic cycle more strongly than other anthropogenic forcing agents. Energy deposited at the surface directly affects evaporation and sensible heat transfer. The instantaneous radiative flux change at the surface (hereafter called 'surface forcing') is a useful diagnostic tool for understanding changes in the heat and moisture surface budgets and the accompanying climate change. However, unlike radiative forcing, it cannot be used to quantitatively compare the effects of different agents on the equilibrium global mean surface temperature change. Net radiative forcing and surface forcing have different equator-to-pole gradients in the NH, and are different between the NH and SH. {2.9, 7.2, 7.5, 9.5}

TS.3 Observations of Changes in Climate

This assessment evaluates changes in the Earth's climate system, considering not only the atmosphere, but also the ocean and the cryosphere, as well as phenomena such as atmospheric circulation changes, in order to increase understanding of trends, variability and processes of climate change at global and regional scales. Observational records employing direct methods are of variable length as described below, with global temperature estimates now beginning as early as 1850. Observations of extremes of weather and climate are discussed, and observed changes in extremes are described. The consistency of observed changes among different climate variables that allows an increasingly comprehensive picture to be drawn is also described. Finally, palaeoclimatic information that generally employs indirect proxies to infer information about climate change over longer time scales (up to millions of years) is also assessed.

TS.3.1 Atmospheric Changes: Instrumental Record

This assessment includes analysis of global and hemispheric means, changes over land and ocean and distributions of trends in latitude, longitude and altitude. Since the TAR, improvements in observations and their calibration, more detailed analysis of methods and extended time series allow more in-depth analyses of changes including atmospheric temperature, precipitation, humidity, wind and circulation. Extremes of climate are a key expression of climate variability, and this assessment includes new data that permit improved insights into the changes in many types of extreme events including heat waves, droughts, heavy precipitation and tropical cyclones (including hurricanes and typhoons). {3.2–3.4, 3.8}

Furthermore, advances have occurred since the TAR in understanding how a number of seasonal and long-term anomalies can be described by patterns of climate variability. These patterns arise from internal interactions and from the differential effects on the atmosphere of land and ocean, mountains and large changes in heating. Their response is often felt in regions far removed from their physical source through atmospheric teleconnections associated with large-scale waves in the atmosphere. Understanding temperature and precipitation anomalies associated with the dominant patterns of climate variability is essential to understanding many regional climate anomalies and why these may differ from those at the global scale. Changes in storm tracks, the jet streams,

regions of preferred blocking anticyclones and changes in monsoons can also occur in conjunction with these preferred patterns of variability. {3.5–3.7}

TS.3.1.1   Global Average Temperatures

2005 and 1998 were the warmest two years in the instrumental global surface air temperature record since 1850. Surface temperatures in 1998 were enhanced by the major 1997–1998 El Niño but no such strong anomaly was present in 2005. Eleven of the last 12 years (1995 to 2006) – the exception being 1996 – rank among the 12 warmest years on record since 1850. {3.2}

The global average surface temperature has increased, especially since about 1950. The updated 100-year trend (1906–2005) of 0.74°C ± 0.18°C is larger than the 100-year warming trend at the time of the TAR (1901–2000) of 0.6°C ± 0.2°C due to additional warm years. The total temperature increase from 1850-1899 to 2001-2005 is 0.76°C ± 0.19°C. The rate of warming averaged over the last 50 years (0.13°C ± 0.03°C per decade) is nearly twice that for the last 100 years. Three different global estimates all show consistent warming trends. There is also consistency between the data sets in their separate land and ocean domains, and between sea surface temperature (SST) and nighttime marine air temperature (see Figure TS.6). {3.2}

Recent studies confirm that effects of urbanisation and land use change on the global temperature record are negligible (less than 0.006°C per decade over land and zero over the ocean) as far as hemispheric- and continental-scale averages are concerned. All observations are subject to data quality and consistency checks to correct for potential biases. The real but local effects of urban areas are accounted for in the land temperature data sets used. Urbanisation and land use effects are not relevant to the widespread oceanic warming that has been observed. Increasing evidence suggests that urban heat island effects also affect precipitation, cloud and diurnal temperature range (DTR). {3.2}

The global average DTR has stopped decreasing. A decrease in DTR of approximately 0.1°C per decade was reported in the TAR for the period 1950 to 1993. Updated observations reveal that DTR has not changed from 1979 to 2004 as both day- and night time temperature have risen at about the same rate. The trends are highly variable from one region to another. {3.2}

New analyses of radiosonde and satellite measurements of lower- and mid-tropospheric temperature show warming rates that are generally consistent with each other and with those in the surface temperature record within their respective uncertainties for the periods 1958 to 2005 and 1979 to 2005. This largely resolves a discrepancy noted in the TAR (see Figure TS.7). The radiosonde record is markedly less spatially complete than the surface record and increasing evidence suggests that a number of radiosonde data sets are unreliable, especially in the tropics. Disparities remain among different tropospheric temperature trends estimated from satellite Microwave Sounding Unit (MSU) and advanced MSU measurements since 1979, and all likely still contain residual errors. However, trend estimates have been substantially improved and data set differences reduced since the TAR, through adjustments for changing satellites, orbit decay and drift in local crossing time (diurnal cycle effects). It appears that the satellite tropospheric temperature record is broadly consistent with surface temperature trends provided that the stratospheric influence on MSU channel 2 is accounted for. The range across different data sets of global surface warming since 1979 is 0.16°C to 0.18°C per decade, compared to 0.12°C to 0.19°C per decade for MSU-derived estimates of tropospheric temperatures. It is likely that there is increased warming with altitude from the surface through much of the troposphere in the tropics, pronounced cooling in the stratosphere, and a trend towards a higher tropopause. {3.4}

Stratospheric temperature estimates from adjusted radiosondes, satellites and reanalyses are all in qualitative agreement, with a cooling of between 0.3°C and 0.6°C per decade since 1979 (see Figure TS.7). Longer radiosonde records (back to 1958) also indicate stratospheric cooling but are subject to substantial instrumental uncertainties. The rate of cooling increased after 1979 but has slowed in the last decade. It is *likely* that radiosonde records overestimate stratospheric cooling, owing to changes in sondes not yet taken into account. The trends are not monotonic, because of stratospheric warming episodes that follow major volcanic eruptions. {3.4}
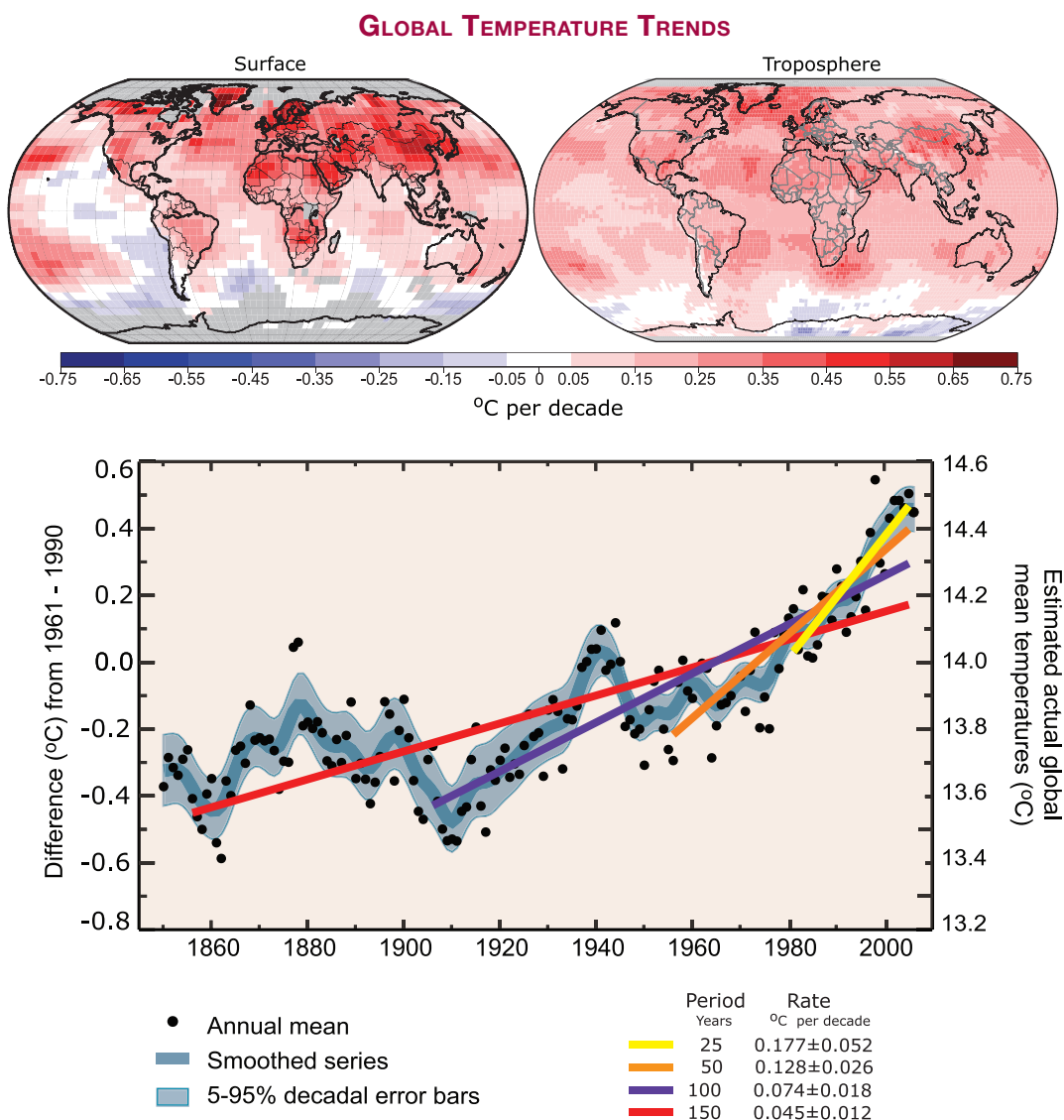
Figure TS.6. *(Top) Patterns of linear global temperature trends over the period 1979 to 2005 estimated at the surface (left), and for the troposphere from satellite records (right). Grey indicates areas with incomplete data. (Bottom) Annual global mean temperatures (black dots) with linear fits to the data. The left hand axis shows temperature anomalies relative to the 1961 to 1990 average and the right hand axis shows estimated actual temperatures, both in °C. Linear trends are shown for the last 25 (yellow), 50 (orange), 100 (purple) and 150 years (red). The smooth blue curve shows decadal variations (see Appendix 3.A), with the decadal 90% error range shown as a pale blue band about that line. The total temperature increase from the period 1850 to 1899 to the period 2001 to 2005 is 0.76°C ± 0.19°C. {FAQ 3.1, Figure 1.}*

TS.3.1.2   Spatial Distribution of Changes in Temperature, Circulation and Related Variables

Surface temperatures over land regions have warmed at a faster rate than over the oceans in both hemispheres. Longer records now available show significantly faster rates of warming over land than ocean in the past two decades (about 0.27°C vs. 0.13°C per decade). {3.2}

The warming in the last 30 years is widespread over the globe, and is greatest at higher northern latitudes. The greatest warming has occurred in the NH winter (DJF) and spring (MAM). Average arctic temperatures have been increasing at almost twice the rate of the rest of the world in the past 100 years. However, arctic temperatures are highly variable. A slightly longer arctic warm period, almost as warm as the present, was observed from 1925 to 1945, but its geographical distribution appears to have been different from the recent warming since its extent was not global. {3.2}

There is evidence for long-term changes in the large-scale atmospheric circulation, such as a poleward shift and strengthening of the westerly winds. Regional climate trends can be very different from the global average, reflecting changes in the circulations and interactions of the atmosphere and ocean and the other components of the climate system. Stronger mid-latitude westerly wind maxima have occurred in both hemispheres in most seasons from at least 1979 to the late 1990s, and poleward displacements of corresponding Atlantic and southern polar front jet streams have been documented. The westerlies in the NH increased from the 1960s to the 1990s but have since returned to values close to the long-term average. The increased strength of the westerlies in the NH changes the flow from oceans to continents, and is a major factor in the observed winter changes in storm tracks and related patterns of precipitation and temperature trends at mid- and high-latitudes. Analyses of wind and significant wave height support reanalysis-based evidence for changes in NH extratropical storms from the start of the reanalysis record in the late 1970s until the late 1990s. These changes are accompanied by a tendency towards stronger winter polar vortices throughout the troposphere and lower stratosphere. {3.2, 3.5}

Many regional climate changes can be described in terms of preferred patterns of climate variability and therefore as changes in the occurrence of indices that characterise the strength and phase of these patterns. The importance, over all time scales, of fluctuations in the westerlies and storm tracks in the North Atlantic has often been noted, and these fluctuations are described by the NAO (see Box TS.2 for an explanation of this and other preferred patterns). The characteristics of fluctuations in the zonally averaged westerlies in the two hemispheres have more recently been described by their respective 'annular modes', the Northern and Southern Annular Modes (NAM and SAM). The observed changes can be expressed as a shift of the circulation towards the structure associated with one sign of these preferred patterns. The increased mid-latitude westerlies in the North Atlantic can be largely viewed as reflecting either NAO or NAM changes; multi-decadal variability is also evident in the Atlantic, both in the atmosphere and the ocean. In the SH, changes in circulation related to an increase in the

OBSERVED AIR TEMPERATURES
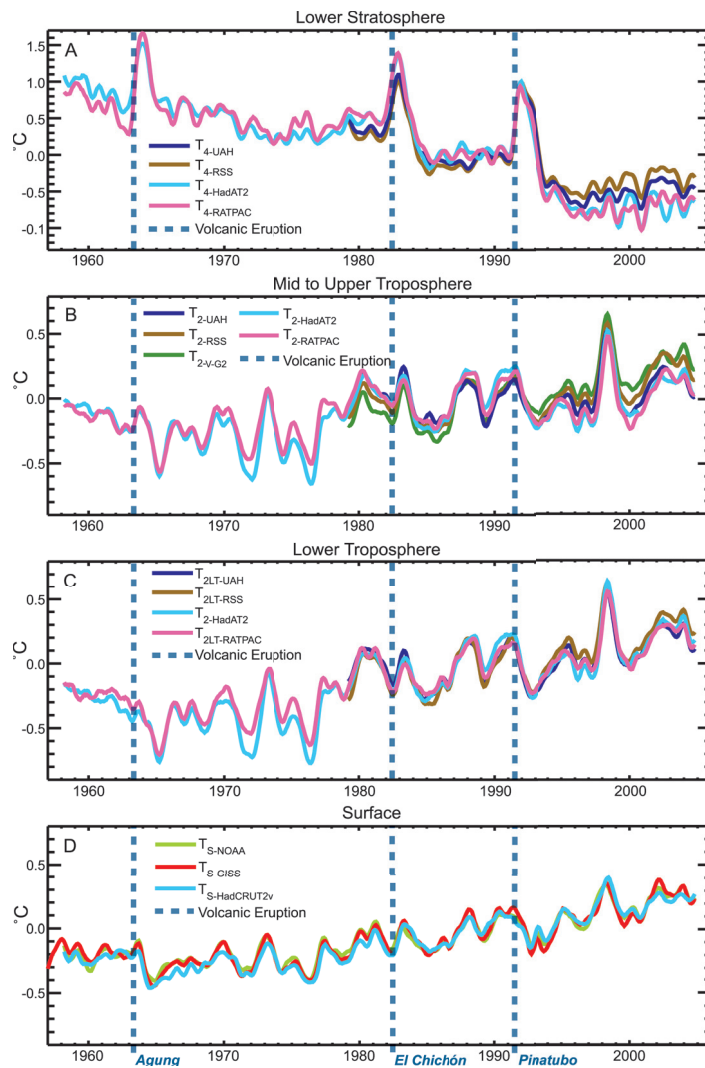
Figure TS.7. *Observed surface (D) and upper air temperatures for the lower troposphere (C), mid- to upper troposphere (B) and lower stratosphere (A), shown as monthly mean anomalies relative to the period 1979 to 1997 smoothed with a seven-month running mean filter. Dashed lines indicate the times of major volcanic eruptions. {Figure 3.17}*

SAM from the 1960s to the present are associated with strong warming over the Antarctic Peninsula and, to a lesser extent, cooling over parts of continental Antarctica. Changes have also been observed in ocean-atmosphere interactions in the Pacific. The ENSO is the dominant mode of global-scale variability on interannual time scales although there have been times when it is less apparent. The 1976–1977 climate shift, related to the phase change in the Pacific Decadal Oscillation (PDO) towards more El Niño events and changes in the evolution of ENSO, has affected many areas, including most tropical monsoons. For instance, over North America, ENSO and Pacific-

Box TS.2: Patterns (Modes) of Climate Variability

Analysis of atmospheric and climatic variability has shown that a significant component of it can be described in terms of fluctuations in the amplitude and sign of indices of a relatively small number of preferred patterns of variability. Some of the best known of these are:

- El Niño-Southern Oscillation (ENSO), a coupled fluctuation in the atmosphere and the equatorial Pacific Ocean, with preferred time scales of two to about seven years. ENSO is often measured by the difference in surface pressure anomalies between Tahiti and Darwin and the SSTs in the central and eastern equatorial Pacific. ENSO has global teleconnections.

- North Atlantic Oscillation (NAO), a measure of the strength of the Icelandic Low and the Azores High, and of the westerly winds between them, mainly in winter. The NAO has associated fluctuations in the storm track, temperature and precipitation from the North Atlantic into Eurasia (see Box TS.2, Figure 1).

- Northern Annular Mode (NAM), a winter fluctuation in the amplitude of a pattern characterised by low surface pressure in the Arctic and strong mid-latitude westerlies. The NAM has links with the northern polar vortex and hence the stratosphere.

- Southern Annular Mode (SAM), the fluctuation of a pattern with low antarctic surface pressure and strong mid-latitude westerlies, analogous to the NAM, but present year round.

- Pacific-North American (PNA) pattern, an atmospheric large-scale wave pattern featuring a sequence of tropospheric high- and low-pressure anomalies stretching from the subtropical west Pacific to the east coast of North America.

- Pacific Decadal Oscillation (PDO), a measure of the SSTs in the North Pacific that has a very strong correlation with the North Pacific Index (NPI) measure of the depth of the Aleutian Low. However, it has a signature throughout much of the Pacific.

POSITIVE PHASE OF NAO AND NAM

With higher than normal atmospheric pressure over the central Atlantic, strong westerly winds push warmth and precipitation toward northern Europe.

WARMER THAN NORMAL

COOLER THAN NORMAL

DRIER THAN NORMAL

WETTER THAN NORMAL

©IPCC 2007: WG1-AR4
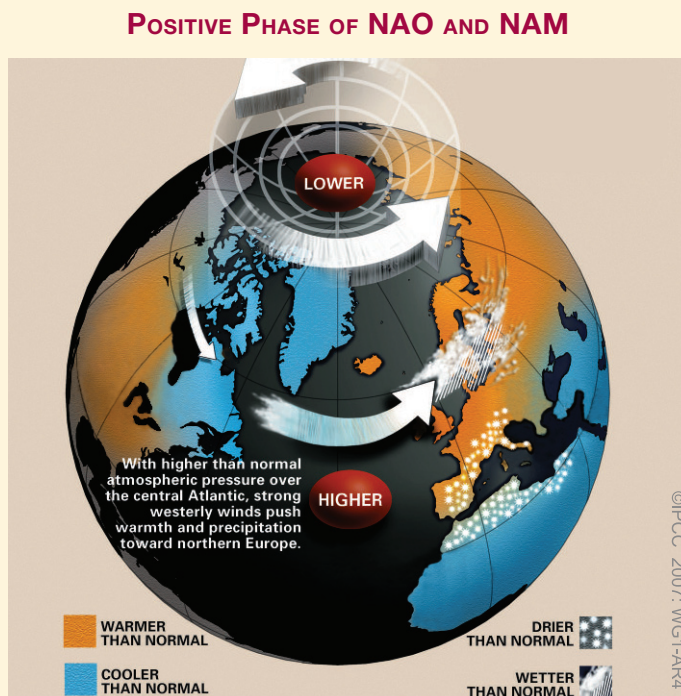
Box TS.2, Figure 1. *A schematic of the changes associated with the positive phase of the NAO and NAM. The changes in pressure and winds are shown, along with precipitation changes. Warm colours indicate areas that are warmer than normal and blue indicates areas that are cooler than normal.*

The extent to which all these preferred patterns of variability can be considered to be true modes of the climate system is a topic of active research. However, there is evidence that their existence can lead to larger-amplitude regional responses to forcing than would otherwise be expected. In particular, a number of the observed 20th-century climate changes can be viewed in terms of changes in these patterns. It is therefore important to test the ability of climate models to simulate them (see Section TS.4, Box TS.7) and to consider the extent to which observed changes related to these patterns are linked to internal variability or to anthropogenic climate change. {3.6, 8.4}

North American (PNA) teleconnection-related changes appear to have led to contrasting changes across the continent, as the western part has warmed more than the eastern part, while the latter has become cloudier and wetter. There is substantial low-frequency atmospheric variability in the Pacific sector over the 20th century, with extended periods of weakened (1900–1924; 1947–1976) as well as strengthened (1925–1946; 1977–2003) circulation. {3.2, 3.5, 3.6}

Changes in extremes of temperature are consistent with warming. Observations show widespread reductions in the number of frost days in mid-latitude regions, increases in the number of warm extremes (warmest 10% of days or nights) and a reduction in the number of daily cold extremes (coldest 10% of days or nights) (see Box TS.5). The most marked changes are for cold nights, which have declined over the 1951 to 2003 period for all regions where data are available (76% of the land). {3.8}

Heat waves have increased in duration beginning in the latter half of the 20th century. The record-breaking heat wave over western and central Europe in the summer of 2003 is an example of an exceptional recent extreme. That summer (JJA) was the warmest since comparable instrumental records began around 1780 (1.4°C above the previous warmest in 1807). Spring drying of the land surface over Europe was an important factor in the occurrence of the extreme 2003 temperatures. Evidence suggests that heat waves have also increased in frequency and duration in other locations. The very strong correlation between observed dryness and high temperatures over land in the tropics during summer highlights the important role moisture plays in moderating climate. {3.8, 3.9}

There is insufficient evidence to determine whether trends exist in such events as tornadoes, hail, lightning and dust storms which occur at small spatial scales. {3.8}

TS.3.1.3 *Changes in the Water Cycle: Water Vapour, Clouds, Precipitation and Tropical Storms*

Tropospheric water vapour is increasing (Figure TS.8). Surface specific humidity has generally increased since 1976 in close association with higher temperatures over both land and ocean. Total column water vapour has increased over the global oceans by 1.2 ± 0.3% per decade (95% confidence limits) from 1988 to 2004. The observed regional changes are consistent in pattern and amount with the changes in SST and the assumption of a near-constant relative humidity increase in water vapour mixing ratio. The additional atmospheric water vapour implies increased moisture availability for precipitation. {3.4}

ATMOSPHERIC WATER VAPOUR

a) Column Water Vapour, Ocean only: Trend,1988-2004

b) Global ocean mean (%) 1.2% per decade

c) Global mean T2−T12 (°C) 0.17 °C per decade
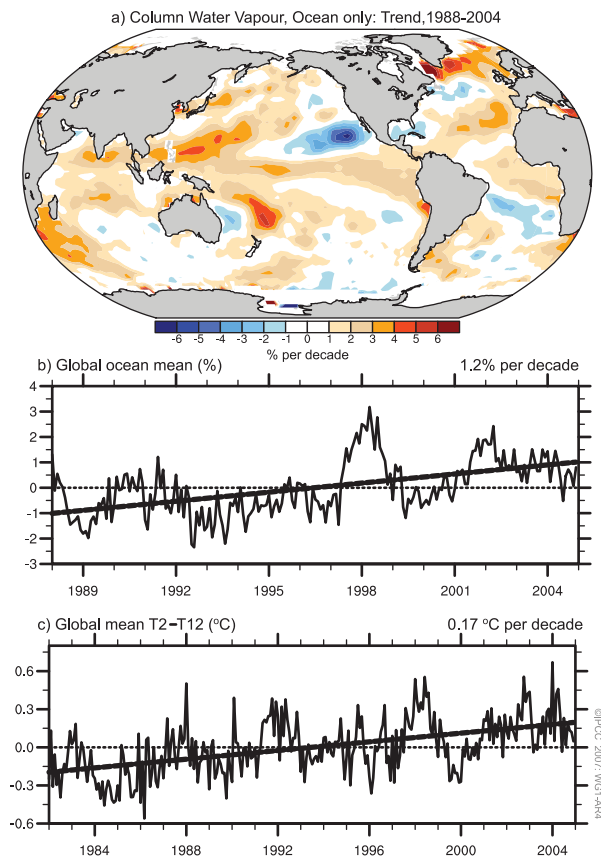
Figure TS.8. *(a) Linear trends in precipitable water (total column water vapour) over the period 1988 to 2004 (% per decade) and (b) the monthly time series of anomalies, relative to the period shown, over the global ocean with linear trend. (c) The global mean (80°N to 80°S) radiative signature of upper-tropospheric moistening is given by monthly time series of combinations of satellite brightness temperature anomalies (°C), relative to the period 1982 to 2004, with the dashed line showing the linear trend of the key brightness temperature in °C per decade. {3.4, Figures 3.20 and 3.21}*

Upper-tropospheric water vapour is also increasing. Due to instrumental limitations, it is difficult to assess long-term changes in water vapour in the upper troposphere, where it is of radiative importance. However, the available data now show evidence for global increases in upper-tropospheric specific humidity over the past two decades (Figure TS.8). These observations are consistent with the observed increase in temperatures and represent an important advance since the TAR. {3.4}

Cloud changes are dominated by ENSO. Widespread (but not ubiquitous) decreases in continental DTR have coincided with increases in cloud amounts. Surface and satellite observations disagree on changes in total and low-level cloud changes over the ocean. However, radiation

changes at the top of the atmosphere from the 1980s to 1990s (possibly related in part to the ENSO phenomenon) appear to be associated with reductions in tropical upper-level cloud cover, and are consistent with changes in the energy budget and in observed ocean heat content. {3.4}

'Global dimming' is not global in extent and it has not continued after 1990. Reported decreases in solar radiation at the Earth's surface from 1970 to 1990 have an urban bias. Further, there have been increases since about 1990. An increasing aerosol load due to human activities decreases regional air quality and the amount of solar radiation reaching the Earth's surface. In some areas, such as Eastern Europe, recent observations of a reversal in the sign of this effect link changes in solar radiation to concurrent air quality improvements. {3.4}

Long-term trends in precipitation amounts from 1900 to 2005 have been observed in many large regions (Figure TS.9). Significantly increased precipitation has been observed in the eastern parts of North and South America, northern Europe and northern and central Asia. Drying has been observed in the Sahel, the Mediterranean, southern Africa and parts of southern Asia. Precipitation is highly variable spatially and temporally, and robust long-term trends have not been established for other large regions.[5] {3.3}

Substantial increases in heavy precipitation events have been observed. It is *likely* that there have been increases in the number of heavy precipitation events (e.g., above the 95th percentile) in many land regions since about 1950, even in those regions where there has been a reduction in total precipitation amount. Increases have also been reported for rarer precipitation events (1 in 50 year return period), but only a few regions have sufficient data to assess such trends reliably (see Figure TS.10). {3.8}

There is observational evidence for an increase of intense tropical cyclone activity in the North Atlantic since about 1970, correlated with increases in tropical SSTs. There are also suggestions of increased intense tropical cyclone activity in some other regions where concerns over data quality are greater. Multi-decadal variability and the quality of the tropical cyclone records prior to routine satellite observations in about 1970 complicate the detection of long-term trends in tropical cyclone activity and there is no clear trend in the annual numbers of tropical cyclones. Estimates of the potential destructiveness of tropical cyclones suggest a substantial upward trend since the mid-1970s, with a trend towards longer lifetimes and greater intensity. Trends are also apparent in SST, a critical variable known to influence

GLOBAL MEAN PRECIPITATION
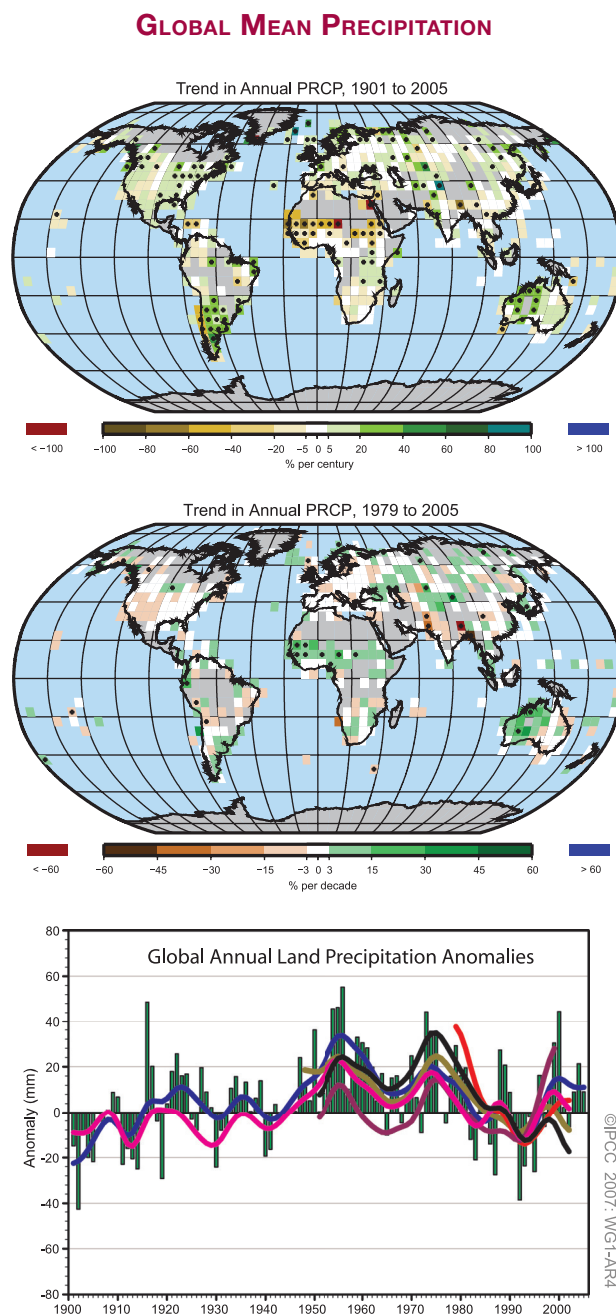
Figure TS.9. *(Top) Distribution of linear trends of annual land precipitation amounts over the period 1901 to 2005 (% per century) and (middle) 1979 to 2005 (% per decade). Areas in grey have insufficient data to produce reliable trends. The percentage is based on the 1961 to 1990 period. (Bottom) Time series of annual global land precipitation anomalies with respect to the 1961 to 1990 base period for 1900 to 2005. The smooth curves show decadal variations (see Appendix 3.A) for different data sets. {3.3, Figures 3.12 and 3.13}*

---

[5] The assessed regions are those considered in the regional projections chapter of the TAR and in Chapter 11 of this report.

ANNUAL PRECIPITATION TRENDS

Trend % per decade 1951 - 2003 contribution from very wet days
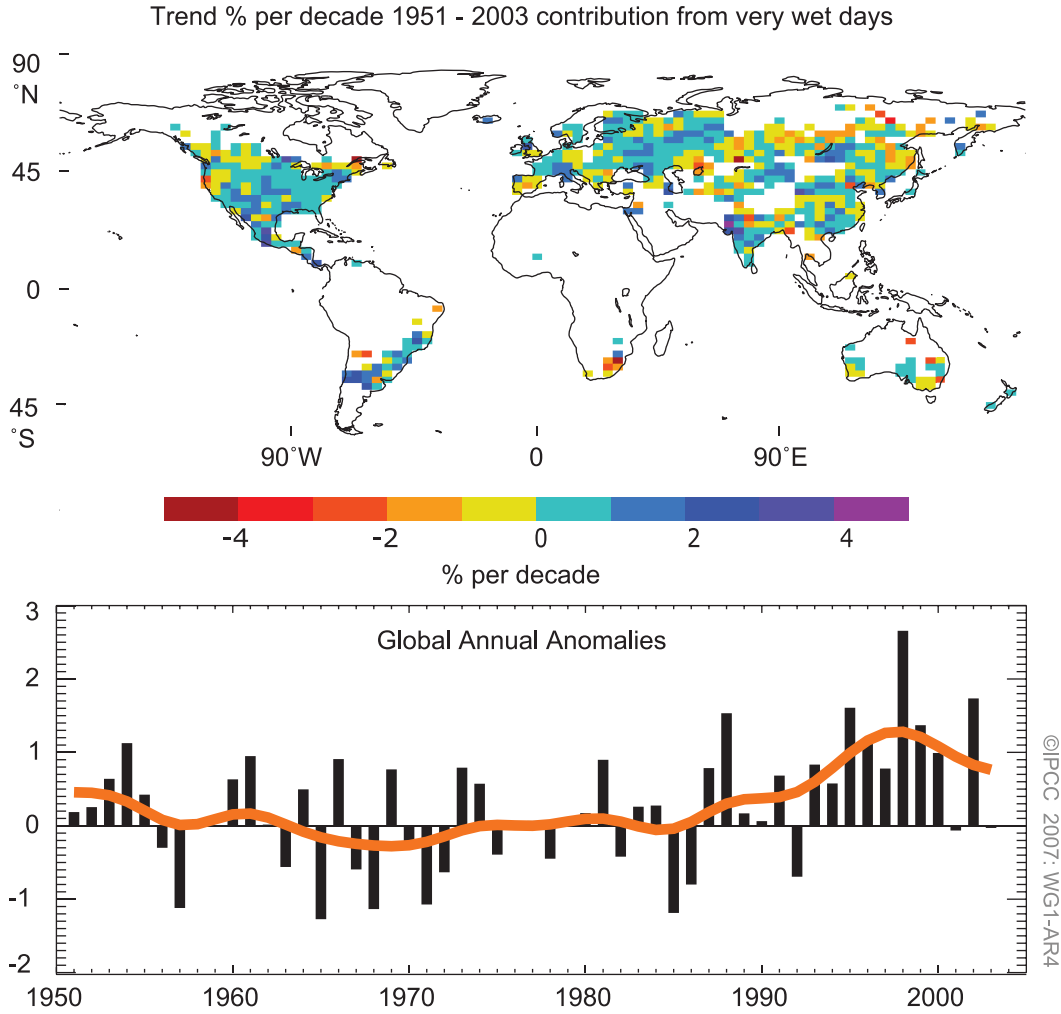
Figure TS.10. *(Top) Observed trends (% per decade) over the period 1951 to 2003 in the contribution to total annual precipitation from very wet days (i.e., corresponding to the 95th percentile and above). White land areas have insufficient data for trend determination. (Bottom) Anomalies (%) of the global (regions with data shown in top panel) annual time series of very wet days (with respect to 1961– 1990) defined as the percentage change from the base period average (22.5%). The smooth orange curve shows decadal variations (see Appendix 3.A). {Figure 3.39}*

ANNUAL SEA-SURFACE TEMPERATURE ANOMALIES
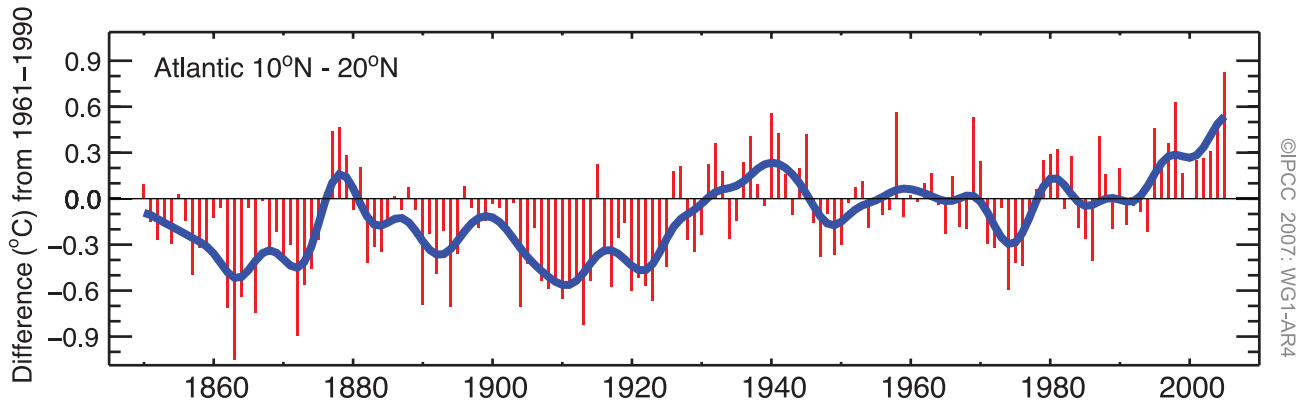
Figure TS.11. *Tropical Atlantic (10°N–20°N) sea surface temperature annual anomalies (°C) in the region of Atlantic hurricane formation, relative to the 1961 to 1990 mean. {Figure 3.33}*

tropical cyclone development (see Figure TS.11). Variations in the total numbers of tropical cyclones result from ENSO and decadal variability, which also lead to a redistribution of tropical storm numbers and tracks. The numbers of hurricanes in the North Atlantic have been above normal (based on 1981–2000) in nine of the years from 1995 to 2005. {3.8}

More intense and longer droughts have been observed over wider areas, particularly in the tropics and subtropics since the 1970s. While there are many different measures of drought, many studies use precipitation changes together with temperature.[6] Increased drying due to higher temperatures and decreased land precipitation have contributed to these changes. {3.3}

TS.3.2 Changes in the Cryosphere: Instrumental Record

Currently, ice permanently covers 10% of the land surface, with only a tiny fraction occurring outside Antarctica and Greenland. Ice also covers approximately 7% of the oceans in the annual mean. In midwinter, snow covers approximately 49% of the land surface in the NH. An important property of snow and ice is its high surface albedo. Because up to 90% of the incident solar radiation is reflected by snow and ice surfaces, while only about 10% is reflected by the open ocean or forested lands, changes in snow and ice cover are important feedback mechanisms in climate change. In addition, snow and ice are effective insulators. Seasonally frozen ground is more extensive than snow cover, and its presence is important for energy and moisture fluxes. Therefore, frozen surfaces play important roles in energy and climate processes. {4.1}

The cryosphere stores about 75% of the world's freshwater. At a regional scale, variations in mountain snowpack, glaciers and small ice caps play a crucial role in freshwater availability. Since the change from ice to liquid water occurs at specific temperatures, ice is a component of the climate system that could be subject to abrupt change following sufficient warming. Observations and analyses of changes in ice have expanded and improved since the TAR, including shrinkage of mountain glacier volume, decreases in snow cover, changes in permafrost and frozen ground, reductions in arctic sea ice extent, coastal thinning of the Greenland Ice Sheet exceeding inland thickening from increased snowfall, and reductions in seasonally frozen ground and river and lake ice cover.

These allow an improved understanding of how the cryosphere is changing, including its contributions to recent changes in sea level. The periods from 1961 to the present and from 1993 to the present are a focus of this report, due to the availability of directly measured glacier mass balance data and altimetry observations of the ice sheets, respectively. {4.1}

Snow cover has decreased in most regions, especially in spring. Northern Hemisphere snow cover observed by satellite over the 1966 to 2005 period decreased in every month except November and December, with a stepwise drop of 5% in the annual mean in the late 1980s (see Figure TS.12). In the SH, the few long records or proxies mostly show either decreases or no changes in the past 40 years or more. Northern Hemisphere April snow cover extent is strongly correlated with 40°N to 60°N April temperature, reflecting the feedback between snow and temperature. {4.2}

Decreases in snowpack have been documented in several regions worldwide based upon annual time series of mountain snow water equivalent and snow depth. Mountain snow can be sensitive to small changes in temperature, particularly in temperate climatic zones where the transition from rain to snow is generally closely associated with the altitude of the freezing level. Declines in mountain snowpack in western North America and in the Swiss Alps are largest at lower, warmer elevations. Mountain snow water equivalent has declined since 1950 at 75% of the stations monitored in western North America. Mountain snow depth has also declined in the Alps and in southeastern Australia. Direct observations of snow depth are too limited to determine changes in the Andes, but temperature measurements suggest that the altitude where snow occurs (above the snow line) has probably risen in mountainous regions of South America. {4.2}

Permafrost and seasonally frozen ground in most regions display large changes in recent decades. Changes in permafrost conditions can affect river runoff, water supply, carbon exchange and landscape stability, and can cause damage to infrastructure. Temperature increases at the top of the permafrost layer of up to 3°C since the 1980s have been reported. Permafrost warming has also been observed with variable magnitude in the Canadian Arctic, Siberia, the Tibetan Plateau and Europe. The permafrost base is thawing at a rate ranging from 0.04 m yr^{-1} in Alaska to 0.02 m yr^{-1} on the Tibetan Plateau. {4.7}

The maximum area covered by seasonally frozen ground decreased by about 7% in the NH over the

---

[6] Precipitation and temperature are combined in the Palmer Drought Severity Index (PDSI), considered in this report as one measure of drought. The PDSI does not include variables such as wind speed, solar radiation, cloudiness and water vapour but is a superior measure to precipitation alone.

Box TS.3: Ice Sheet Dynamics and Stability

Ice sheets are thick, broad masses of ice formed mainly from compaction of snow. They spread under their own weight, transferring mass towards their margins where it is lost primarily by runoff of surface melt water or by calving of icebergs into marginal seas or lakes. Ice sheets flow by deformation within the ice or melt water-lubricated sliding over materials beneath. Rapid basal motion requires that the basal temperature be raised to the melting point by heat from the Earth's interior, delivered by melt water transport, or from the 'friction' of ice motion. Sliding velocities under a given gravitational stress can differ by several orders of magnitude, depending on the presence or absence of deformable sediment, the roughness of the substrate and the supply and distribution of water. Basal conditions are generally poorly characterised, introducing important uncertainties to the understanding of ice sheet stability. {4.6}

Ice flow is often channelled into fast-moving ice streams (that flow between slower-moving ice walls) or outlet glaciers (with rock walls). Enhanced flow in ice streams arises either from higher gravitational stress linked to thicker ice in bedrock troughs, or from increased basal lubrication. {4.6}

Ice discharged across the coast often remains attached to the ice sheet to become a floating ice shelf. An ice shelf moves forward, spreading and thinning under its own weight, and fed by snowfall on its surface and ice input from the ice sheet. Friction at ice shelf sides and over local shoals slows the flow of the ice shelf and thus the discharge from the ice sheet. An ice shelf loses mass by calving icebergs from the front and by basal melting into the ocean cavity beneath. Studies suggest an ocean warming of 1°C could increase ice shelf basal melt by 10 m yr^{-1}, but inadequate knowledge of the largely inaccessible ice shelf cavities restricts the accuracy of such estimates. {4.6}

The palaeo-record of previous ice ages indicates that ice sheets shrink in response to warming and grow in response to cooling, and that shrinkage can be far faster than growth. The volumes of the Greenland and Antarctic Ice Sheets are equivalent to approximately 7 m and 57 m of sea level rise, respectively. Palaeoclimatic data indicate that substantial melting of one or both ice sheets has likely occurred in the past. However, ice core data show that neither ice sheet was completely removed during warm periods of at least the past million years. Ice sheets can respond to environmental forcing over very long time scales, implying that commitments to future changes may result from current warming. For example, a surface warming may take more than 10,000 years to penetrate to the bed and change temperatures there. Ice velocity over most of an ice sheet changes slowly in response to changes in the ice sheet shape or surface temperature, but large velocity changes may occur rapidly in ice streams and outlet glaciers in response to changing basal conditions, penetration of surface melt water to the bed or changes in the ice shelves into which they flow. {4.6, 6.4}

Models currently configured for long integrations remain most reliable in their treatment of surface accumulation and ablation, as for the TAR, but do not include full treatments of ice dynamics; thus, analyses of past changes or future projections using such models may underestimate ice flow contributions to sea level rise, but the magnitude of such an effect is unknown. {8.2}

latter half of the 20th century, with a decrease in spring of up to 15%. Its maximum depth has decreased by about 0.3 m in Eurasia since the mid-20th century. In addition, maximum seasonal thaw depth increased by about 0.2 m in the Russian Arctic from 1956 to 1990. {4.7}

On average, the general trend in NH river and lake ice over the past 150 years indicates that the freeze-up date has become later at an average rate of 5.8 ± 1.9 days per century, while the breakup date has occurred earlier, at a rate of 6.5 ± 1.4 days per century. However, considerable spatial variability has also been observed, with some regions showing trends of opposite sign. {4.3}

Annual average arctic sea ice extent has shrunk by about 2.7 ± 0.6% per decade since 1978 based upon satellite observations (see Figure TS.13). The decline in summer extent is larger than in winter extent, with the summer minimum declining at a rate of about 7.4 ± 2.4% per decade. Other data indicate that the summer decline began around 1970. Similar observations in the Antarctic reveal larger interannual variability but no consistent trends during the period of satellite observations. In contrast to changes in continental ice such as ice sheets and glaciers, changes in sea ice do not directly contribute to sea level change (because this ice is already floating), but can contribute to salinity changes through input of freshwater. {4.4}

During the 20th century, glaciers and ice caps have experienced widespread mass losses and have contributed to sea level rise. Mass loss of glaciers and ice caps (excluding those around the ice sheets of Greenland and Antarctica) is estimated to be 0.50 ± 0.18 mm yr^{-1} in sea level equivalent (SLE) between 1961 and 2003, and 0.77 ± 0.22 mm yr^{-1} SLE between 1991 and 2003. The late 20th-century glacier wastage *likely* has been a response to post-1970 warming. {4.5}

Recent observations show evidence for rapid changes in ice flow in some regions, contributing to sea level rise and suggesting that the dynamics of ice

motion may be a key factor in future responses of ice shelves, coastal glaciers and ice sheets to climate change. Thinning or loss of ice shelves in some near-coastal regions of Greenland, the Antarctic Peninsula and West Antarctica has been associated with accelerated flow of nearby glaciers and ice streams, suggesting that ice shelves (including short ice shelves of kilometres or tens of kilometres in length) could play a larger role

in stabilising or restraining ice motion than previously thought. Both oceanic and atmospheric temperatures appear to contribute to the observed changes. Large summer warming in the Antarctic Peninsula region *very likely* played a role in the subsequent rapid breakup of the Larsen B Ice Shelf in 2002 by increasing summer melt water, which drained into crevasses and wedged them open. Models do not accurately capture all of the physical processes that appear to be involved in observed iceberg calving (as in the breakup of Larsen B). {4.6}

Changes in Snow Cover

Changes in Sea Ice Extent
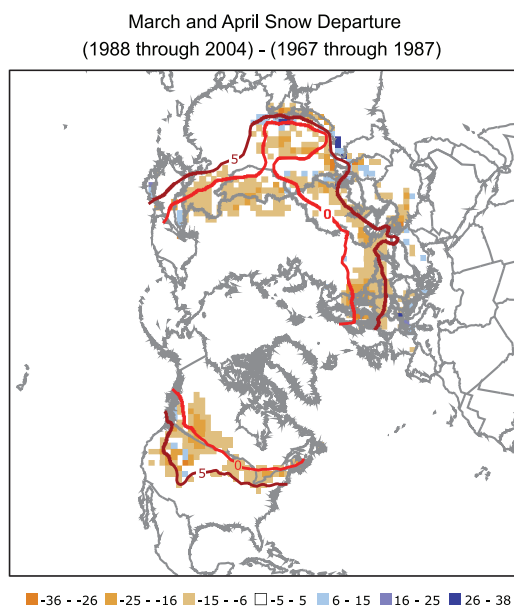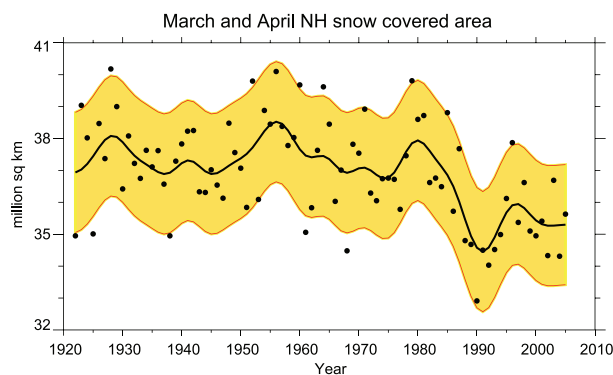
Figure TS.12. *(Top) Northern Hemisphere March-April snow-covered area from a station-derived snow cover index (prior to 1972) and from satellite data (during and after 1972). The smooth curve shows decadal variations (see Appendix 3.A) with the 5 to 95% data range shaded in yellow. (Bottom) Differences in the distribution of March-April snow cover between earlier (1967–1987) and later (1988–2004) portions of the satellite era (expressed in percent coverage). Tan colours show areas where snow cover has declined. Red curves show the 0°C and 5°C isotherms averaged for March-April 1967 to 2004, from the Climatic Research Unit (CRU) gridded land surface temperature version 2 (CRUTEM2v) data. The greatest decline generally tracks the 0°C and 5°C isotherms, reflecting the strong feedback between snow and temperature. {Figures 4.2, 4.3}*

Figure TS.13. *(a) Arctic minimum sea ice extent; (b) arctic sea ice extent anomalies; and (c) antarctic sea ice extent anomalies all for the period 1979 to 2005. Symbols indicate annual values while the smooth blue curves show decadal variations (see Appendix 3.A). The dashed lines indicate the linear trends. (a) Results show a linear trend of $-60 \pm 20 \times 10^3$ km^2 yr^{-1}, or approximately -7.4% per decade. (b) The linear trend is $-33 \pm 7.4 \times 10^3$ km^2 yr^{-1} (equivalent to approximately -2.7% per decade) and is significant at the 95% confidence level. (c) Antarctic results show a small positive trend of $5.6 \pm 9.2 \times 10^3$ km^2 yr^{-1}, which is not statistically significant. {Figures 4.8 and 4.9}*

45

The Greenland and Antarctic Ice Sheets taken together have *very likely* contributed to the sea level rise of the past decade. It is *very likely* that the Greenland Ice Sheet shrunk from 1993 to 2003, with thickening in central regions more than offset by increased melting in coastal regions. Whether the ice sheets have been growing or shrinking over time scales of longer than a decade is not well established from observations. Lack of agreement between techniques and the small number of estimates preclude assignment of best estimates or statistically rigorous error bounds for changes in ice sheet mass balances. However, acceleration of outlet glaciers drains ice from the interior and has been observed in both ice sheets (see Figure TS.14). Assessment of the data and techniques suggests a mass balance for the Greenland Ice Sheet of –50 to –100 Gt yr^{-1} (shrinkage contributing to raising global sea level by 0.14 to 0.28 mm yr^{-1}) during 1993 to 2003, with even larger losses in 2005. There are greater uncertainties for earlier time periods and for Antarctica. The estimated range in mass balance for the Greenland Ice Sheet over the period 1961 to 2003 is between growth of 25 Gt yr^{-1} and shrinkage by 60 Gt yr^{-1} (–0.07 to +0.17 mm yr^{-1} SLE). Assessment of all the data yields an estimate for the overall Antarctic Ice Sheet mass balance ranging from growth of 100 Gt yr^{-1} to shrinkage of 200 Gt yr^{-1} (–0.27 to +0.56 mm yr^{-1} SLE) from 1961 to 2003, and from +50 to –200 Gt yr^{-1} (–0.14 to +0.55 mm yr^{-1} SLE) from 1993 to 2003. The recent changes in ice flow are *likely* to be sufficient to explain much or all of the estimated antarctic mass imbalance, with recent changes in ice flow, snowfall and melt water runoff sufficient to explain the mass imbalance of Greenland. {4.6, 4.8}

RATES OF OBSERVED SURFACE ELEVATION CHANGE
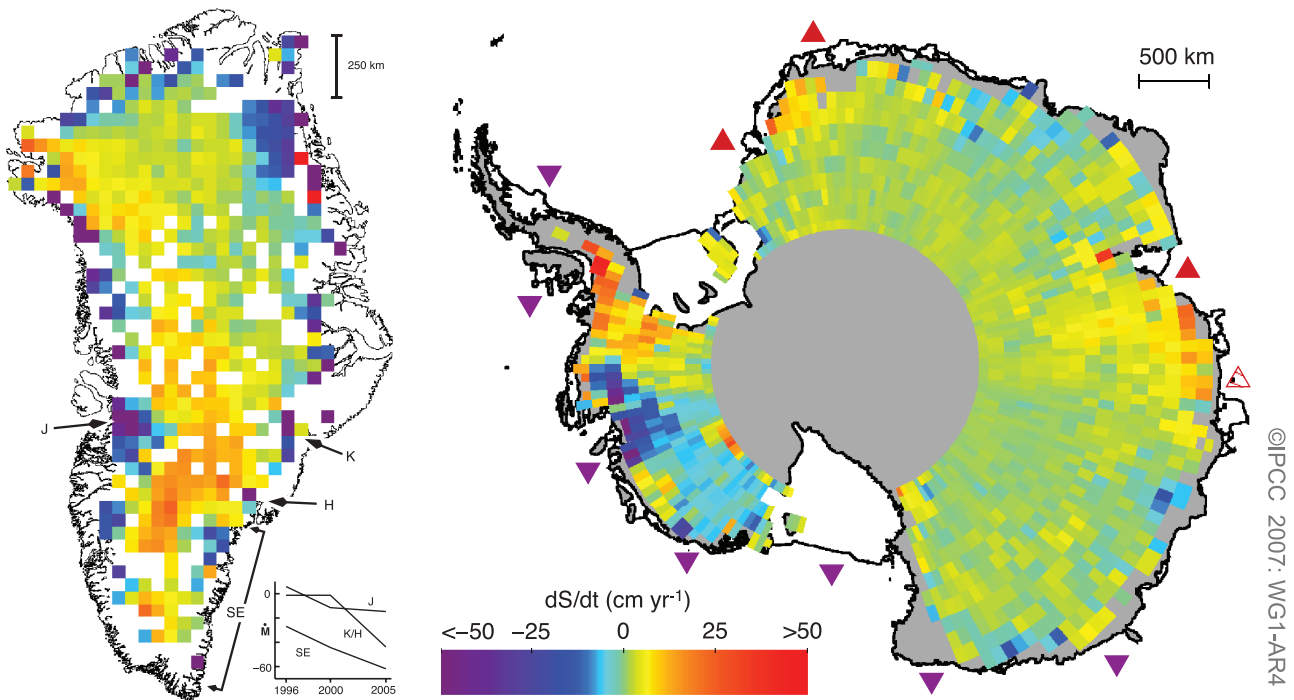
Figure TS.14. *Rates of observed recent surface elevation change for Greenland (left; 1989–2005) and Antarctica (right; 1992–2005). Red hues indicate a rising surface and blue hues a falling surface, which typically indicate an increase or loss in ice mass at a site, although changes over time in bedrock elevation and in near-surface density can be important. For Greenland, the rapidly thinning outlet glaciers Jakobshavn (J), Kangerdlugssuaq (K), Helheim (H) and areas along the southeast coast (SE) are shown, together with their estimated mass balance vs. time (with K and H combined, in Gt yr^{-1}, with negative values indicating loss of mass from the ice sheet to the ocean). For Antarctica, ice shelves estimated to be thickening or thinning by more than 30 cm yr^{-1} are shown by point-down purple triangles (thinning) and point-up red triangles (thickening) plotted just seaward of the relevant ice shelves. {Figures 4.17 and 4.19}*

TS.3.3 Changes in the Ocean: Instrumental Record

The ocean plays an important role in climate and climate change. The ocean is influenced by mass, energy and momentum exchanges with the atmosphere. Its heat capacity is about 1000 times larger than that of the atmosphere and the ocean's net heat uptake is therefore many times greater than that of the atmosphere (see Figure TS.15). Global observations of the heat taken up by the ocean can now be shown to be a definitive test of changes in the global energy budget. Changes in the amount of energy taken up by the upper layers of the ocean also play a crucial role for climate variations on seasonal to interannual time scales, such as El Niño. Changes in the transport of heat and SSTs have important effects upon many regional climates worldwide. Life in the sea is dependent on the biogeochemical status of the ocean and is affected by changes in its physical state and circulation. Changes in ocean biogeochemistry can also feed back into the climate system, for example, through changes in uptake or release of radiatively active gases such as CO_2. {5.1, 7.3}

ENERGY CONTENT IN THE CLIMATE SYSTEM
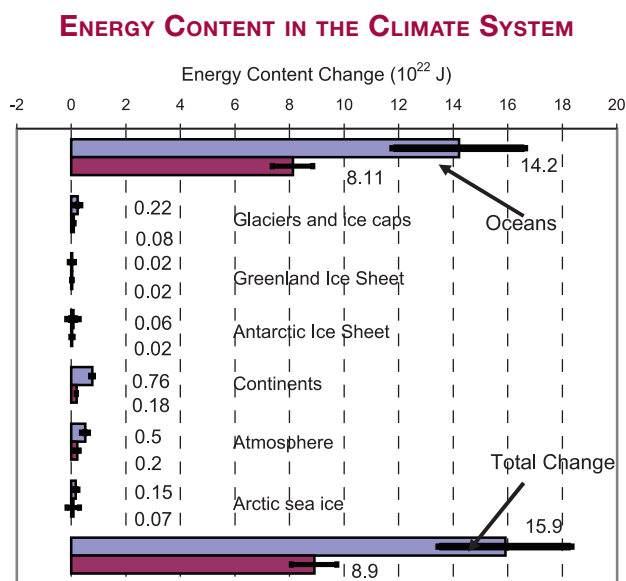
Figure TS.15. *Energy content changes in different components of the Earth system for two periods (1961–2003 and 1993–2003). Blue bars are for 1961 to 2003; burgundy bars are for 1993 to 2003. Positive energy content change means an increase in stored energy (i.e., heat content in oceans, latent heat from reduced ice or sea ice volumes, heat content in the continents excluding latent heat from permafrost changes, and latent and sensible heat and potential and kinetic energy in the atmosphere). All error estimates are 90% confidence intervals. No estimate of confidence is available for the continental heat gain. Some of the results have been scaled from published results for the two respective periods. {Figure 5.4}*

Global mean sea level variations are driven in part by changes in density, through thermal expansion or contraction of the ocean's volume. Local changes in sea level also have a density-related component due to temperature and salinity changes. In addition, exchange of water between oceans and other reservoirs (e.g., ice sheets, mountain glaciers, land water reservoirs and the atmosphere) can change the ocean's mass and hence contribute to changes in sea level. Sea level change is not geographically uniform because processes such as ocean circulation changes are not uniform across the globe (see Box TS.4). {5.5}

Oceanic variables can be useful for climate change detection, in particular temperature and salinity changes below the surface mixed layer where the variability is smaller and signal-to-noise ratio is higher. Observations analysed since the TAR have provided new evidence for changes in global ocean heat content and salinity, sea level, thermal expansion contributions to sea level rise, water mass evolution and biogeochemical cycles. {5.5}

TS.3.3.1 Changes in Ocean Heat Content and Circulation

The world ocean has warmed since 1955, accounting over this period for more than 80% of the changes in the energy content of the Earth's climate system. A total of 7.9 million vertical profiles of ocean temperature allows construction of improved global time series (see Figure TS.16). Analyses of the global oceanic heat budget have been replicated by several independent analysts and are robust to the method used. Data coverage limitations require averaging over decades for the deep ocean and observed decadal variability in the global heat content is not fully understood. However, inadequacies in the distribution of data (particularly coverage in the Southern Ocean and South Pacific) could contribute to the apparent decadal variations in heat content. During the period 1961 to 2003, the 0 to 3000 m ocean layer has taken up about 14.1×10^{22} J, equivalent to an average heating rate of 0.2 W m^{-2} (per unit area of the Earth's surface). During 1993 to 2003, the corresponding rate of warming in the shallower 0 to 700 m ocean layer was higher, about 0.5 ± 0.18 W m^{-2}. Relative to 1961 to 2003, the period 1993 to 2003 had high rates of warming but in 2004 and 2005 there has been some cooling compared to 2003. {5.1–5.3}

Warming is widespread over the upper 700 m of the global ocean. The Atlantic has warmed south of 45°N. The warming is penetrating deeper in the Atlantic Ocean Basin than in the Pacific, Indian and Southern Oceans, due to the

GLOBAL OCEAN HEAT CONTENT (0 - 700 M)
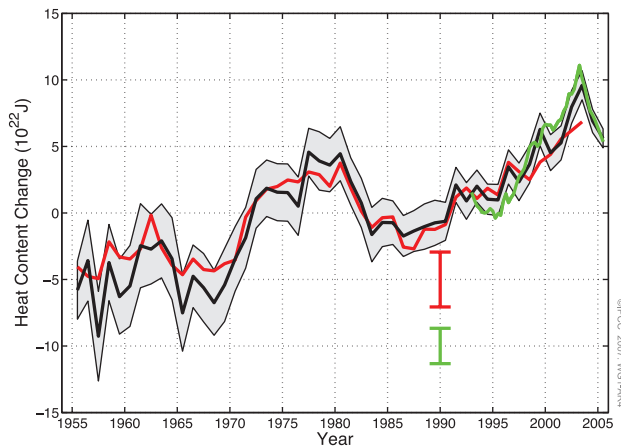
Figure TS.16. *Time series of global ocean heat content (10²² J) for the 0 to 700 m layer. The three coloured lines are independent analyses of the oceanographic data. The black and red curves denote the deviation from their 1961 to 1990 average and the shorter green curve denotes the deviation from the average of the black curve for the period 1993 to 2003. The 90% uncertainty range for the black curve is indicated by the grey shading and for the other two curves by the error bars. {Figure 5.1}*

deep overturning circulation cell that occurs in the North Atlantic. The SH deep overturning circulation shows little evidence of change based on available data. However, the upper layers of the Southern Ocean contribute strongly to the overall warming. At least two seas at subtropical latitudes (Mediterranean and Japan/East China Sea) are warming. While the global trend is one of warming, significant decadal variations have been observed in the global time series, and there are large regions where the oceans are cooling. Parts of the North Atlantic, North Pacific and equatorial Pacific have cooled over the last 50 years. The changes in the Pacific Ocean show ENSO-like spatial patterns linked in part to the PDO. {5.2, 5.3}

Parts of the Atlantic meridional overturning circulation exhibit considerable decadal variability, but data do not support a coherent trend in the overturning circulation. {5.3}

TS.3.3.2   *Changes in Ocean Biogeochemistry and Salinity*

The uptake of anthropogenic carbon since 1750 has led to the ocean becoming more acidic, with an average decrease in surface pH of 0.1 units.[7] Uptake of CO_2 by the ocean changes its chemical equilibrium. Dissolved CO_2 forms a weak acid, so as dissolved CO_2 increases, pH decreases (i.e., the ocean becomes more acidic). The overall pH change is computed from estimates of anthropogenic carbon uptake and simple ocean models. Direct observations of pH at available stations for the last 20 years also show trends of decreasing pH, at a rate of about 0.02 pH units per decade. Decreasing ocean pH decreases the depth below which calcium carbonate dissolves and increases the volume of the ocean that is undersaturated with respect to the minerals aragonite (a meta-stable form of calcium carbonate) and calcite, which are used by marine organisms to build their shells. Decreasing surface ocean pH and rising surface temperatures also act to reduce the ocean buffer capacity for CO_2 and the rate at which the ocean can take up excess atmospheric CO_2. {5.4, 7.3}

The oxygen concentration of the ventilated thermocline (about 100 to 1000 m) decreased in most ocean basins between 1970 and 1995. These changes may reflect a reduced rate of ventilation linked to upper-level warming and/or changes in biological activity. {5.4}

There is now widespread evidence for changes in ocean salinity at gyre and basin scales in the past half century (see Figure TS.17) with the near-surface waters in the more evaporative regions increasing in salinity in almost all ocean basins. These changes in salinity imply changes in the hydrological cycle over the oceans. In the high-latitude regions in both hemispheres, the surface waters show an overall freshening consistent with these regions having greater precipitation, although higher runoff, ice melting, advection and changes in the meridional overturning circulation may also contribute. The subtropical latitudes in both hemispheres are characterised by an increase in salinity in the upper 500 m. The patterns are consistent with a change in the Earth's hydrological cycle, in particular with changes in precipitation and inferred larger water transport in the atmosphere from low latitudes to high latitudes and from the Atlantic to the Pacific. {5.2}

TS.3.3.3   *Changes in Sea Level*

Over the 1961 to 2003 period, the average rate of global mean sea level rise is estimated from tide gauge data to be 1.8 ± 0.5 mm yr^{-1} (see Figure TS.18). For the purpose of examining the sea level budget, best estimates and 5 to 95% confidence intervals are provided for all land ice contributions. The average

---

[7] Acidity is a measure of the concentration of H⁺ ions and is reported in pH units, where pH = –log(H⁺). A pH decrease of 1 unit means a 10-fold increase in the concentration of H⁺, or acidity.

LINEAR TRENDS OF ZONALLY AVERAGED SALINITY (1955 - 1998)
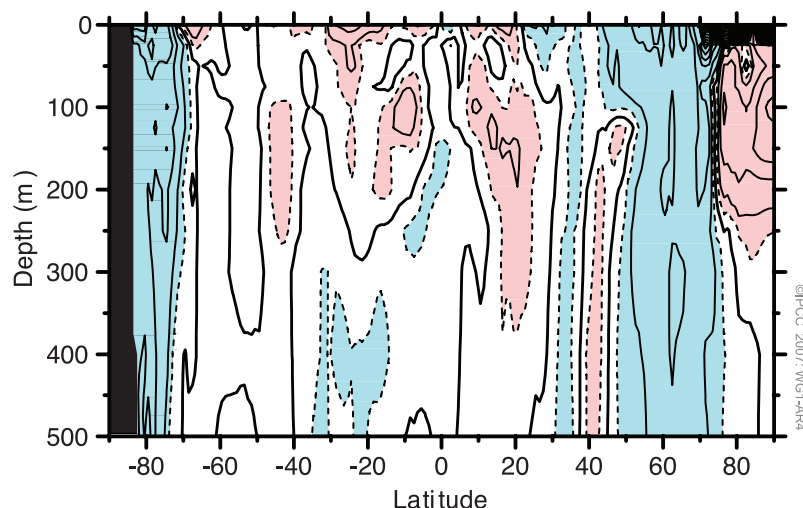
Figure TS.17. *Linear trends (1955–1998) of zonally averaged salinity (Practical Salinity Scale) for the World Ocean. The contour interval is 0.01 per decade and dashed contours are ±0.005 per decade. The dark, solid line is the zero contour. Red shading indicates values equal to or greater than 0.005 per decade and blue shading indicates values equal to or less than –0.005 per decade. {Figure 5.5}*

thermal expansion contribution to sea level rise for this period was 0.42 ± 0.12 mm yr^{-1}, with significant decadal variations, while the contribution from glaciers, ice caps and ice sheets is estimated to have been 0.7 ± 0.5 mm yr^{-1} (see Table TS.3). The sum of these estimated climate-related contributions for about the past four decades thus amounts to 1.1 ± 0.5 mm yr^{-1}, which is less than the best estimate from the tide gauge observations (similar to the discrepancy noted in the TAR). Therefore, the sea level budget for 1961 to 2003 has not been closed satisfactorily. {4.8, 5.5}

The global average rate of sea level rise measured by TOPEX/Poseidon satellite altimetry during 1993 to 2003 is 3.1 ± 0.7 mm yr^{-1}. This observed rate for the recent period is close to the estimated total of 2.8 ± 0.7 mm yr^{-1} for the climate-related contributions due to thermal expansion (1.6 ± 0.5 mm yr^{-1}) and changes in land ice (1.2 ± 0.4 mm yr^{-1}). Hence, the understanding of the budget has improved significantly for this recent period, with the climate contributions constituting the main factors in the sea level budget (which is closed to within known errors). Whether the faster rate for 1993 to 2003 compared to 1961 to 2003 reflects decadal variability or an increase in the longer-term trend is unclear. The

tide gauge record indicates that faster rates similar to that observed in 1993 to 2003 have occurred in other decades since 1950. {5.5, 9.5}

There is *high confidence* that the rate of sea level rise accelerated between the mid-19th and the mid-20th centuries based upon tide gauge and geological data. A recent reconstruction of sea level change back to 1870 using the best available tide records provides high confidence that the rate of sea level rise accelerated over the period 1870 to 2000. Geological observations indicate that during the previous 2000 years, sea level change was small, with average rates in the range 0.0 to 0.2 mm yr^{-1}. The use of proxy sea level data from archaeological sources is well established in the Mediterranean and indicates that oscillations in sea level from about AD 1 to AD 1900 did not exceed ±0.25 m. The available evidence indicates that the onset of modern sea level rise started between the mid-19th and mid-20th centuries. {5.5}

Precise satellite measurements since 1993 now provide unambiguous evidence of regional variability of sea level change. In some regions, rates of rise during this period are up to several times the global mean,

GLOBAL MEAN SEA LEVEL
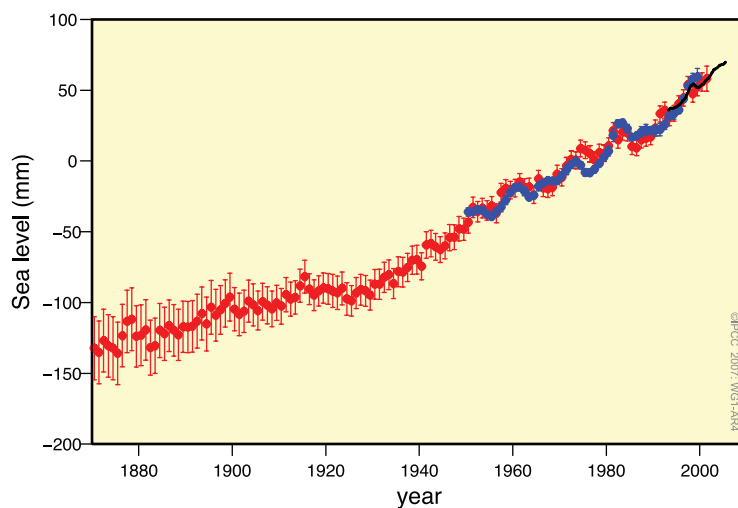
Figure TS.18. *Annual averages of the global mean sea level based on reconstructed sea level fields since 1870 (red), tide gauge measurements since 1950 (blue) and satellite altimetry since 1992 (black). Units are in mm relative to the average for 1961 to 1990. Error bars are 90% confidence intervals. {Figure 5.13}*

Table TS.3. *Contributions to sea level rise based upon observations (left columns) compared to models used in this assessment (right columns; see Section 9.5 and Appendix 10.A for details). Values are presented for 1993 to 2003 and for the last four decades, including observed totals. {Adapted from Tables 5.3 and 9.2}*

Sources of Sea Level Rise	Sea Level Rise (mm yr⁻¹)			
	1961–2003		1993–2003	
	Observed	Modelled	Observed	Modelled
Thermal expansion	0.42 ± 0.12	0.5 ± 0.2	1.6 ± 0.5	1.5 ± 0.7
Glaciers and ice caps	0.50 ± 0.18	0.5 ± 0.2	0.77 ± 0.22	0.7 ± 0.3
Greenland Ice Sheet	0.05 ± 0.12[a]		0.21 ± 0.07[a]	
Antarctic Ice Sheet	0.14 ± 0.41[a]		0.21 ± 0.35[a]	
Sum of individual climate contributions to sea level rise	1.1 ± 0.5	1.2 ± 0.5	2.8 ± 0.7	2.6 ± 0.8
Observed total sea level rise	1.8 ± 0.5 (tide gauges)		3.1 ± 0.7 (satellite altimeter)	
Difference (Observed total minus the sum of observed climate contributions)	0.7 ± 0.7		0.3 ± 1.0	

Notes:
[a] prescribed based upon observations (see Section 9.5)

while in other regions sea level is falling. The largest sea level rise since 1992 has taken place in the western Pacific and eastern Indian Oceans (see Figure TS.19). Nearly all of the Atlantic Ocean shows sea level rise during the past decade, while sea level in the eastern Pacific and western Indian Oceans has been falling. These temporal and spatial variations in regional sea level rise are influenced in part by patterns of coupled ocean-atmosphere variability, including ENSO and the NAO. The pattern of observed sea level change since 1992 is similar to the thermal expansion computed from ocean temperature changes, but different from the thermal expansion pattern of the last 50 years, indicating the importance of regional decadal variability. {5.5}

Observations suggest increases in extreme high water at a broad range of sites worldwide since 1975. Longer records are limited in space and under-sampled in time, so a global analysis over the entire 20th century is not feasible. In many locations, the secular changes in extremes were similar to those in mean sea level. At others, changes in atmospheric conditions such as storminess were more important in determining long-term trends. Interannual variability in high water extremes was positively correlated with regional mean sea level, as well as to indices of regional climate such as ENSO in the Pacific and NAO in the Atlantic. {5.5}

SEA LEVEL CHANGE PATTERNS
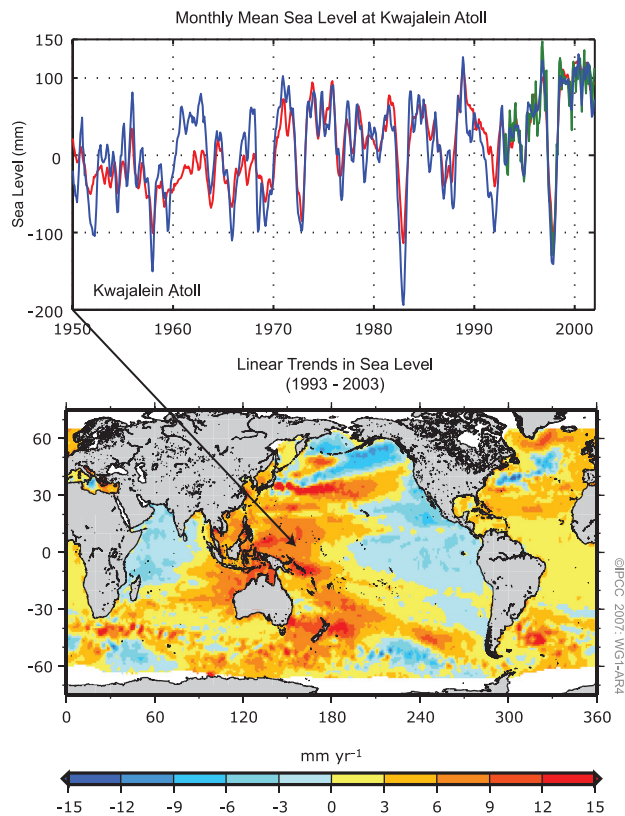
Figure TS.19. *(Top) Monthly mean sea level (mm) curve for 1950 to 2000 at Kwajalein (8°44'N, 167°44'E). The observed sea level (from tide gauge measurements) is in blue, the reconstructed sea level in red and the satellite altimetry record in green. Annual and semiannual signals have been removed from each time series and the tide gauge data have been smoothed. (Bottom) Geographic distribution of short-term linear trends in mean sea level for 1993 to 2003 (mm yr⁻¹) based on TOPEX/Poseidon satellite altimetry. {Figures 5.15 and 5.18}*

Box TS.4: Sea Level

The level of the sea at the shoreline is determined by many factors that operate over a great range of temporal scales: hours to days (tides and weather), years to millennia (climate), and longer. The land itself can rise and fall and such regional land movements need to be accounted for when using tide gauge measurements for evaluating the effect of oceanic climate change on coastal sea level. Coastal tide gauges indicate that global average sea level rose during the 20th century. Since the early 1990s, sea level has also been observed continuously by satellites with near-global coverage. Satellite and tide gauge data agree at a wide range of spatial scales and show that global average sea level has continued to rise during this period. Sea level changes show geographical variation because of several factors, including the distributions of changes in ocean temperature, salinity, winds and ocean circulation. Regional sea level is affected by climate variability on shorter time scales, for instance associated with El Niño and the NAO, leading to regional interannual variations which can be much greater or weaker than the global trend.

Based on ocean temperature observations, the thermal expansion of seawater as it warms has contributed substantially to sea level rise in recent decades. Climate models are consistent with the ocean observations and indicate that thermal expansion is expected to continue to contribute to sea level rise over the next 100 years. Since deep ocean temperatures change only slowly, thermal expansion would continue for many centuries even if atmospheric concentrations of greenhouse gases were stabilised.

Global average sea level also rises or falls when water is transferred from land to ocean or vice versa. Some human activities can contribute to sea level change, especially by the extraction of groundwater and construction of reservoirs. However, the major land store of freshwater is the water frozen in glaciers, ice caps and ice sheets. Sea level was more than 100 m lower during the glacial periods because of the ice sheets covering large parts of the NH continents. The present-day retreat of glaciers and ice caps is making a substantial contribution to sea level rise. This is expected to continue during the next 100 years. Their contribution should decrease in subsequent centuries as this store of freshwater diminishes.

The Greenland and Antarctic Ice Sheets contain much more ice and could make large contributions over many centuries. In recent years the Greenland Ice Sheet has experienced greater melting, which is projected to increase further. In a warmer climate, models suggest that the ice sheets could accumulate more snowfall, tending to lower sea level. However, in recent years any such tendency has probably been outweighed by accelerated ice flow and greater discharge observed in some marginal areas of the ice sheets. The processes of accelerated ice flow are not yet completely understood but could result in overall net sea level rise from ice sheets in the future.

The greatest climate- and weather-related impacts of sea level are due to extremes on time scales of days and hours, associated with tropical cyclones and mid-latitude storms. Low atmospheric pressure and high winds produce large local sea level excursions called 'storm surges', which are especially serious when they coincide with high tide. Changes in the frequency of occurrence of these extreme sea levels are affected both by changes in mean sea level and in the meteorological phenomena causing the extremes. {5.5}

TS.3.4   Consistency Among Observations

In this section, variability and trends within and across different climate variables including the atmosphere, cryosphere and oceans are examined for consistency based upon conceptual understanding of physical relationships between the variables. For example, increases in temperature will enhance the moisture-holding capacity of the atmosphere. Changes in temperature and/or precipitation should be consistent with those evident in glaciers. Consistency between independent observations using different techniques and variables provides a key test of understanding, and hence enhances confidence. {3.9}

Changes in the atmosphere, cryosphere and ocean show unequivocally that the world is warming. {3.2, 3.9, 4.2, 4.4–4.8, 5.2, 5.5}

Both land surface air temperatures and SSTs show warming. In both hemispheres, land regions have warmed at a faster rate than the oceans in the past few decades, consistent with the much greater thermal inertia of the oceans. {3.2}

The warming of the climate is consistent with observed increases in the number of daily warm extremes, reductions in the number of daily cold extremes and reductions in the number of frost days at mid-latitudes. {3.2, 3.8}

Surface air temperature trends since 1979 are now consistent with those at higher altitudes. It is *likely* that there is slightly greater warming in the troposphere than at the surface, and a higher tropopause, consistent with expectations from basic physical processes and observed increases in greenhouse gases together with depletion of stratospheric ozone. {3.4, 9.4}

Changes in temperature are broadly consistent with the observed nearly worldwide shrinkage of the cryosphere. There have been widespread reductions in mountain glacier mass and extent. Changes in climate consistent with warming are also indicated by decreases in snow cover, snow depth, arctic sea ice extent, permafrost thickness and temperature, the extent of seasonally frozen ground and the length of the freeze season of river and lake ice. {3.2, 3.9, 4.2–4.5, 4.7}

Observations of sea level rise since 1993 are consistent with observed changes in ocean heat content and the cryosphere. Sea level rose by 3.1 ± 0.7 mm yr^{-1} from 1993 to 2003, the period of availability of global altimetry measurements. During this time, a near balance was observed between observed total sea level rise and contributions from glacier, ice cap and ice sheet retreat together with increases in ocean heat content and associated ocean expansion. This balance gives increased

Table TS.4. *Recent trends, assessment of human influence on trends, and projections of extreme weather and climate events for which there is evidence of an observed late 20th-century trend. An asterisk in the column headed 'D' indicates that formal detection and attribution studies were used, along with expert judgement, to assess the likelihood of a discernible human influence. Where this is not available, assessments of likelihood of human influence are based on attribution results for changes in the mean of a variable or changes in physically related variables and/or on the qualitative similarity of observed and simulated changes, combined with expert judgement. {3.8, 5.5, 9.7, 11.2–11.9; Tables 3.7, 3.8, 9.4}*

Phenomenon[a] and direction of trend	Likelihood that trend occurred in late 20th century (typically post-1960)	Likelihood of a human contribution to observed trend	D	Likelihood of future trend based on projections for 21st century using SRES[b] scenarios
Warmer and fewer cold days and nights over most land areas	*Very likely*[c]	*Likely*[e]	*	*Virtually certain*[e]
Warmer and more frequent hot days and nights over most land areas	*Very likely*[d]	*Likely* (nights) [e]	*	*Virtually certain*[e]
Warm spells / heat waves: Frequency increases over most land areas	*Likely*	*More likely than not*		*Very likely*
Heavy precipitation events. Frequency (or proportion of total rainfall from heavy falls) increases over most areas	*Likely*	*More likely than not*		*Very likely*
Area affected by droughts increases	*Likely* in many regions since 1970s	*More likely than not*	*	*Likely*
Intense tropical cyclone activity increases	*Likely* in some regions since 1970	*More likely than not*		*Likely*
Increased incidence of extreme high sea level (excludes tsunamis)[f]	*Likely*	*More likely than not* [g]		*Likely* [h]

Notes:
[a] See Table 3.7 for further details regarding definitions.
[b] SRES refers to the IPCC Special Report on Emission Scenarios. The SRES scenario families and illustrative cases are summarised in a box at the end of the Summary for Policymakers.
[c] Decreased frequency of cold days and nights (coldest 10%)
[d] Increased frequency of hot days and nights (hottest 10%)
[e] Warming of the most extreme days/nights each year
[f] Extreme high sea level depends on average sea level and on regional weather systems. It is defined here as the highest 1% of hourly values of observed sea level at a station for a given reference period.
[g] Changes in observed extreme high sea level closely follow the changes in average sea level {5.5.2.6}. It is *very likely* that anthropogenic activity contributed to a rise in average sea level. {9.5.2}
[h] In all scenarios, the projected global average sea level at 2100 is higher than in the reference period {10.6}. The effect of changes in regional weather systems on sea level extremes has not been assessed.

confidence that the observed sea level rise is a strong indicator of warming. However, the sea level budget is not balanced for the longer period 1961 to 2003. {5.5, 3.9}

Observations are consistent with physical understanding regarding the expected linkage between water vapour and temperature, and with intensification of precipitation events in a warmer world. Column and upper-tropospheric water vapour have increased, providing important support for the hypothesis of simple physical models that specific humidity increases in a warming world and represents an important positive feedback to climate change. Consistent with rising amounts of water vapour in the atmosphere, there are widespread increases in the numbers of heavy precipitation events and increased likelihood of flooding events in many land regions, even those where there has been a reduction in total precipitation. Observations of changes in ocean salinity independently support the view

---

Box TS.5: Extreme Weather Events

People affected by an extreme weather event (e.g., the extremely hot summer in Europe in 2003, or the heavy rainfall in Mumbai, India in July 2005) often ask whether human influences on the climate are responsible for the event. A wide range of extreme weather events is expected in most regions even with an unchanging climate, so it is difficult to attribute any individual event to a change in the climate. In most regions, instrumental records of variability typically extend only over about 150 years, so there is limited information to characterise how extreme rare climatic events could be. Further, several factors usually need to combine to produce an extreme event, so linking a particular extreme event to a single, specific cause is problematic. In some cases, it may be possible to estimate the anthropogenic contribution to such changes in the probability of occurrence of extremes.

However, simple statistical reasoning indicates that substantial changes in the frequency of extreme events (and in the maximum feasible extreme, e.g., the maximum possible 24-hour rainfall at a specific location) can result from a relatively small shift of the distribution of a weather or climate variable.

Extremes are the infrequent events at the high and low end of the range of values of a particular variable. The probability of occurrence of values in this range is called a probability distribution function (PDF) that for some variables is shaped similarly to a 'Normal' or 'Gaussian' curve (the familiar 'bell' curve). Box TS.5, Figure 1 shows a schematic of a such a PDF and illustrates the effect a small shift (corresponding to a small change in the average or centre of the distribution) can have on the frequency of extremes at either end of the distribution. An increase in the frequency of one extreme (e.g., the number of hot days) will often be accompanied by a decline in the opposite extreme (in this case the number of cold days such as frosts). Changes in the variability or shape of the distribution can complicate this simple picture.

The IPCC Second Assessment Report noted that data and analyses of extremes related to climate change were sparse. By the time of the TAR, improved monitoring and data for changes in extremes was

Box TS.5, Figure 1. *Schematic showing the effect on extreme temperatures when the mean temperature increases, for a normal temperature distribution.*

available, and climate models were being analysed to provide projections of extremes. Since the TAR, the observational basis of analyses of extremes has increased substantially, so that some extremes have now been examined over most land areas (e.g., daily temperature and rainfall extremes). More models have been used in the simulation and projection of extremes, and multiple integrations of models with different starting conditions (ensembles) now provide more robust information about PDFs and extremes. Since the TAR, some climate change detection and attribution studies focussed on changes in the global statistics of extremes have become available (Table TS.4). For some extremes (e.g., tropical cyclone intensity), there are still data concerns and/or inadequate models. Some assessments still rely on simple reasoning about how extremes might be expected to change with global warming (e.g., warming could be expected to lead to more heat waves). Others rely on qualitative similarity between observed and simulated changes. The assessed likelihood of anthropogenic contributions to trends is lower for variables where the assessment is based on indirect evidence.

that the Earth's hydrologic cycle has changed, in a manner consistent with observations showing greater precipitation and river runoff outside the tropics and subtropics, and increased transfer of freshwater from the ocean to the atmosphere at lower latitudes. {3.3, 3.4, 3.9, 5.2}

Although precipitation has increased in many areas of the globe, the area under drought has also increased. Drought duration and intensity has also increased. While regional droughts have occurred in the past, the widespread spatial extent of current droughts is broadly consistent with expected changes in the hydrologic cycle under warming. Water vapour increases with increasing global temperature, due to increased evaporation where surface moisture is available, and this tends to increase precipitation. However, increased continental temperatures are expected to lead to greater evaporation and drying, which is particularly important in dry regions where surface moisture is limited. Changes in snowpack, snow cover and in atmospheric circulation patterns and storm tracks can also reduce available seasonal moisture, and contribute to droughts. Changes in SSTs and associated changes in the atmospheric circulation and precipitation have contributed to changes in drought, particularly at low latitudes. The result is that drought has become more common, especially in the tropics and subtropics, since the 1970s. In Australia and Europe, direct links to global warming have been inferred through the extremes in high temperatures and heat waves accompanying recent droughts. {3.3, 3.8, 9.5}

TS.3.5   A Palaeoclimatic Perspective

Palaeoclimatic studies make use of measurements of past change derived from borehole temperatures, ocean sediment pore-water change and glacier extent changes, as well as proxy measurements involving the changes in chemical, physical and biological parameters that reflect past changes in the environment where the proxy grew or existed. Palaeoclimatic studies rely on multiple proxies so that results can be cross-verified and uncertainties better understood. It is now well accepted and verified that many biological organisms (e.g., trees, corals, plankton, animals) alter their growth and/or population dynamics in response to changing climate, and that these climate-induced changes are well recorded in past growth in living and dead (fossil) specimens or assemblages of organisms. Networks of tree ring width and tree ring density chronologies are used to infer past temperature changes based on calibration with temporally overlapping instrumental data. While these methods are heavily used, there are concerns regarding the distributions of available measurements, how well these sample the globe, and such issues as the degree to which the methods have spatial and seasonal biases or apparent divergence in the relationship with recent climate change. {6.2}

It is *very likely* that average NH temperatures during the second half of the 20th century were warmer than any other 50-year period in the last 500 years and *likely* the warmest in at least the past 1300 years. The data supporting these conclusions are most extensive over summer extratropical land areas (particularly for the longer time period; see Figure TS.20). These conclusions are based upon proxy data such as the width and density of a tree ring, the isotopic composition of various elements in ice or the chemical composition of a growth band in corals, requiring analysis to derive temperature information and associated uncertainties. Among the key uncertainties are that temperature and precipitation are difficult to separate in some cases, or are representative of particular seasons rather than full years. There are now improved and expanded data since the TAR, including, for example, measurements at a larger number of sites, improved analysis of borehole temperature data and more extensive analyses of glaciers, corals and sediments. However, palaeoclimatic data are more limited than the instrumental record since 1850 in both space and time, so that statistical methods are employed to construct global averages, and these are subject to uncertainties as well. Current data are too limited to allow a similar evaluation of the SH temperatures prior to the period of instrumental data. {6.6, 6.7}

Some post-TAR studies indicate greater multi-centennial NH variability than was shown in the TAR, due to the particular proxies used and the specific statistical methods of processing and/or scaling them to represent past temperatures. The additional variability implies cooler conditions, predominantly during the 12th to 14th, the 17th and the 19th centuries; these are *likely* linked to natural forcings due to volcanic eruptions and/or solar activity. For example, reconstructions suggest decreased solar activity and increased volcanic activity in the 17th century as compared to current conditions. One reconstruction suggests slightly warmer conditions in the 11th century than those indicated in the TAR, but within the uncertainties quoted in the TAR. {6.6}

The ice core CO_2 record over the past millennium provides an additional constraint on natural climate variability. The amplitudes of the pre-industrial, decadal-scale NH temperature changes from the proxy-based reconstructions (<1°C) are broadly consistent with the ice core CO_2 record and understanding of the strength

NORTHERN HEMISPHERE TEMPERATURE RECONSTRUCTIONS
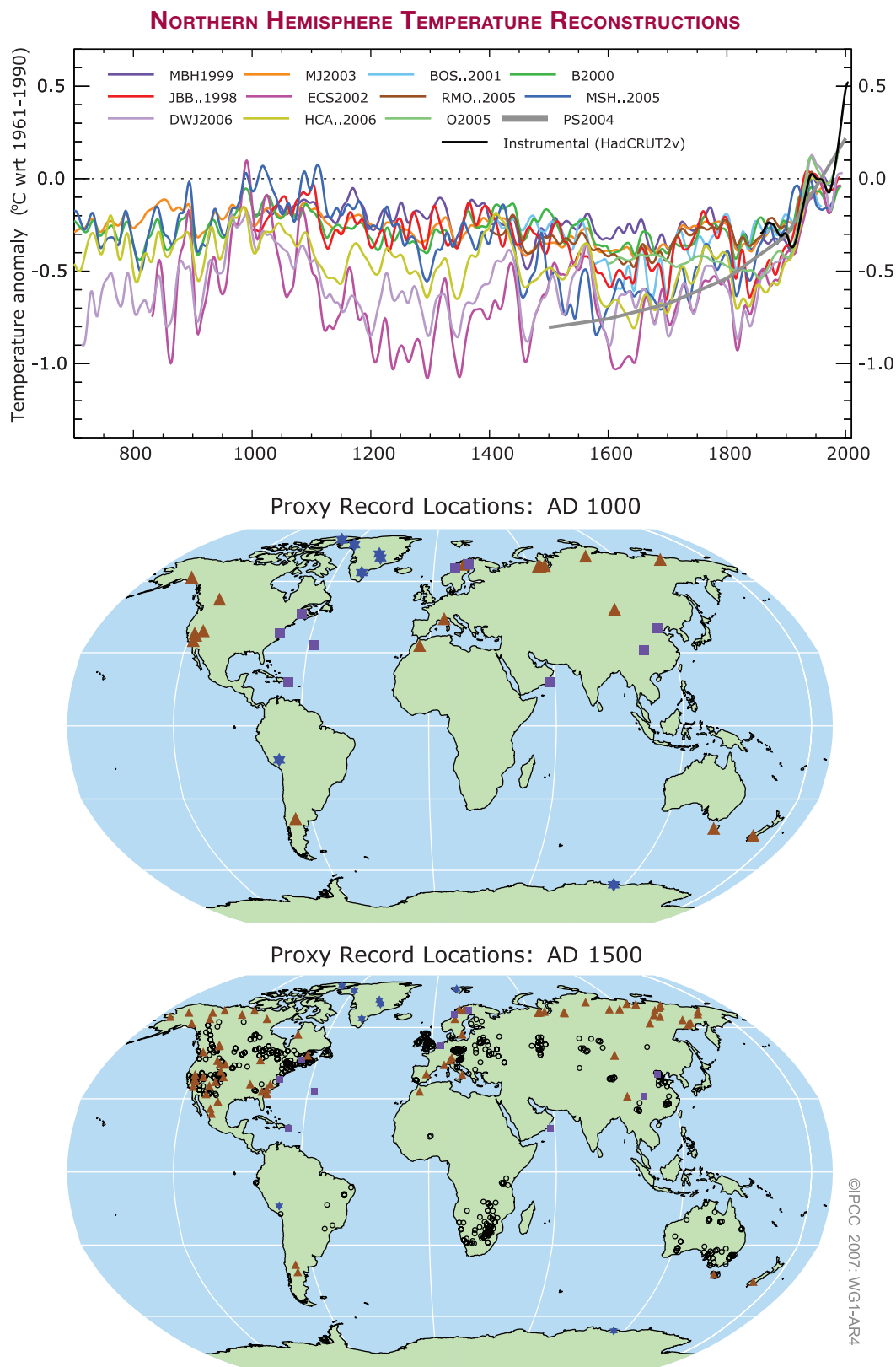
Figure TS.20. *(Top) Records of Northern Hemisphere temperature variation during the last 1300 years with 12 reconstructions using multiple climate proxy records shown in colour and instrumental records shown in black. (Middle and Bottom) Locations of temperature-sensitive proxy records with data back to AD 1000 and AD 1500 (tree rings: brown triangles; boreholes: black circles; ice core/ice boreholes: blue stars; other records including low-resolution records: purple squares). Data sources are given in Table 6.1, Figure 6.10 and are discussed in Chapter 6. {Figures 6.10 and 6.11}*

Box TS.6: Orbital Forcing

It is well known from astronomical calculations that periodic changes in characteristics of the Earth's orbit around the Sun control the seasonal and latitudinal distribution of incoming solar radiation at the top of the atmosphere (hereafter called 'insolation'). Past and future changes in insolation can be calculated over several millions of years with a high degree of confidence. {6.4}

Precession refers to changes in the time of the year when the Earth is closest to the Sun, with quasi-periodicities of about 19,000 and 23,000 years. As a result, changes in the position and duration of the seasons on the orbit strongly modulate the latitudinal and seasonal distribution of insolation. Seasonal changes in insolation are much larger than annual mean changes and can reach 60 W m^{-2} (Box TS.6, Figure 1).

The obliquity (tilt) of the Earth's axis varies between about 22° and 24.5° with two neighbouring quasi-periodicities of around 41,000 years. Changes in obliquity modulate seasonal contrasts as well as annual mean insolation changes with opposite effects at low vs. high latitudes (and therefore no effect on global average insolation) {6.4}.

The eccentricity of the Earth's orbit around the Sun has longer quasi-periodicities at 400,000 years and around 100,000 years. Changes in eccentricity alone have limited impacts on insolation, due to the resulting very small changes in the distance between the Sun and the Earth. However, changes in eccentricity interact with seasonal effects induced by obliquity and precession of the equinoxes. During periods of low eccentricity, such as about 400,000 years ago and during the next 100,000 years, seasonal insolation changes induced by precession are not as large as during periods of larger eccentricity (Box TS.6, Figure 1). {6.4}

Box TS.6, Figure 1. *Schematic of the Earth's orbital changes (Milankovitch cycles) that drive the ice age cycles. 'T' denotes changes in the tilt (or obliquity) of the Earth's axis, 'E' denotes changes in the eccentricity of the orbit and 'P' denotes precession, that is, changes in the direction of the axis tilt at a given point of the orbit. {FAQ 6.1, Figure 1}*

The Milankovitch, or 'orbital' theory of the ice ages is now well developed. Ice ages are generally triggered by minima in high-latitude NH summer insolation, enabling winter snowfall to persist through the year and therefore accumulate to build NH glacial ice sheets. Similarly, times with especially intense high-latitude NH summer insolation, determined by orbital changes, are thought to trigger rapid deglaciations, associated climate change and sea level rise. These orbital forcings determine the pacing of climatic changes, while the large responses appear to be determined by strong feedback processes that amplify the orbital forcing. Over multi-millennial time scales, orbital forcing also exerts a major influence on key climate systems such as the Earth's major monsoons, global ocean circulation and the greenhouse gas content of the atmosphere. {6.4}

Available evidence indicates that the current warming will not be mitigated by a natural cooling trend towards glacial conditions. Understanding of the Earth's response to orbital forcing indicates that the Earth would not naturally enter another ice age for at least 30,000 years. {6.4, FAQ 6.1}

of the carbon cycle-climate feedback. Atmospheric CO_2 and temperature in Antarctica co-varied over the past 650,000 years. Available data suggest that CO_2 acts as an amplifying feedback. {6.4, 6.6}

Changes in glaciers are evident in Holocene data, but these changes were caused by different processes than the late 20th-century retreat. Glaciers of several mountain regions in the NH retreated in response to orbitally forced regional warmth between 11,000 and 5000 years ago, and were smaller than at the end of the 20th century (or even absent) at times prior to 5000 years ago. The current near-global retreat of mountain glaciers cannot be due to the same causes, because decreased summer insolation during the past few thousand years in the NH should be favourable to the growth of glaciers. {6.5}

Palaeoclimatic data provide evidence for changes in many regional climates. The strength and frequency of ENSO events have varied in past climates. There is evidence that the strength of the Asian monsoon, and hence precipitation amount, can change abruptly. The palaeoclimatic records of northern and eastern Africa and of North America indicate that droughts lasting decades to centuries are a recurrent feature of climate in these regions, so that recent droughts in North America and northern Africa are not unprecedented. Individual decadal-resolution palaeoclimatic data sets support the existence of regional quasi-periodic climate variability, but it is *unlikely* that these regional signals were coherent at the global scale. {6.5, 6.6}

Strong evidence from ocean sediment data and from modelling links abrupt climate changes during the last glacial period and glacial-interglacial transition to changes in the Atlantic Ocean circulation. Current understanding suggests that the ocean circulation can become unstable and change rapidly when critical thresholds are crossed. These events have affected temperature by up to 16°C in Greenland and have influenced tropical rainfall patterns. They were probably associated with a redistribution of heat between the NH and SH rather than with large changes in global mean temperature. Such events have not been observed during the past 8000 years. {6.4}

THE ARCTIC AND THE LAST INTERGLACIAL
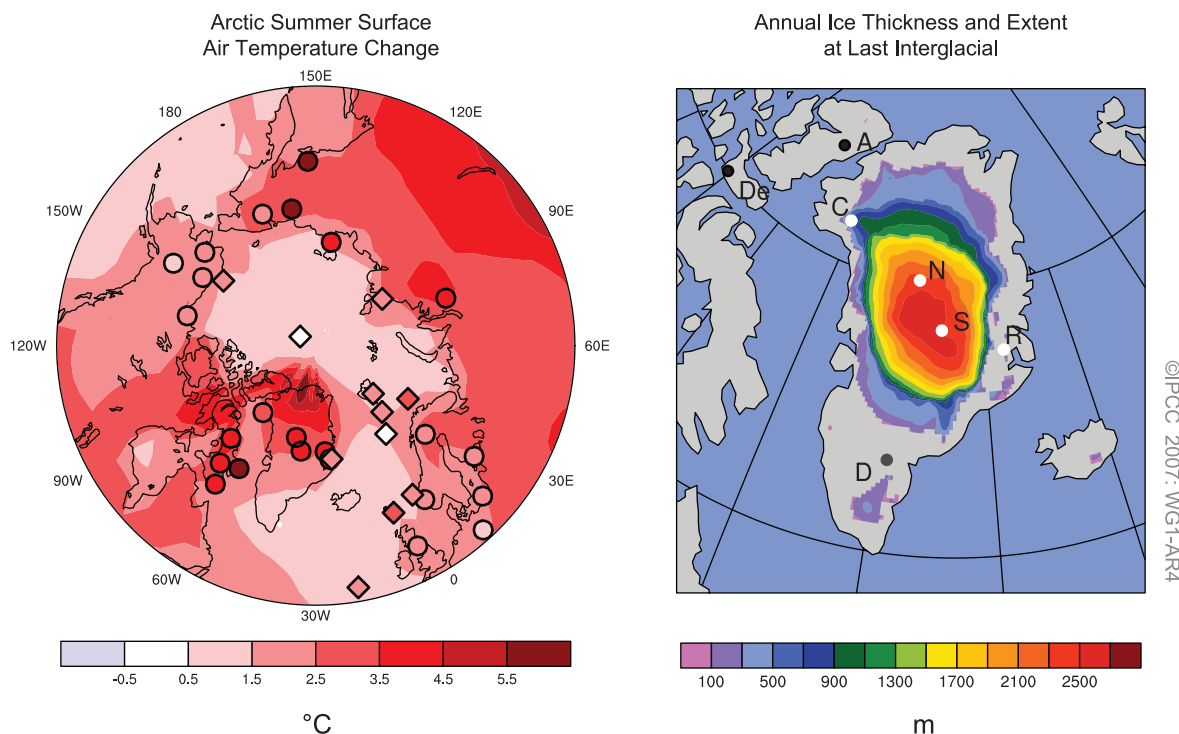
Figure TS.21. *Summer surface air temperature change relative to the present over the Arctic (left) and ice thickness and extent for Greenland and western arctic glaciers (right) for the last interglacial, approximately 125,000 years ago, from a multi-model and multi-proxy synthesis. (Left) A multi-model simulation of summer warming during the last interglacial is overlain by proxy estimates of maximum summer warming from terrestrial (circles) and marine (diamonds) sites. (Right) Extents and thicknesses of the Greenland Ice Sheet and western Canadian and Iceland glaciers at their minimum extent during the last interglacial, shown as a multi-model average from three ice models. Ice core observations indicate ice during the last interglacial at sites (white dots), Renland (R), North Greenland Ice Core Project (N), Summit (S, GRIP and GISP2) and possibly Camp Century (C), but no ice at sites (black dots): Devon (De) and Agassiz (A).Evidence for LIG ice at Dye-3 (D, grey dot) is equivocal. {Figure 6.6}*

Confidence in the understanding of past climate change and changes in orbital forcing is strengthened by the improved ability of current models to simulate past climate conditions. The Last Glacial Maximum (LGM; the last 'ice age' about 21,000 years ago) and the mid-Holocene (6000 years ago) were different from the current climate not because of random variability, but because of altered seasonal and global forcing linked to known differences in the Earth's orbit (see Box TS.6). Biogeochemical and biogeophysical feedbacks amplified the response to orbital forcings. Comparisons between simulated and reconstructed conditions in the LGM demonstrate that models capture the broad features of inferred changes in the temperature and precipitation patterns. For the mid-Holocene, coupled climate models are able to simulate mid-latitude warming and enhanced monsoons, with little change in global mean temperature (<0.4°C), consistent with our understanding of orbital forcing. {6.2, 6.4, 6.5, 9.3}

Global average sea level was likely between 4 and 6 m higher during the last interglacial period, about 125,000 years ago, than during the 20th century, mainly due to the retreat of polar ice (Figure TS.21). Ice core data suggest that the Greenland Summit region was ice-covered during this period, but reductions in the ice sheet extent are indicated in parts of southern Greenland. Ice core data also indicate that average polar temperatures at that time were 3°C to 5°C warmer than the 20th century because of differences in the Earth's orbit. The Greenland Ice Sheet and other arctic ice fields likely contributed no more than 4 m of the observed sea level rise, implying that there may also have been a contribution from Antarctica. {6.4}

TS.4 Understanding and Attributing Climate Change

Attribution evaluates whether observed changes are consistent with quantitative responses to different forcings obtained in well-tested models, and are not consistent with alternative physically plausible explanations. The first IPCC Assessment Report (FAR) contained little observational evidence of a detectable anthropogenic influence on climate. Six years later, the IPCC Second Assessment Report (SAR) concluded that the balance of evidence suggested a discernible human influence on the climate of the 20th century. The TAR concluded that 'most of the observed warming over the last 50 years is likely to have been due to the increase in greenhouse gas concentrations'. Confidence in the assessment of the human contributions to recent climate change has increased considerably since the TAR, in part because of stronger signals obtained from longer records, and an expanded and improved range of observations allowing attribution of warming to be more fully addressed jointly with other changes in the climate system. Some apparent inconsistencies in the observational record (e.g., in the vertical profile of temperature changes) have been largely resolved. There have been improvements in the simulation of many aspects of present mean climate and its variability on seasonal to inter-decadal time scales, although uncertainties remain (see Box TS.7). Models now employ more detailed representations of processes related to aerosol and other forcings. Simulations of 20th-century climate change have used many more models and much more complete anthropogenic and natural forcings than were available for the TAR. Available multi-model ensembles increase confidence in attribution results by providing an improved representation of model uncertainty. An anthropogenic signal has now more clearly emerged in formal attribution studies of aspects of the climate system beyond global-scale atmospheric temperature, including changes in global ocean heat content, continental-scale temperature trends, temperature extremes, circulation and arctic sea ice extent. {9.1}

TS.4.1 Advances in Attribution of Changes in Global-Scale Temperature in the Instrumental Period: Atmosphere, Ocean and Ice

Anthropogenic warming of the climate system is widespread and can be detected in temperature observations taken at the surface, in the free atmosphere and in the oceans. {3.2, 3.4, 9.4}

Evidence of the effect of external influences, both anthropogenic and natural, on the climate system has continued to accumulate since the TAR. Model and data improvements, ensemble simulations and improved representations of aerosol and greenhouse gas forcing along with other influences lead to greater confidence that most current models reproduce large-scale forced variability of the atmosphere on decadal and inter-decadal time scales quite well. These advances confirm that past climate variations at large spatial scales have been strongly influenced by external forcings. However, uncertainties still exist in the magnitude and temporal evolution of estimated contributions from individual forcings other than well-mixed greenhouse gases, due, for

Box TS.7: Evaluation of Atmosphere-Ocean General Circulation Models

Atmosphere-ocean general circulation models (AOGCMs) are the primary tool used for understanding and attribution of past climate variations, and for future projections. Since there are no historical perturbations to radiative forcing that are fully analogous to the human-induced perturbations expected over the 21st century, confidence in the models must be built from a number of indirect methods, described below. In each of these areas there have been substantial advances since the TAR, increasing overall confidence in models. {8.1}

Enhanced scrutiny and analysis of model behaviour has been facilitated by internationally coordinated efforts to collect and disseminate output from model experiments performed under common conditions. This has encouraged a more comprehensive and open evaluation of models, encompassing a diversity of perspectives. {8.1}

Projections for different scales and different periods using global climate models. Climate models project the climate for several decades or longer into the future. Since the details of individual weather systems are not being tracked and forecast, the initial atmospheric conditions are much less important than for weather forecast models. For climate projections, the forcings are of much greater importance. These forcings include the amount of solar energy reaching the Earth, the amount of particulate matter from volcanic eruptions in the atmosphere, and the concentrations of anthropogenic gases and particles in the atmosphere. As the area of interest moves from global to regional to local, or the time scale of interest shortens, the amplitude of variability linked to weather increases relative to the signal of long-term climate change. This makes detection of the climate change signal more difficult at smaller scales. Conditions in the oceans are important as well, especially for interannual and decadal time scales. {FAQ 1.2, 9.4, 11.1}

Model formulation. The formulation of AOGCMs has developed through improved spatial resolution and improvements to numerical schemes and parametrizations (e.g., sea ice, atmospheric boundary layer, ocean mixing). More processes have been included in many models, including a number of key processes important for forcing (e.g., aerosols are now modelled interactively in many models). Most models now maintain a stable climate without use of flux adjustments, although some long-term trends remain in AOGCM control integrations, for example, due to slow processes in the ocean. {8.2, 8.3}

Simulation of present climate. As a result of improvements in model formulation, there have been improvements in the simulation of many aspects of present mean climate. Simulations of precipitation, sea level pressure and surface temperature have each improved overall, but deficiencies remain, notably in tropical precipitation. While significant deficiencies remain in the simulation of clouds (and corresponding feedbacks affecting climate sensitivity), some models have demonstrated improvements in the simulation of certain cloud regimes (notably marine stratocumulus). Simulation of extreme events (especially extreme temperature) has improved, but models generally simulate too little precipitation in the most extreme events. Simulation of extratropical cyclones has improved. Some models used for projections of tropical cyclone changes can simulate successfully the observed frequency and distribution of tropical cyclones. Improved simulations have been achieved for ocean water mass structure, the meridional overturning circulation and ocean heat transport. However most models show some biases in their simulation of the Southern Ocean, leading to some uncertainty in modelled ocean heat uptake when climate changes. {8.3, 8.5, 8.6}

Simulation of modes of climate variability. Models simulate dominant modes of extratropical climate variability that resemble the observed ones (NAM/SAM, PNA, PDO) but they still have problems in representing aspects of them. Some models can now simulate important aspects of ENSO, while simulation of the Madden-Julian Oscillation remains generally unsatisfactory. {8.4}

Simulation of past climate variations. Advances have been made in the simulation of past climate variations. Independently of any attribution of those changes, the ability of climate models to provide a physically self-consistent explanation of observed climate variations on various time scales builds confidence that the models are capturing many key processes for the evolution of 21st-century climate. Recent advances include success in modelling observed changes in a wider range of climate variables over the 20th century (e.g., continental-scale surface temperatures and extremes, sea ice extent, ocean heat content trends and land precipitation). There has also been progress in the ability to model many of the general features of past, very different climate states such as the mid-Holocene and the LGM using identical or related models to those used for studying current climate. Information on factors treated as boundary conditions in palaeoclimate calculations include the different states of ice sheets in those periods. The broad predictions of earlier climate models, of increasing global temperatures in response to increasing greenhouse gases, have been borne out by subsequent observations. This strengthens confidence in near-term climate projections and understanding of related climate change commitments. {6.4, 6.5, 8.1, 9.3–9.5}   *(continued)*

Weather and seasonal prediction using climate models. A few climate models have been tested for (and shown) capability in initial value prediction, on time scales from weather forecasting (a few days) to seasonal climate variations, when initialised with appropriate observations. While the predictive capability of models in this mode of operation does not necessarily imply that they will show the correct response to changes in climate forcing agents such as greenhouse gases, it does increase confidence that they are adequately representing some key processes and teleconnections in the climate system. {8.4}

Measures of model projection accuracy. The possibility of developing model capability measures ('metrics'), based on the above evaluation methods, that can be used to narrow uncertainty by providing quantitative constraints on model climate projections, has been explored for the first time using model ensembles. While these methods show promise, a proven set of measures has yet to be established. {8.1, 9.6, 10.5}

example, to uncertainties in model responses to forcing. Some potentially important forcings such as black carbon aerosols have not yet been considered in most formal detection and attribution studies. Uncertainties remain in estimates of natural internal climate variability. For example, there are discrepancies between estimates of ocean heat content variability from models and observations, although poor sampling of parts of the world ocean may explain this discrepancy. In addition, internal variability is difficult to estimate from available observational records since these are influenced by external forcing, and because records are not long enough in the case of instrumental data, or precise enough in the case of proxy reconstructions, to provide complete descriptions of variability on decadal and longer time scales (see Figure TS.22 and Box TS.7). {8.2–8.4, 8.6, 9.2–9.4}

It is *extremely unlikely* (<5%) that the global pattern of warming observed during the past half century can be explained without external forcing. These changes took place over a time period when non-anthropogenic forcing factors (i.e., the sum of solar and volcanic forcing) would be *likely* to have produced cooling, not warming (see Figure TS.23). Attribution studies show that it is *very likely* that these natural forcing factors alone cannot account for the observed warming (see Figure TS.23). There is also increased confidence that natural internal variability cannot account for the observed changes, due in part to improved studies demonstrating that the warming occurred in both oceans and atmosphere, together with observed ice mass losses. {2.9, 3.2, 5.2, 9.4, 9.5, 9.7}

It is *very likely* that anthropogenic greenhouse gas increases caused most of the observed increase in global average temperatures since the mid-20th century. Without the cooling effect of atmospheric aerosols, it is *likely* that greenhouse gases alone would have caused a greater global mean temperature rise than that observed during the last 50 years. A key

factor in identifying the aerosol fingerprint, and therefore the amount of cooling counteracting greenhouse warming, is the temperature change through time (see Figure TS.23), as well as the hemispheric warming contrast. The conclusion that greenhouse gas forcing has been dominant takes into account observational and forcing uncertainties, and is robust to the use of different climate models, different methods for estimating the responses to external forcing and different analysis techniques. It also allows for possible amplification of the response to solar forcing. {2.9, 6.6, 9.1, 9.2, 9.4}

Widespread warming has been detected in ocean temperatures. Formal attribution studies now suggest that it is *likely* that anthropogenic forcing has contributed to the observed warming of the upper several hundred metres of the global ocean during the latter half of the 20th century. {5.2, 9.5}

Anthropogenic forcing has *likely* contributed to recent decreases in arctic sea ice extent. Changes in arctic sea ice are expected given the observed enhanced arctic warming. Attribution studies and improvements in the modelled representation of sea ice and ocean heat transport strengthen the confidence in this conclusion. {3.3, 4.4, 8.2, 8.3, 9.5}

It is *very likely* that the response to anthropogenic forcing contributed to sea level rise during the latter half of the 20th century, but decadal variability in sea level rise remains poorly understood. Modelled estimates of the contribution to sea level rise from thermal expansion are in good agreement with estimates based on observations during 1961 to 2003, although the budget for sea level rise over that interval is not closed. The observed increase in the rate of loss of mass from glaciers and ice caps is proportional to the global average temperature rise, as expected qualitatively from physical considerations (see Table TS.3). The greater rate of sea level rise in 1993 to 2003 than in 1961 to 2003 may be linked to increasing anthropogenic forcing, which has

GLOBAL AND CONTINENTAL TEMPERATURE CHANGE
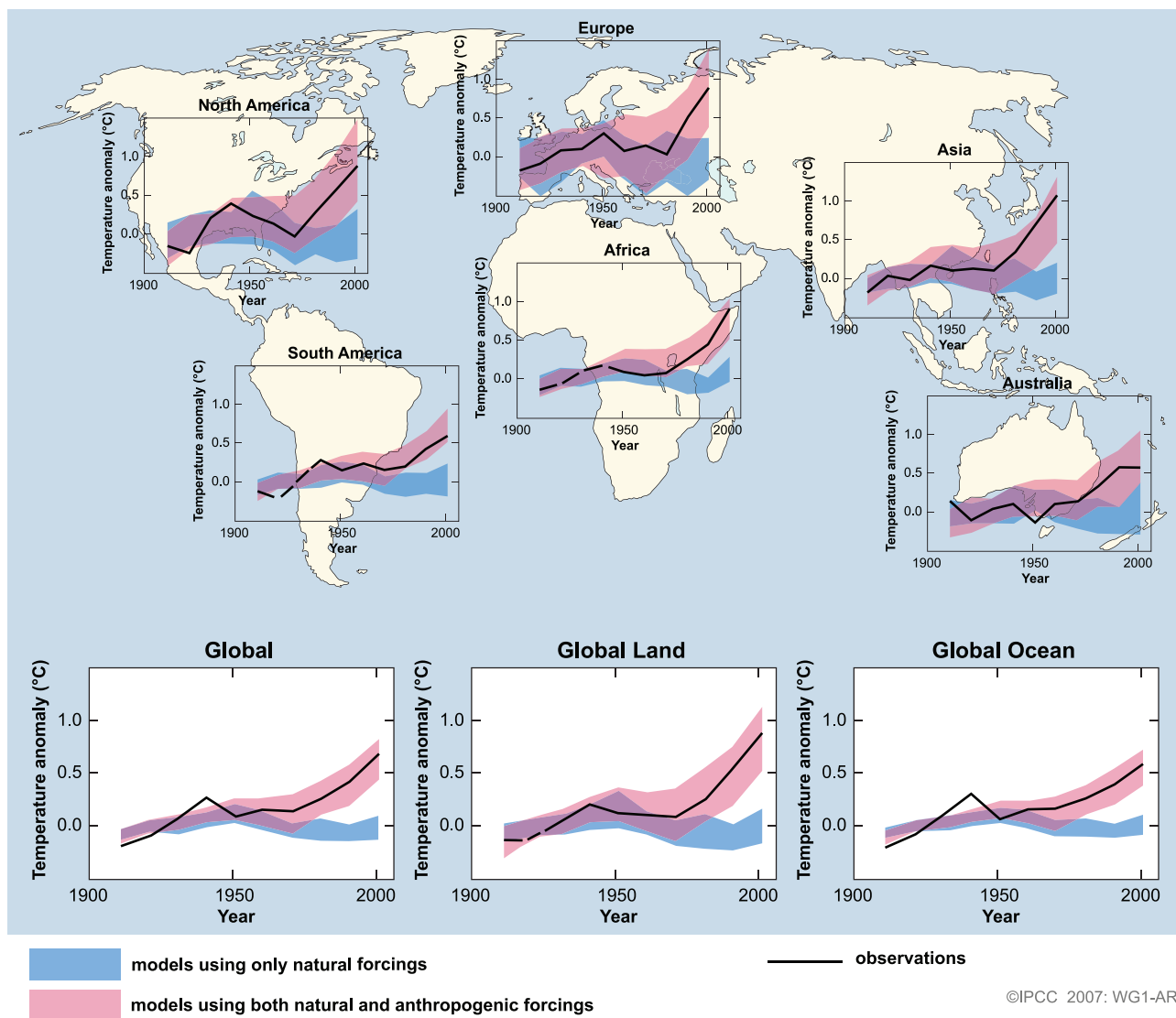
Figure TS.22. *Comparison of observed continental- and global-scale changes in surface temperature with results simulated by climate models using natural and anthropogenic forcings. Decadal averages of observations are shown for the period 1906 to 2005 (black line) plotted against the centre of the decade and relative to the corresponding average for 1901 to 1950. Lines are dashed where spatial coverage is less than 50%. Blue shaded bands show the 5% to 95% range for 19 simulations from 5 climate models using only the natural forcings due to solar activity and volcanoes. Red shaded bands show the 5% to 95% range for 58 simulations from 14 climate models using both natural and anthropogenic forcings. Data sources and models used are described in Section 9.4, FAQ 9.2, Table 8.1 and the supplementary information for Chapter 9. {FAQ 9.2, Figure 1}*

likely contributed to the observed warming of the upper ocean and widespread glacier retreat. On the other hand, the tide gauge record of global mean sea level suggests that similarly large rates may have occurred in previous 10-year periods since 1950, implying that natural internal variability could also be a factor in the high rates for 1993 to 2003 period. Observed decadal variability in the tide gauge record is larger than can be explained by variability in observationally based estimates of thermal expansion

and land ice changes. Further, the observed decadal variability in thermal expansion is larger than simulated by models for the 20th century. Thus, the physical causes of the variability seen in the tide gauge record are uncertain. These unresolved issues relating to sea level change and its decadal variability during 1961 to 2003 make it unclear how much of the higher rate of sea level rise in 1993 to 2003 is due to natural internal variability and how much to anthropogenic climate change. {5.5, 9.5}

TS.4.2   Attribution of Spatial and Temporal Changes in Temperature

The observed pattern of tropospheric warming and stratospheric cooling is *very likely* due to the influence of anthropogenic forcing, particularly that due to greenhouse gas increases and stratospheric ozone depletion. New analyses since the TAR show that this pattern corresponds to an increase in the height of the tropopause that is *likely* due largely to greenhouse gas and stratospheric ozone changes. Significant uncertainty remains in the estimation of tropospheric temperature trends, particularly from the radiosonde record. {3.2, 3.4, 9.4}

It is *likely* that there has been a substantial anthropogenic contribution to surface temperature increases averaged over every continent except Antarctica since the middle of the 20th century. Antarctica has insufficient observational coverage to make an assessment. Anthropogenic warming has also been identified in some sub-continental land areas. The ability of coupled climate models to simulate the temperature evolution on each of six continents provides stronger evidence of human influence on the global climate than was available in the TAR. No coupled global climate model that has used natural forcing only has reproduced the observed global mean warming trend, or the continental mean warming trends in individual

GLOBAL MEAN SURFACE TEMPERATURE ANOMALIES
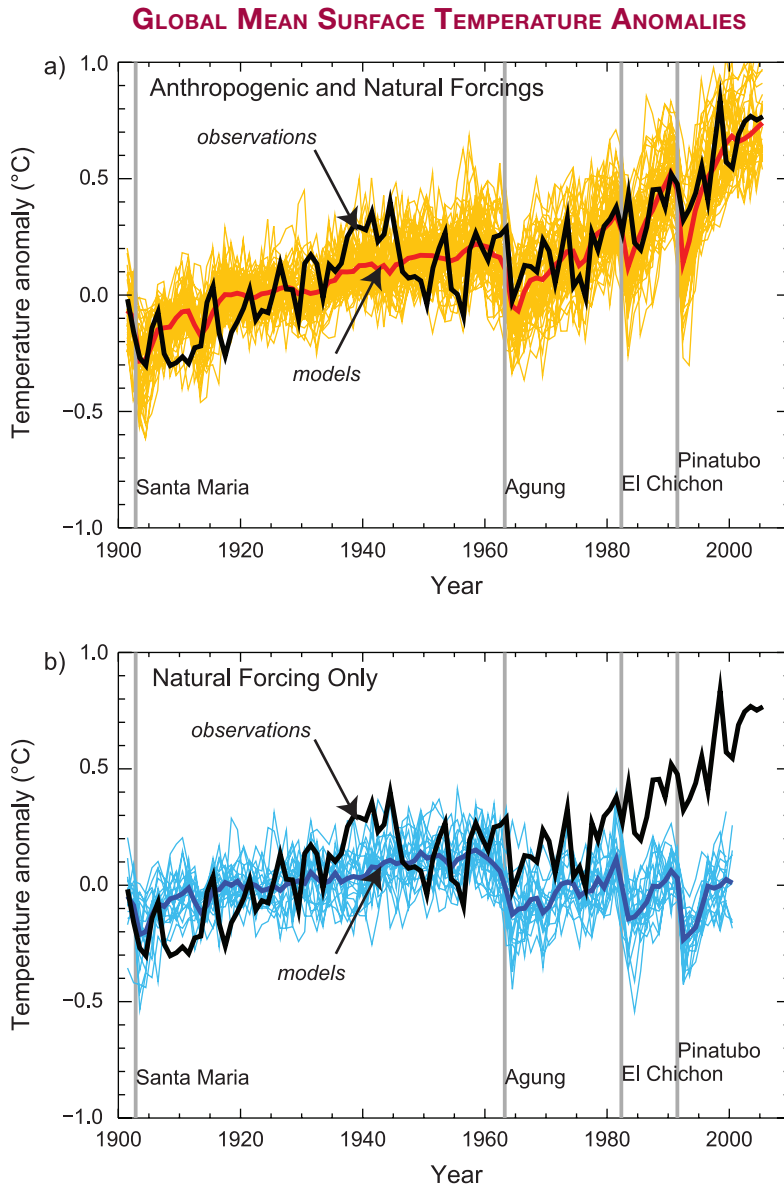
Figure TS.23. *(a) Global mean surface temperature anomalies relative to the period 1901 to 1950, as observed (black line) and as obtained from simulations with both anthropogenic and natural forcings. The thick red curve shows the multi-model ensemble mean and the thin yellow curves show the individual simulations. Vertical grey lines indicate the timing of major volcanic events. (b) As in (a), except that the simulated global mean temperature anomalies are for natural forcings only. The thick blue curve shows the multi-model ensemble mean and the thin lighter blue curves show individual simulations. Each simulation was sampled so that coverage corresponds to that of the observations. {Figure 9.5}*

©IPCC 2007: WG1-AR4

continents (except Antarctica) over the second half of the 20th century. {9.4}

Difficulties remain in attributing temperature changes at smaller than continental scales and over time scales of less than 50 years. Attribution results at these scales have, with limited exceptions, not been established. Averaging over smaller regions reduces the natural variability less than does averaging over large regions, making it more difficult to distinguish between changes expected from external forcing and variability. In addition, temperature changes associated with some modes of variability are poorly simulated by models in some regions and seasons. Furthermore, the small-scale

details of external forcing and the response simulated by models are less credible than large-scale features. {8.3, 9.4}

Surface temperature extremes have _likely_ been affected by anthropogenic forcing. Many indicators of extremes, including the annual numbers and most extreme values of warm and cold days and nights, as well as numbers of frost days, show changes that are consistent with warming. Anthropogenic influence has been detected in some of these indices, and there is evidence that anthropogenic forcing may have substantially increased the risk of extremely warm summer conditions regionally, such as the 2003 European heat wave. {9.4}
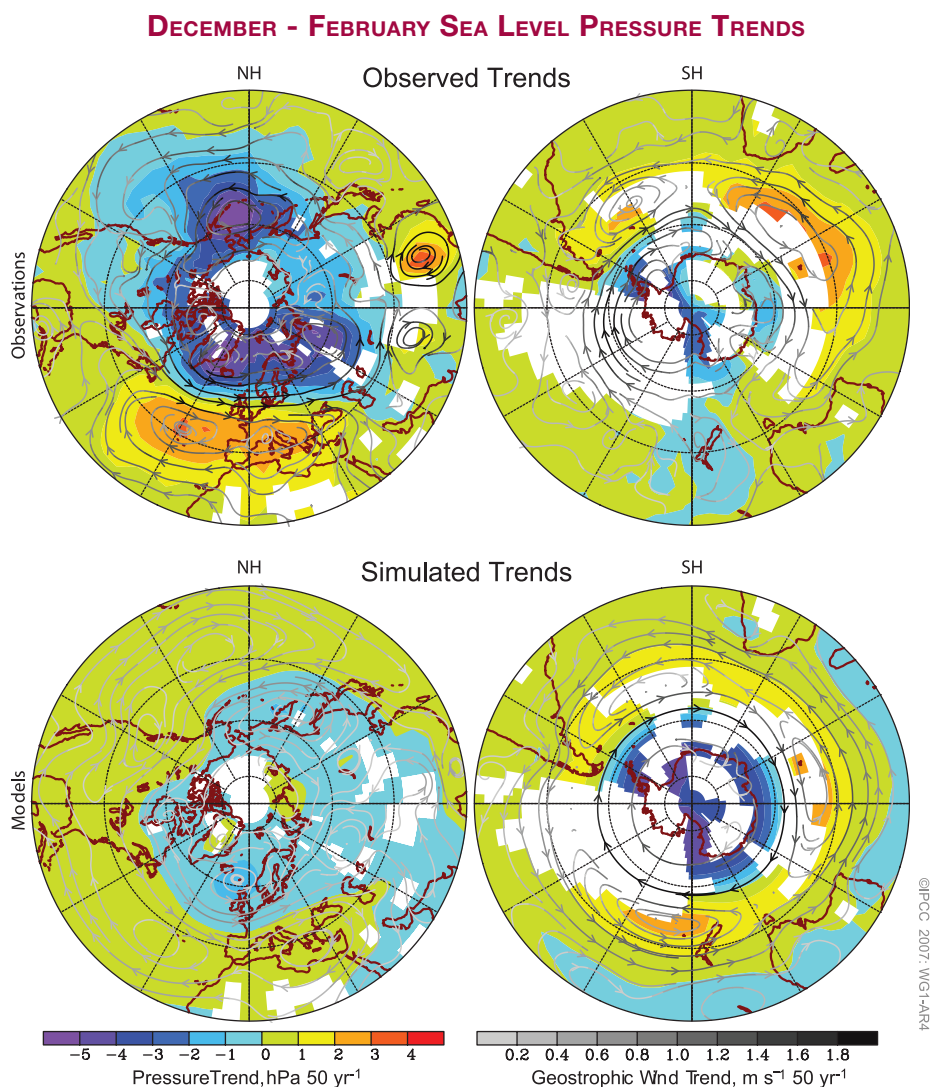
Figure TS.24. *December through February sea level pressure trends based on decadal means for the period 1955 to 2005. (Top) Trends estimated from an observational data set and displayed in regions where there is observational coverage. (Bottom) Mean trends simulated in response to natural and anthropogenic forcing changes in eight coupled models. The model-simulated trends are displayed only where observationally based trends are displayed. Streamlines, which are not masked, indicate the direction of the trends in the geostrophic wind derived from the trends in sea level pressure, and the shading of the streamlines indicates the magnitude of the change, with darker streamlines corresponding to larger changes in geostrophic wind. Data sources and models are described in Chapter 9 and its supplementary material, and Table 8.1 provides model details. {Figure 9.16}*

TS.4.3 Attribution of Changes in Circulation, Precipitation and Other Climate Variables

Trends in the Northern and Southern Annular Modes over recent decades, which correspond to sea level pressure reductions over the poles and related changes in atmospheric circulation, are *likely* related in part to human activity (see Figure TS.24). Models reproduce the sign of the NAM trend, but the simulated response is smaller than observed. Models including both greenhouse gas and stratospheric ozone changes simulate a realistic trend in the SAM, leading to a detectable human influence on global sea level pressure that is also consistent with the observed cooling trend in surface climate over parts of Antarctica. These changes in hemispheric circulation and their attribution to human activity imply that anthropogenic effects have *likely* contributed to changes in mid- and high-latitude patterns of circulation and temperature, as well as changes in winds and storm tracks. However, quantitative effects are uncertain because simulated responses to 20th century forcing change for the NH agree only qualitatively and not quantitatively with observations of these variables. {3.6, 9.5, 10.3}

There is some evidence of the impact of external influences on the hydrological cycle. The observed large-scale pattern of changes in land precipitation over the 20th century is qualitatively consistent with simulations, suggestive of a human influence. An observed global trend towards increases in drought in the second half of the 20th century has been reproduced with a model by taking anthropogenic and natural forcing into account. A number of studies have now demonstrated that changes in land use, due for example to overgrazing and conversion of woodland to agriculture, are *unlikely* to have been the primary cause of Sahelian and Australian droughts. Comparisons between observations and models suggest that changes in monsoons, storm intensities and Sahelian rainfall are related at least in part to changes in observed SSTs. Changes in global SSTs are expected to be affected by anthropogenic forcing, but an association of regional SST changes with forcing has not been established. Changes in rainfall depend not just upon SSTs but also upon changes in the spatial and temporal SST patterns and regional changes in atmospheric circulation, making attribution to human influences difficult. {3.3, 9.5, 10.3, 11.2}

TS.4.4 Palaeoclimate Studies of Attribution

It is *very likely* that climate changes of at least the seven centuries prior to 1950 were not due to unforced variability alone. Detection and attribution studies indicate that a substantial fraction of pre-industrial NH inter-decadal temperature variability contained in reconstructions for those centuries is *very likely* attributable to natural external forcing. Such forcing includes episodic cooling due to known volcanic eruptions, a number of which were larger than those of the 20th century (based on evidence such as ice cores), and long-term variations in solar irradiance, such as reduced radiation during the Maunder Minimum. Further, it is *likely* that anthropogenic forcing contributed to the early 20th-century warming evident in these records. Uncertainties are unlikely to lead to a spurious agreement between temperature reconstructions and forcing reconstructions as they are derived from independent proxies. Insufficient data are available to make a similar SH evaluation. {6.6, 9.3}

TS.4.5 Climate Response to Radiative Forcing

Specification of a *likely* range and a most *likely* value for equilibrium climate sensitivity[8] in this report represents significant progress in quantifying the climate system response to radiative forcing since the TAR and an advance in challenges to understanding that have persisted for over 30 years. A range for equilibrium climate sensitivity – the equilibrium global average warming expected if CO_2 concentrations were to be sustained at double their pre-industrial values (about 550 ppm) – was given in the TAR as between 1.5°C and 4.5°C. It has not been possible previously to provide a best estimate or to estimate the probability that climate sensitivity might fall outside that quoted range. Several approaches are used in this assessment to constrain climate sensitivity, including the use of AOGCMs, examination of the transient evolution of temperature (surface, upper air and ocean) over the last 150 years and examination of the rapid response of the global climate system to changes in the forcing caused by volcanic eruptions (see Figure TS.25). These are complemented by estimates based upon palaeoclimate studies such as reconstructions of the NH temperature record of the past millennium and the LGM. Large ensembles of climate model simulations have shown that the ability of models to simulate present climate has value in constraining climate sensitivity. {8.1, 8.6, 9.6, Box 10.2}

---

[8] See the Glossary for a detailed definition of climate sensitivity.

Analysis of models together with constraints from observations suggest that the equilibrium climate sensitivity is *likely* to be in the range 2°C to 4.5°C, with a best estimate value of about 3°C. It is *very unlikely* to be less than 1.5°C. Values substantially higher than 4.5°C cannot be excluded, but agreement with observations is not as good for those values. Probability density functions derived from different information and approaches generally tend to have a long tail towards high values exceeding 4.5°C. Analysis of climate and forcing evolution over previous centuries and model ensemble studies do not rule out climate sensitivity being as high as 6°C or more. One factor in this is the possibility of small net radiative forcing over the 20th century if aerosol indirect cooling effects were at the upper end of their uncertainty range, thus cancelling most of the positive forcing due to greenhouse gases. However, there is no well-established way of estimating a single probability distribution function from individual results taking account of the different assumptions in each study. The lack of strong constraints limiting high climate sensitivities prevents the specification of a 95th percentile bound or a very likely range for climate sensitivity. {Box 10.2}

There is now increased confidence in the understanding of key climate processes that are important to climate sensitivity due to improved analyses and comparisons of models to one another and to observations. Water vapour changes dominate the feedbacks affecting climate sensitivity and are now better understood. New observational and modelling evidence strongly favours a combined water vapour-lapse rate[9] feedback of around the strength found in General Circulation Models (GCMs), that is, approximately 1 W m^{-2} per degree global temperature increase, corresponding to about a 50% amplification of global mean warming. Such GCMs have demonstrated an ability to simulate seasonal to inter-decadal humidity variations in the upper troposphere over land and ocean, and have successfully simulated the observed surface temperature and humidity changes associated with volcanic eruptions. Cloud feedbacks (particularly from low clouds) remain the largest source of uncertainty. Cryospheric feedbacks such as changes in snow cover have been shown to contribute less to the spread in model estimates of climate sensitivity than cloud or water vapour feedbacks, but they

CUMULATIVE DISTRIBUTIONS OF CLIMATE SENSITIVITY
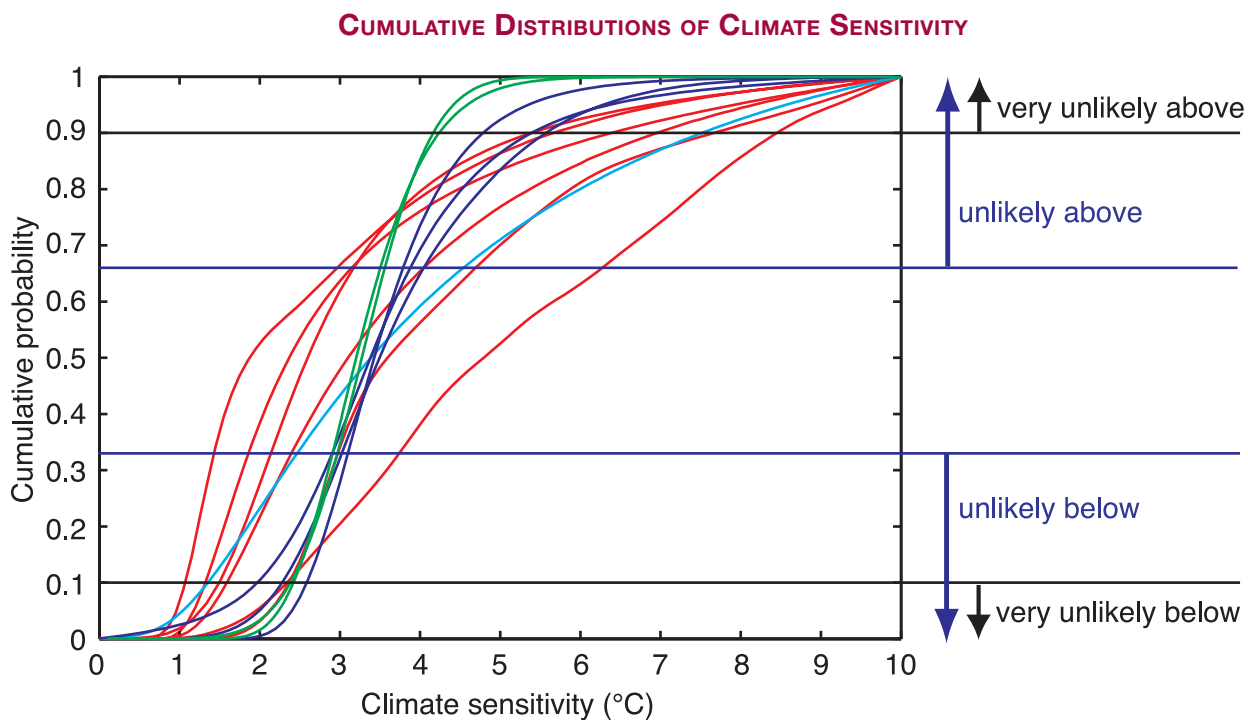
Figure TS.25. *Cumulative distributions of climate sensitivity derived from observed 20th-century warming (red), model climatology (blue), proxy evidence (cyan) and from climate sensitivities of AOGCMs (green). Horizontal lines and arrows mark the boundaries of the likelihood estimates defined in the IPCC Fourth Assessment Uncertainty Guidance Note (see Box TS.1). {Box 10.2, Figures 1 and 2}*

©IPCC 2007: WG1-AR4

---

[9] The rate at which air temperature decreases with altitude.

can be important for regional climate responses at mid- and high latitudes. A new model intercomparison suggests that differences in radiative transfer formulations also contribute to the range. {3.4, 8.6, 9.3, 9.4, 9.6, 10.2, Box 10.2}

Improved quantification of climate sensitivity allows estimation of best estimate equilibrium temperatures and ranges that could be expected if concentrations of CO_2 were to be stabilised at various levels based on global energy balance considerations (see Table TS.5). As in the estimate of climate sensitivity, a very likely upper bound cannot be established. Limitations to the concept of radiative forcing and climate sensitivity should be noted. Only a few AOGCMs have been run to equilibrium under elevated CO_2 concentrations, and some results show that climate feedbacks may change over long time scales, resulting in substantial deviations from estimates of warming based on equilibrium climate sensitivity inferred from mixed layer ocean models and past climate change. {10.7}

Agreement among models for projected transient climate change has also improved since the TAR. The range of transient climate responses (defined as the global average surface air temperature averaged over a 20-year period centred at the time of CO_2 doubling in a 1% yr^{-1} increase experiment) among models is smaller than the range in the equilibrium climate sensitivity. This parameter is now better constrained by multi-model ensembles and comparisons with observations; it is *very likely* to be greater than 1°C and *very unlikely* to be greater than 3°C. The transient climate response

Table TS.5. *Best estimate, likely ranges and very likely lower bounds of global mean equilibrium surface temperature increase (°C) over pre-industrial temperatures for different levels of CO_2-equivalent radiative forcing, as derived from the climate sensitivity.*

Equilibrium CO_2–eq (ppm)	Temperature Increase (°C)		
	Best Estimate	*Very Likely* Above	*Likely* in the Range
350	1.0	0.5	0.6–1.4
450	2.1	1.0	1.4–3.1
550	2.9	1.5	1.9–4.4
650	3.6	1.8	2.4–5.5
750	4.3	2.1	2.8–6.4
1000	5.5	2.8	3.7–8.3
1200	6.3	3.1	4.2–9.4

is related to sensitivity in a nonlinear way such that high sensitivities are not immediately manifested in the short-term response. Transient climate response is strongly affected by the rate of ocean heat uptake. Although the ocean models have improved, systematic model biases and limited ocean temperature data to evaluate transient ocean heat uptake affect the accuracy of current estimates. {8.3, 8.6, 9.4, 9.6, 10.5}

TS.5 Projections of Future Changes in Climate

Since the TAR, there have been many important advances in the science of climate change projections. An unprecedented effort has been initiated to make new model results available for prompt scrutiny by researchers outside of the modelling centres. A set of coordinated, standard experiments was performed by 14 AOGCM modelling groups from 10 countries using 23 models. The resulting multi-model database of outputs, analysed by hundreds of researchers worldwide, forms the basis for much of this assessment of model results. Many advances have come from the use of multi-member ensembles from single models (e.g., to test the sensitivity of response to initial conditions) and from multi-model ensembles. These two different types of ensembles allow more robust studies of the range of model results and more quantitative model evaluation against observations, and provide new information on simulated statistical variability. {8.1, 8.3, 9.4, 9.5, 10.1}

A number of methods for providing probabilistic climate change projections, both for global means and geographical depictions, have emerged since the TAR and are a focus of this report. These include methods based on results of AOGCM ensembles without formal application of observational constraints as well as methods based on detection algorithms and on large model ensembles that provide projections consistent with observations of climate change and their uncertainties. Some methods now explicitly account for key uncertainty sources such as climate feedbacks, ocean heat uptake, radiative forcing and the carbon cycle. Short-term projections are similarly constrained by observations of recent trends. Some studies have probed additional probabilistic issues, such as the likelihood of future changes in extremes such as heat waves that could occur due to human influences. Advances have also occurred since the TAR through broader ranges

of studies of committed climate change and of carbon-climate feedbacks. {8.6, 9.6, 10.1, 10.3, 10.5}

These advances in the science of climate change modelling provide a probabilistic basis for distinguishing projections of climate change for different SRES marker scenarios. This is in contrast to the TAR where ranges for different marker scenarios could not be given in probabilistic terms. As a result, this assessment identifies and quantifies the difference in character between uncertainties that arise in climate modelling and those that arise from a lack of prior knowledge of decisions that will affect greenhouse gas emissions. A loss of policy-relevant information would result from combining probabilistic projections. For these reasons, projections for different emission scenarios are not combined in this report.

Model simulations used here consider the response of the physical climate system to a range of possible future conditions through use of idealised emissions or concentration assumptions. These include experiments with greenhouse gases and aerosols held constant at year 2000 levels, CO_2 doubling and quadrupling experiments, SRES marker scenarios for the 2000 to 2100 period, and experiments with greenhouse gases and aerosols held constant after 2100, providing new information on the physical aspects of long-term climate change and stabilisation. The SRES scenarios did not include climate initiatives. This Working Group I assessment does not evaluate the plausibility or likelihood of any specific emission scenario. {10.1, 10.3}

A new multi-model data set using Earth System Models of Intermediate Complexity (EMICs) complements AOGCM experiments to extend the time horizon for several more centuries in the future. This provides a more comprehensive range of model responses in this assessment as well as new information on climate change over long time scales when greenhouse gas and aerosol concentrations are held constant. Some AOGCMs and EMICs contain prognostic carbon cycle components, which permit estimation of the likely effects and associated uncertainties of carbon cycle feedbacks. {10.1}

Box TS.8: Hierarchy of Global Climate Models

Estimates of change in global mean temperature and sea level rise due to thermal expansion can be made using Simple Climate Models (SCMs) that represent the ocean-atmosphere system as a set of global or hemispheric boxes, and predict global surface temperature using an energy balance equation, a prescribed value of climate sensitivity and a basic representation of ocean heat uptake. Such models can also be coupled to simplified models of biogeochemical cycles and allow rapid estimation of the climate response to a wide range of emission scenarios. {8.8, 10.5}

Earth System Models of Intermediate Complexity (EMICs) include some dynamics of the atmospheric and oceanic circulations, or parametrizations thereof, and often include representations of biogeochemical cycles, but they commonly have reduced spatial resolution. These models can be used to investigate continental-scale climate change and long-term, large-scale effects of coupling between Earth system components using large ensembles of model runs or runs over many centuries. For both SCMs and EMICs it is computationally feasible to sample parameter spaces thoroughly, taking account of parameter uncertainties derived from tuning to more comprehensive climate models, matching observations and use of expert judgment. Thus, both types of model are well suited to the generation of probabilistic projections of future climate and allow a comparison of the 'response uncertainty' arising from uncertainty in climate model parameters with the 'scenario range' arising from the range of emission scenarios being considered. Earth System Models of Intermediate Complexity have been evaluated in greater depth than previously and intercomparison exercises have demonstrated that they are useful for studying questions involving long time scales or requiring large ensembles of simulations. {8.8, 10.5, 10.7}

The most comprehensive climate models are the AOGCMs. They include dynamical components describing atmospheric, oceanic and land surface processes, as well as sea ice and other components. Much progress has been made since the TAR (see Box TS.7), and there are over 20 models from different centres available for climate simulations. Although the large-scale dynamics of these models are comprehensive, parametrizations are still used to represent unresolved physical processes such as the formation of clouds and precipitation, ocean mixing due to wave processes and the formation of water masses, etc. Uncertainty in parametrizations is the primary reason why climate projections differ between different AOGCMs. While the resolution of AOGCMs is rapidly improving, it is often insufficient to capture the fine-scale structure of climatic variables in many regions. In such cases, the output from AOGCMs can be used to drive limited-area (or regional climate) models that combine the comprehensiveness of process representations comparable to AOGCMs with much higher spatial resolution. {8.2}

TS.5.1 Understanding Near-Term Climate Change

Knowledge of the climate system together with model simulations confirm that past changes in greenhouse gas concentrations will lead to a committed warming (see Box TS.9 for a definition) and future climate change. New model results for experiments in which concentrations of all forcing agents were held constant provide better estimates of the committed changes in atmospheric variables that would follow because of the long response time of the climate system, particularly the oceans. {10.3, 10.7}

Previous IPCC projections of future climate changes can now be compared to recent observations, increasing confidence in short-term projections and the underlying physical understanding of committed climate change over a few decades. Projections for 1990 to 2005 carried out for the FAR and the SAR suggested global mean temperature increases of about 0.3°C and 0.15°C per decade, respectively.[10] The difference between the two was due primarily to the inclusion of aerosol cooling effects in the SAR, whereas there was no quantitative basis for doing so in the FAR. Projections given in the TAR were similar to those of the SAR. These results are comparable to observed values of about 0.2°C per decade, as shown in Figure TS.26, providing broad confidence in such short-term projections. Some of this warming is the committed effect of changes in the concentrations of greenhouse gases prior to the times of those earlier assessments. {1.2, 3.2}

Committed climate change (see Box TS.9) due to atmospheric composition in the year 2000 corresponds to a warming trend of about 0.1°C per decade over the next two decades, in the absence of large changes in volcanic or solar forcing. About twice as much warming (0.2°C per decade) would be expected if emissions were to fall within the range of the SRES marker scenarios. This result is insensitive to the choice among the SRES marker scenarios, none of which considered climate initiatives. By 2050, the range of expected warming shows limited sensitivity to the choice among SRES scenarios (1.3°C to 1.7°C relative to 1980–1999) with about a quarter being due to the committed climate change if all radiative forcing agents were stabilised today. {10.3, 10.5, 10.7}

Sea level is expected to continue to rise over the next several decades. During 2000 to 2020 under the SRES A1B scenario in the ensemble of AOGCMs, the rate of thermal expansion is projected to be 1.3 ± 0.7 mm yr^{-1}, and is not significantly different under the A2 or B1 scenarios. These projected rates are within the uncertainty of the observed contribution of thermal expansion for 1993 to 2003 of 1.6 ± 0.6 mm yr^{-1}. The ratio of committed thermal expansion, caused by constant atmospheric composition at year 2000 values, to total thermal expansion (that is the ratio of expansion occurring after year 2000 to that occurring before and after) is larger than the corresponding ratio for global average surface temperature. {10.6, 10.7}

Box TS.9: Committed Climate Change

If the concentrations of greenhouse gases and aerosols were held fixed after a period of change, the climate system would continue to respond due to the thermal inertia of the oceans and ice sheets and their long time scales for adjustment. 'Committed warming' is defined here as the further change in global mean temperature after atmospheric composition, and hence radiative forcing, is held constant. Committed change also involves other aspects of the climate system, in particular sea level. Note that holding concentrations of radiatively active species constant would imply that ongoing emissions match natural removal rates, which for most species would be equivalent to a large reduction in emissions, although the corresponding model experiments are not intended to be considered as emission scenarios. {FAQ 10.3}

The troposphere adjusts to changes in its boundary conditions over time scales shorter than a month or so. The upper ocean responds over time scales of several years to decades, and the deep ocean and ice sheet response time scales are from centuries to millennia. When the radiative forcing changes, internal properties of the atmosphere tend to adjust quickly. However, because the atmosphere is strongly coupled to the oceanic mixed layer, which in turn is coupled to the deeper oceanic layer, it takes a very long time for the atmospheric variables to come to an equilibrium. During the long periods where the surface climate is changing very slowly, one can consider that the atmosphere is in a quasi-equilibrium state, and most energy is being absorbed by the ocean, so that ocean heat uptake is a key measure of climate change. {10.7}

---

[10] See IPCC First Assessment Report, Policymakers Summary, and Second Assessment Report, Technical Summary, Figure 18.

GLOBAL MEAN WARMING:
MODEL PROJECTIONS COMPARED WITH OBSERVATIONS
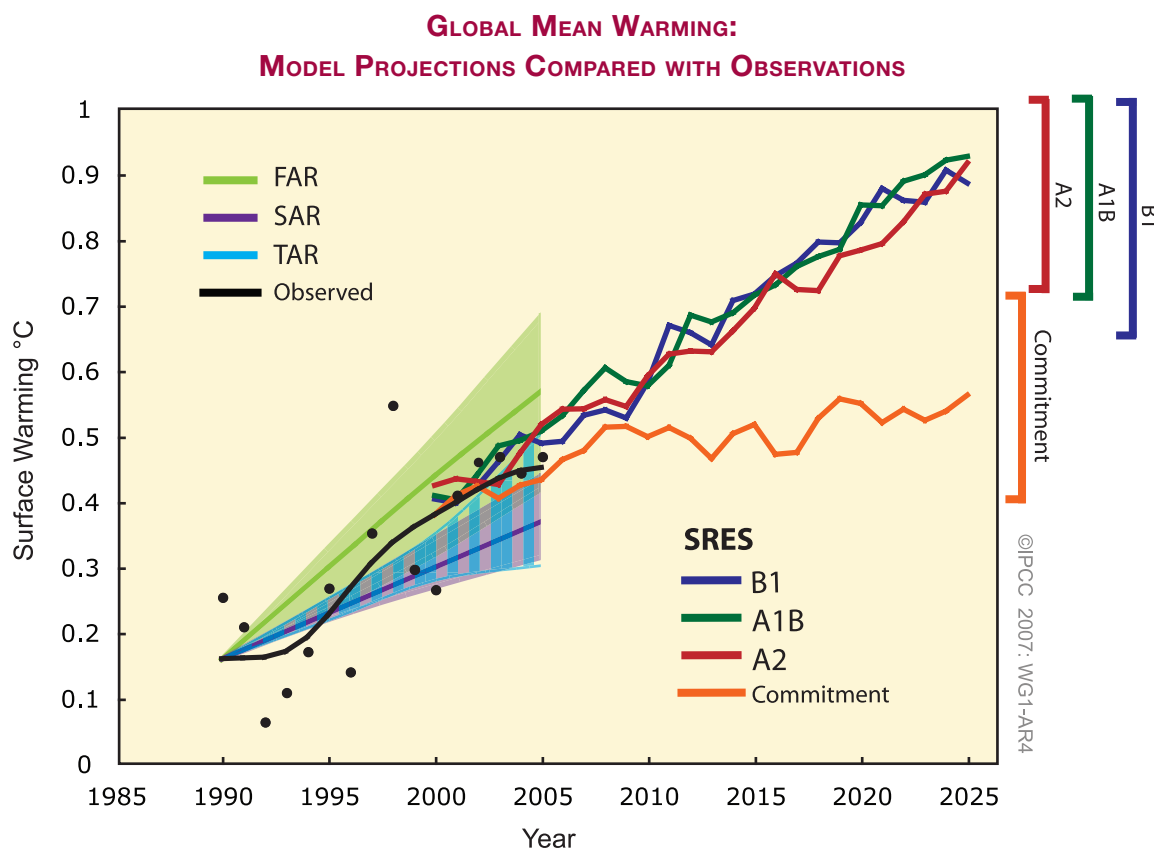
Figure TS.26. *Model projections of global mean warming compared to observed warming. Observed temperature anomalies, as in Figure TS.6, are shown as annual (black dots) and decadal average values (black line). Projected trends and their ranges from the IPCC First (FAR) and Second (SAR) Assessment Reports are shown as green and magenta solid lines and shaded areas, and the projected range from the TAR is shown by vertical blue bars. These projections were adjusted to start at the observed decadal average value in 1990. Multi-model mean projections from this report for the SRES B1, A1B and A2 scenarios, as in Figure TS.32, are shown for the period 2000 to 2025 as blue, green and red curves with uncertainty ranges indicated against the right-hand axis. The orange curve shows model projections of warming if greenhouse gas and aerosol concentrations were held constant from the year 2000 – that is, the committed warming. {Figures 1.1 and 10.4}*

TS.5.2   Large-Scale Projections for the 21st Century

This section covers advances in understanding global-scale climate projections and the processes that will influence their large-scale patterns in the 21st century. More specific discussion of regional-scale changes follows in TS.5.3.

Projected global average surface warming for the end of the 21st century (2090–2099) is scenario-dependent and the actual warming will be significantly affected by the actual emissions that occur. Warmings compared to 1980 to 1999 for six SRES scenarios[11] and for constant year 2000 concentrations, given as best estimates and corresponding *likely* **ranges,** are shown in Table TS.6. These results are based on AOGCMs, observational constraints and other methods to quantify the range of model response (see Figure TS.27). The combination of multiple lines of evidence allows likelihoods to be assigned to the resulting ranges, representing an important advance since the TAR. {10.5}

Assessed uncertainty ranges are larger than those given in the TAR because they consider a more complete range of models and climate-carbon cycle feedbacks. Warming tends to reduce land and ocean uptake of atmospheric CO_2, increasing the fraction of anthropogenic emissions that remains in the atmosphere. For the A2 scenario for example, the CO_2 feedback increases the corresponding global average warming in 2100 by more than 1°C. {7.3, 10.5}

---

[11]   Approximate CO_2 equivalent concentrations corresponding to the computed radiative forcing due to anthropogenic greenhouse gases and aerosols in 2100 (see p. 823 of the TAR) for the SRES B1, A1T, B2, A1B, A2 and A1FI illustrative marker scenarios are about 600, 700, 800, 850, 1,250 and 1,550 ppm respectively. Constant emission at year 2000 levels would lead to a concentration for CO_2 alone of about 520 ppm by 2100.

Table TS.6. *Projected global average surface warming and sea level rise at the end of the 21st century.* {10.5, 10.6, Table 10.7}

Case	Temperature Change (°C at 2090-2099 relative to 1980-1999) [a]		Sea Level Rise (m at 2090-2099 relative to 1980-1999)
	Best estimate	*Likely* range	Model-based range excluding future rapid dynamical changes in ice flow
Constant Year 2000 concentrations [b]	0.6	0.3 – 0.9	NA
B1 scenario	1.8	1.1 – 2.9	0.18 – 0.38
A1T scenario	2.4	1.4 – 3.8	0.20 – 0.45
B2 scenario	2.4	1.4 – 3.8	0.20 – 0.43
A1B scenario	2.8	1.7 – 4.4	0.21 – 0.48
A2 scenario	3.4	2.0 – 5.4	0.23 – 0.51
A1FI scenario	4.0	2.4 – 6.4	0.26 – 0.59

Notes:

[a] These estimates are assessed from a hierarchy of models that encompass a simple climate model, several Earth Models of Intermediate Complexity (EMICs), and a large number of Atmosphere-Ocean Global Circulation Models (AOGCMs).

[b] Year 2000 constant composition is derived from AOGCMs only.

Projected global-average sea level rise at the end of the 21st century (2090 to 2099), relative to 1980 to 1999 for the six SRES marker scenarios, given as 5% to 95% ranges based on the spread of model results, are shown in Table TS.6. Thermal expansion contributes 70 to 75% to the best estimate for each scenario. An improvement since the TAR is the use of AOGCMs to evaluate ocean heat uptake and thermal expansion. This has also reduced the projections as compared to the simple model used in the TAR. In all the SRES marker scenarios except B1, the average rate of sea level rise during the 21st century *very likely* exceeds the 1961–2003 average rate (1.8 ± 0.5 mm yr⁻¹). For an average model, the scenario spread in sea level rise is only 0.02 m by the middle of the century, but by the end of the century it is 0.15 m. These ranges do not include uncertainties in carbon-cycle feedbacks or ice flow processes because a basis in published literature is lacking. {10.6, 10.7}

For each scenario, the midpoint of the range given here is within 10% of the TAR model average for 2090–2099, noting that the TAR projections were given for 2100, whereas projections in this report are for 2090–2099. The uncertainty in these projections is less than in the TAR for several reasons: uncertainty in land ice models is assumed independent of uncertainty in temperature and expansion projections; improved observations of recent mass loss from glaciers provide a better observational constraint; and the present report gives uncertainties as 5% to 95% ranges, equivalent to ±1.65 standard deviations, whereas the TAR gave

uncertainty ranges of ±2 standard deviations. The TAR would have had similar ranges for sea level projections to those in this report if it had treated the uncertainties in the same way. {10.6, 10.7}

Changes in the cryosphere will continue to affect sea level rise during the 21st century. Glaciers, ice caps and the Greenland Ice Sheet are projected to lose mass in the 21st century because increased melting will exceed increased snowfall. Current models suggest that the Antarctic Ice Sheet will remain too cold for widespread melting and may gain mass in future through increased snowfall, acting to reduce sea level rise. However, changes in ice dynamics could increase the contributions of both Greenland and Antarctica to 21st-century sea level rise. Recent observations of some Greenland outlet glaciers give strong evidence for enhanced flow when ice shelves are removed. The observations in west-central Greenland of seasonal variation in ice flow rate and of a correlation with summer temperature variation suggest that surface melt water may join a sub-glacially routed drainage system lubricating the ice flow. By both of these mechanisms, greater surface melting during the 21st century could cause acceleration of ice flow and discharge and increase the sea level contribution. In some parts of West Antarctica, large accelerations of ice flow have recently occurred, which may have been caused by thinning of ice shelves due to ocean warming. Although this has not been formally attributed to anthropogenic climate change due to greenhouse gases, it suggests that future warming could cause faster mass loss and greater

PROJECTED WARMING IN 2090–2099
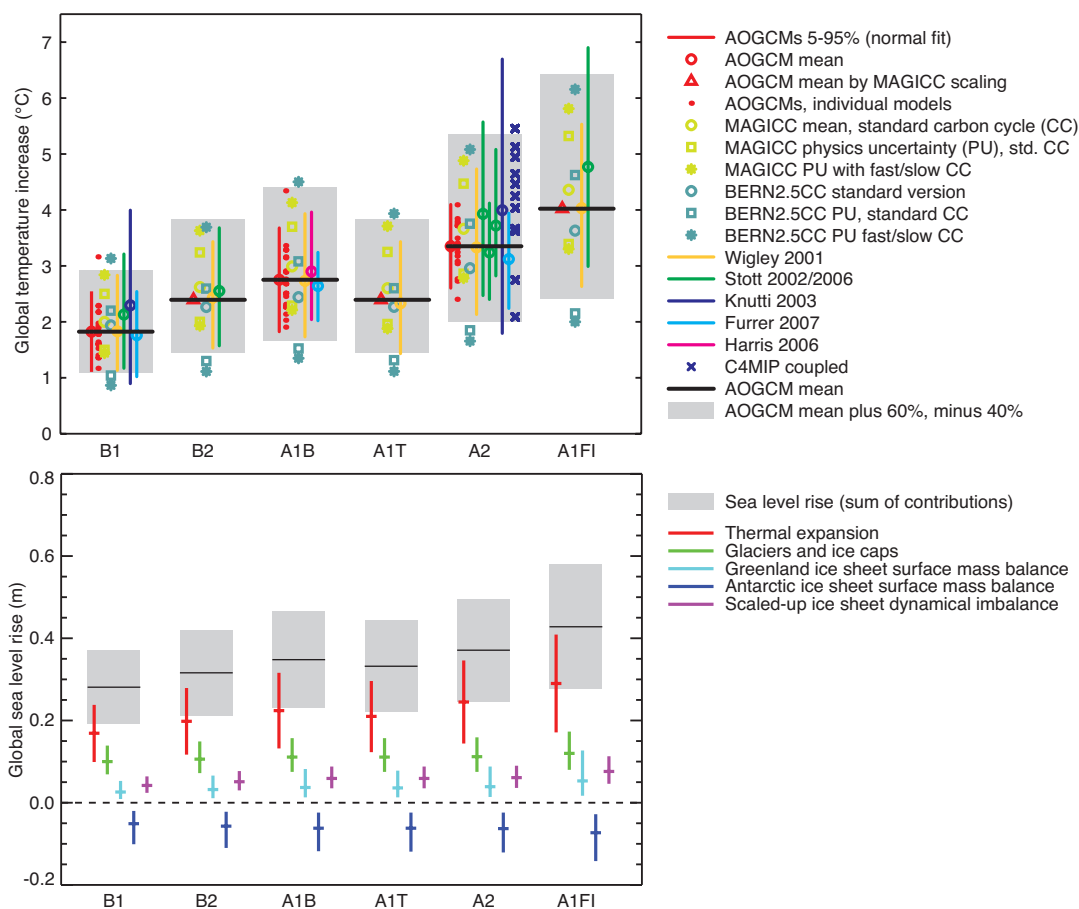
Figure TS.27. *(Top) Projected global mean temperature change in 2090 to 2099 relative to 1980 to 1999 for the six SRES marker scenarios based on results from different and independent models. The multi-model AOGCM mean and the range of the mean minus 40% to the mean plus 60% are shown as black horizontal solid lines and grey bars, respectively. Carbon cycle uncertainties are estimated for scenario A2 based on Coupled Carbon Cycle Climate Model Intercomparison Project (C4MIP) models (dark blue crosses), and for all marker scenarios using an EMIC (pale blue symbols). Other symbols represent individual studies (see Figure 10.29 for details of specific models). (Bottom) Projected global average sea level rise and its components in 2090 to 2099 (relative to 1980–1999) for the six SRES marker scenarios. The uncertainties denote 5 to 95% ranges, based on the spread of model results, and not including carbon cycle uncertainties. The contributions are derived by scaling AOGCM results and estimating land ice changes from temperature changes (see Appendix 10.A for details). Individual contributions are added to give the total sea level rise, which does not include the contribution shown for ice sheet dynamical imbalance, for which the current level of understanding prevents a best estimate from being given. {Figures 10.29 and 10.33}*

sea level rise. Quantitative projections of this effect cannot be made with confidence. If recently observed increases in ice discharge rates from the Greenland and Antarctic Ice Sheets were to increase linearly with global average temperature change, that would add 0.1 to 0.2 m to the upper bound of sea level rise. Understanding of these effects is too limited to assess their likelihood or to give a best estimate. {4.6, 10.6}

Many of the global and regional patterns of temperature and precipitation seen in the TAR projections remain in the new generation of models and across ensemble results (see Figure TS.28). Confidence

in the robustness of these patterns is increased by the fact that they have remained largely unchanged while overall model simulations have improved (Box TS.7). This adds to confidence that these patterns reflect basic physical constraints on the climate system as it warms. {8.3–8.5, 10.3, 11.2–11.9}

The projected 21st-century temperature change is positive everywhere. It is greatest over land and at most high latitudes in the NH during winter, and increases going from the coasts into the continental interiors. In otherwise geographically similar areas, warming is typically larger in arid than in moist regions. {10.3, 11.2–11.9}

In contrast, warming is least over the southern oceans and parts of the North Atlantic Ocean. Temperatures are projected to increase, including over the North Atlantic and Europe, despite a projected slowdown of the meridional overturning circulation (MOC) in most models, due to the much larger influence of the increase in greenhouse gases. The projected pattern of zonal mean temperature change in the atmosphere displays a maximum warming in the upper tropical troposphere and cooling in the stratosphere. Further zonal mean warming in the ocean is expected to occur first near the surface and in the northern mid-latitudes, with the warming gradually reaching the ocean interior, most evident at high latitudes where vertical mixing is greatest. The projected pattern of change is very similar among the late-century cases irrespective of the scenario. Zonally averaged fields normalised by the mean warming are very similar for the scenarios examined (see Figure TS.28). {10.3}

It is *very likely* that the Atlantic MOC will slow down over the course of the 21st century. The multi-model average reduction by 2100 is 25% (range from zero to about 50%) for SRES emission scenario A1B. Temperatures in the Atlantic region are projected to increase despite such changes due to the much larger warming associated with projected increases of greenhouse gases. The projected reduction of the Atlantic MOC is due to the combined effects of an increase in high latitude temperatures and precipitation, which reduce the density of the surface waters in the North Atlantic. This could lead to a significant reduction in Labrador Sea Water formation. Very few AOGCM studies have included the impact of additional freshwater from melting of the Greenland Ice Sheet, but those that have do not suggest that this will lead to a complete MOC shutdown. Taken together, it is *very likely* that the MOC will reduce, but very *unlikely* that the MOC will undergo a large abrupt transition during the course of the 21st century. Longer-term changes in the MOC cannot be assessed with confidence. {8.7, 10.3}

PROJECTIONS OF SURFACE TEMPERATURES

©IPCC 2007: WG1-AR4
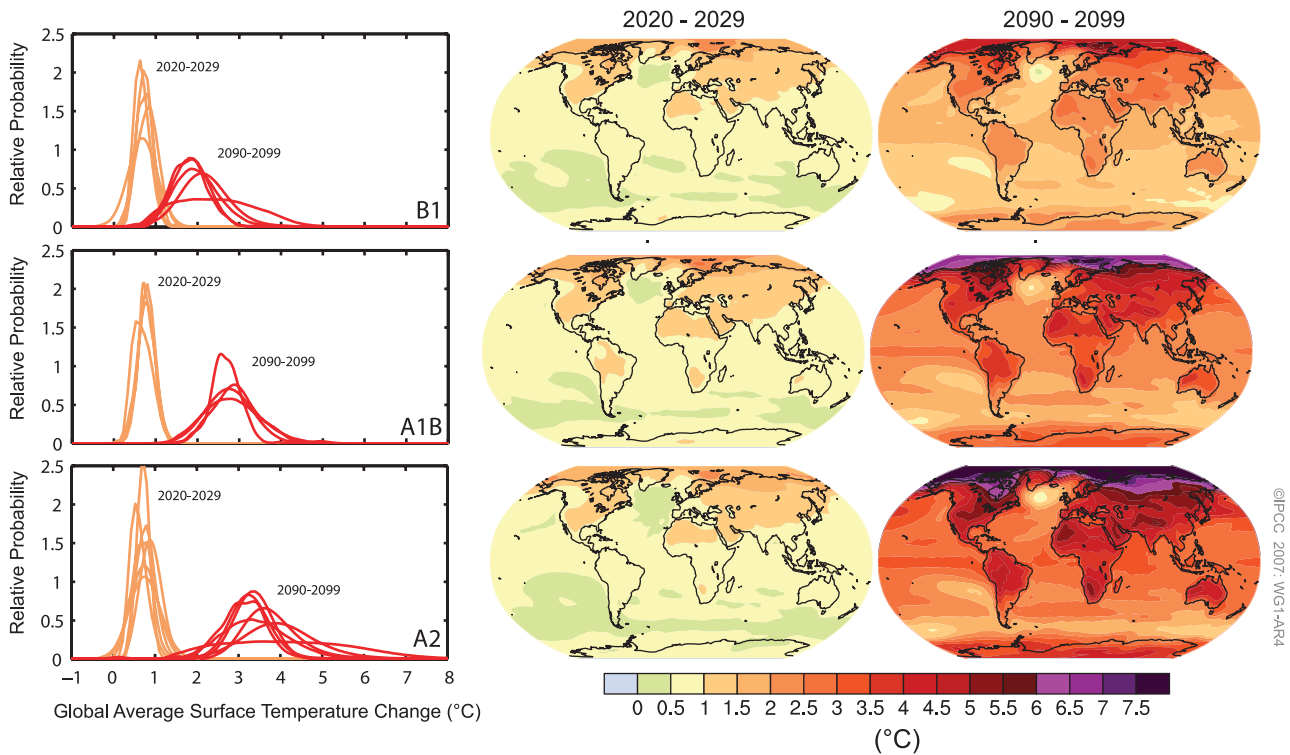
Figure TS.28. *Projected surface temperature changes for the early and late 21st century relative to the period 1980 to 1999. The central and right panels show the AOGCM multi-model average projections (°C) for the B1 (top), A1B (middle) and A2 (bottom) SRES scenarios averaged over the decades 2020 to 2029 (centre) and 2090 to 2099 (right). The left panel shows corresponding uncertainties as the relative probabilities of estimated global average warming from several different AOGCM and EMIC studies for the same periods. Some studies present results only for a subset of the SRES scenarios, or for various model versions. Therefore the difference in the number of curves, shown in the left-hand panels, is due only to differences in the availability of results. {Adapted from Figures 10.8 and 10.28}*

Models indicate that sea level rise during the 21st century will not be geographically uniform. Under scenario A1B for 2070 to 2099, AOGCMs give a median spatial standard deviation of 0.08 m, which is about 25% of the central estimate of the global average sea level rise. The geographic patterns of future sea level change arise mainly from changes in the distribution of heat and salinity in the ocean and consequent changes in ocean circulation. Projected patterns display more similarity across models than those analysed in the TAR. Common features are a smaller than average sea level rise in the Southern Ocean, larger than average sea level rise in the Arctic and a narrow band of pronounced sea level rise stretching across the southern Atlantic and Indian Oceans. {10.6}

Projections of changes in extremes such as the frequency of heat waves are better quantified than in the TAR, due to improved models and a better assessment of model spread based on multi-model ensembles. The TAR concluded that there was a risk of increased temperature extremes, with more extreme heat episodes in a future climate. This result has been confirmed and expanded in more recent studies. Future increases in temperature extremes are projected to follow increases in mean temperature over most of the world except where surface properties (e.g., snow cover or soil moisture) change. A multi-model analysis, based on simulations of 14 models for three scenarios, investigated changes in extreme seasonal (DJF and JJA) temperatures where 'extreme' is defined as lying above the 95th percentile of the simulated temperature distribution for the 20th century. By the end of the 21st century, the projected probability of extreme warm seasons rises above 90% in many tropical areas, and reaches around 40% elsewhere. Several recent studies have addressed possible future changes in heat waves, and found that, in a future climate, heat waves are expected to be more intense, longer lasting and more frequent. Based on an eight-member multi-model ensemble, heat waves are simulated to have been increasing for the latter part of the 20th century, and are projected to increase globally and over most regions. {8.5, 10.3}

For a future warmer climate, models project a 50 to 100% decline in the frequency of cold air outbreaks relative to the present in NH winters in most areas. Results from a nine-member multi-model ensemble show simulated decreases in frost days for the 20th century continuing into the 21st century globally and in most regions. Growing season length is related to frost days and is projected to increase in future climates. {10.3, FAQ 10.1}

Snow cover is projected to decrease. Widespread increases in thaw depth are projected to occur over most permafrost regions. {10.3}

Under several different scenarios (SRES A1B, A2 and B1), large parts of the Arctic Ocean are expected to no longer have year-round ice cover by the end of the 21st century. Arctic sea ice responds sensitively to warming. While projected changes in winter sea ice extent are moderate, late-summer sea ice is projected to disappear almost completely towards the end of the 21st century under the A2 scenario in some models. The reduction is accelerated by a number of positive feedbacks in the climate system. The ice-albedo feedback allows open water to receive more heat from the Sun during summer, the insulating effect of sea ice is reduced and the increase in ocean heat transport to the Arctic further reduces ice cover. Model simulations indicate that the late-summer sea ice cover decreases substantially and generally evolves over the same time scale as global warming. Antarctic sea ice extent is also projected to decrease in the 21st century. {8.6, 10.3, Box 10.1}

Sea level pressure is projected to increase over the subtropics and mid-latitudes, and decrease over high latitudes associated with an expansion of the Hadley Circulation and annular mode changes (NAM/NAO and SAM, see Box TS.2). A positive trend in the NAM/NAO as well as the SAM index is projected by many models. The magnitude of the projected increase is generally greater for the SAM, and there is considerable spread among the models. As a result of these changes, storm tracks are projected to move poleward, with consequent changes in wind, precipitation and temperature patterns outside the tropics, continuing the broad pattern of observed trends over the last half century. Some studies suggest fewer storms in mid-latitude regions. There are also indications of changes in extreme wave height associated with changing storm tracks and circulation. {3.6, 10.3}

In most models, the central and eastern equatorial Pacific SSTs warm more than those in the western equatorial Pacific, with a corresponding mean eastward shift in precipitation. ENSO interannual variability is projected to continue in all models, although changes differ from model to model. Large inter-model differences in projected changes in El Niño amplitude, and the inherent centennial time-scale variability of El Niño in the models, preclude a definitive projection of trends in ENSO variability. {10.3}

Recent studies with improved global models, ranging in resolution from about 100 to 20 km, suggest future changes in the number and intensity of future tropical cyclones (typhoons and hurricanes).

A synthesis of the model results to date indicates, for a warmer future climate, increased peak wind intensities and increased mean and peak precipitation intensities in future tropical cyclones, with the possibility of a decrease in the number of relatively weak hurricanes, and increased numbers of intense hurricanes. However, the total number of tropical cyclones globally is projected to decrease. The apparent observed increase in the proportion of very intense hurricanes since 1970 in some regions is in the same direction but much larger than predicted by theoretical models. {10.3, 8.5, 3.8}

Since the TAR, there is an improving understanding of projected patterns of precipitation. Increases in the amount of precipitation are *very likely* at high latitudes while decreases are *likely* in most subtropical land regions (by as much as about 20% in the A1B scenario in 2100). Poleward of 50°, mean precipitation is projected to increase due to the increase in water vapour in the atmosphere and the resulting increase in vapour transport from lower latitudes. Moving equatorward, there is a transition to mostly decreasing precipitation in the subtropics (20°–40° latitude). Due to increased water vapour transport out of the subtropics and a poleward expansion of the subtropical high-pressure systems, the drying tendency is especially pronounced at the higher-latitude margins of the subtropics (see Figure TS.30). {8.3, 10.3, 11.2–11.9}

Models suggest that changes in mean precipitation amount, even where robust, will rise above natural variability more slowly than the temperature signal. {10.3, 11.1}

Available research indicates a tendency for an increase in heavy daily rainfall events in many regions, including some in which the mean rainfall is projected to decrease. In the latter cases, the rainfall decrease is often attributable to a reduction in the number of rain days rather than the intensity of rain when it occurs. {11.2–11.9}

TS.5.3   Regional-Scale Projections

For each of the continental regions, the projected warming over 2000 to 2050 resulting from the SRES emissions scenarios is greater than the global average and greater than the observed warming over the past century. The warming projected for the next few decades of the 21st century, when averaged over the continents individually, would substantially exceed estimated 20th-century natural forced and unforced variability in all cases except Antarctica (Figure TS.29). Model best-estimate projections indicate that decadal average warming over each continent except Antarctica by 2030 is *very likely* to be at least twice as large as the corresponding model-estimated natural variability during the 20th century. The simulated warming over this period is not very sensitive to the choice of scenarios across the SRES set as is illustrated in Figure TS.32. Over longer time scales, the choice of scenario is more important, as shown in Figure TS.28. The projected warming in the SRES scenarios over 2000 to 2050 also exceeds estimates of natural variability when averaged over most sub-continental regions. {11.1}

Box TS.10. Regional Downscaling

Simulation of regional climates has improved in AOGCMs and, as a consequence, in nested regional climate models and in empirical downscaling techniques. Both dynamic and empirical downscaling methodologies show improving skill in simulating local features in present-day climates when the observed state of the atmosphere at scales resolved by current AOGCMs is used as input. The availability of downscaling and other regionally focused studies remains uneven geographically, causing unevenness in the assessments that can be provided, particularly for extreme weather events. Downscaling studies demonstrate that local precipitation changes can vary significantly from those expected from the large-scale hydrological response pattern, particularly in areas of complex topography. {11.10}

There remain a number of important sources of uncertainty limiting the ability to project regional climate change. While hydrological responses are relatively robust in certain core subpolar and subtropical regions, there is uncertainty in the precise location of these boundaries between increasing and decreasing precipitation. There are some important climate processes that have a significant effect on regional climate, but for which the climate change response is still poorly known. These include ENSO, the NAO, blocking, the thermohaline circulation and changes in tropical cyclone distribution. For those regions that have strong topographical controls on their climatic patterns, there is often insufficient climate change information at the fine spatial resolution of the topography. In some regions there has been only very limited research on extreme weather events. Further, the projected climate change signal becomes comparable to larger internal variability at smaller spatial and temporal scales, making it more difficult to utilise recent trends to evaluate model performance. {Box 11.1, 11.2–11.9}

CONTINENTAL SURFACE TEMPERATURE ANOMALIES:
OBSERVATIONS AND PROJECTIONS
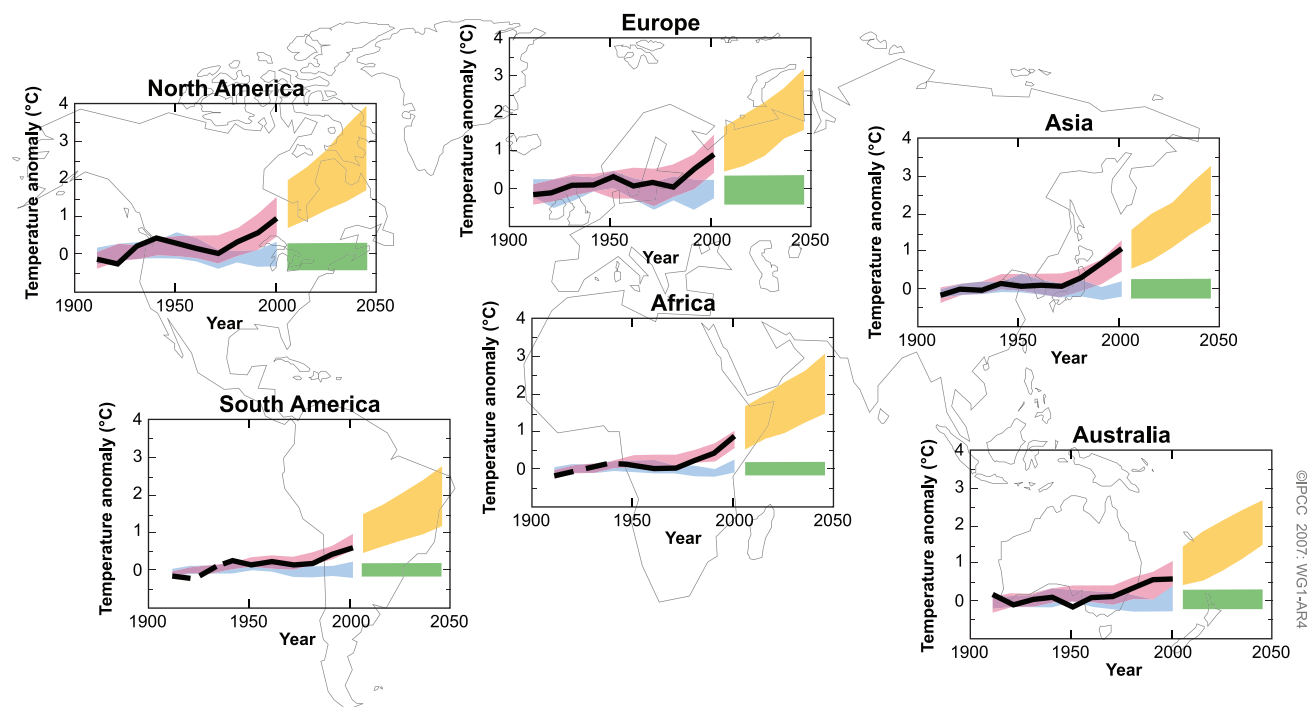
**Figure TS.29.** *Decadal mean continental surface temperature anomalies (°C) in observations and simulations for the period 1906 to 2005 and in projections for 2001 to 2050. Anomalies are calculated from the 1901 to 1950 average. The black lines represent the observations and the red and blue bands show simulated average temperature anomalies as in Figure TS.22 for the 20th century (i.e., red includes anthropogenic and natural forcings and blue includes only natural forcings). The yellow shading represents the 5th to 95th percentile range of projected changes according to the SRES A1B emissions scenario. The green bar denotes the 5th to 95th percentile range of decadal mean anomalies from the 20th-century simulations with only natural forcings (i.e., a measure of the natural decadal variability). For the observed part of these graphs, the decadal averages are centred on calendar decade boundaries (i.e., the last point is at 2000 for 1996 to 2005), whereas for the future period they are centred on calendar decade mid-points (i.e., the first point is at 2005 for 2001 to 2010). To construct the ranges, all simulations from the set of models involved were considered independent realisations of the possible evolution of the climate given the forcings applied. This involved 58 simulations from 14 models for the red curve, 19 simulations from 5 models (a subset of the 14) for the blue curve and green bar and 47 simulations from 18 models for the yellow curve. {FAQ 9.2.1, Figure 1 and Box 11.1, Figure 1}*

In the NH a robust pattern of increased subpolar and decreased subtropical precipitation dominates the projected precipitation pattern for the 21st century over North America and Europe, while subtropical drying is less evident over Asia (see Figure TS.30). Nearly all models project increased precipitation over most of northern North America and decreased precipitation over Central America, with much of the continental USA and northern Mexico in a more uncertain transition zone that moves north and south following the seasons. Decreased precipitation is confidently projected for southern Europe and Mediterranean Africa, with a transition to increased precipitation in northern Europe. In both continents, summer drying is extensive due both to the poleward movement of this transition zone in summer and to increased evaporation. Subpolar increases in precipitation are projected over much of northern Asia but with the subtropical drying spreading from the Mediterranean displaced by distinctive monsoonal signatures as one moves from central Asia eastward. {11.2–11.5}

SEASONAL MEAN PRECIPITATION RATES
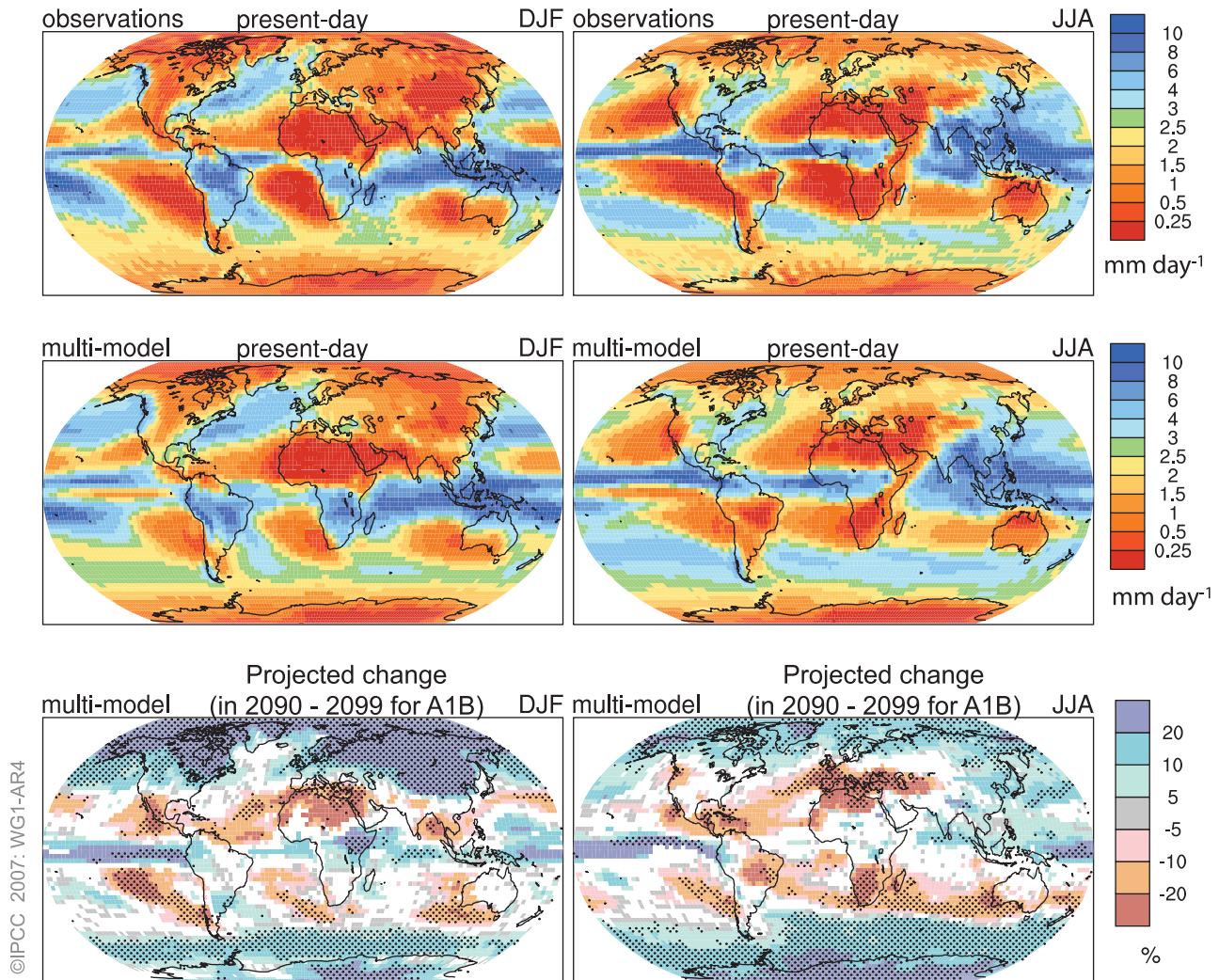
Figure TS.30. *Spatial patterns of observed (top row) and multi-model mean (middle row) seasonal mean precipitation rate (mm day⁻¹) for the period 1979 to 1993 and the multi-model mean for changes by the period 2090 to 2099 relative to 1980 to 1999 (% change) based on the SRES A1B scenario (bottom row). December to February means are in the left column, June to August means in the right column. In the bottom panel, changes are plotted only where more than 66% of the models agree on the sign of the change. The stippling indicates areas where more than 90% of the models agree on the sign of the change. {Based on same datasets as shown in Figures 8.5 and 10.9}*

In the SH, there are few land areas in the zone of projected subpolar moistening during the 21st century, with the subtropical drying more prominent (see Figure TS.30). The South Island of New Zealand and Tierra del Fuego fall within the subpolar precipitation increase zone, with southernmost Africa, the southern Andes in South America and southern Australia experiencing the drying tendency typical of the subtropics. {11.2, 11.6, 11.7}

Projections of precipitation over tropical land regions are more uncertain than those at higher latitudes, but, despite significant inadequacies in modelling tropical convection and atmosphere-ocean interactions, and the added uncertainty associated with tropical cyclones, some robust features emerge in models. Rainfall in the summer monsoon season of South and Southeast Asia increases in most models, as does rainfall in East Africa. The sign of the precipitation response is considered less certain over both the Amazon and the African Sahel. These are regions in which there is added uncertainty due to potential vegetation-climate links, and there is less robustness across models even when vegetation feedbacks are not included. {8.3, 11.2, 11.4, 11.6}

TS.5.4 Coupling Between Climate Change and Changes in Biogeochemical Cycles

All models that treat the coupling of the carbon cycle to climate change indicate a positive feedback effect with warming acting to suppress land and ocean uptake of CO_2, leading to larger atmospheric CO_2 increases and greater climate change for a given emissions scenario, but the strength of this feedback effect varies markedly among models. Since the TAR, several new projections based on fully coupled carbon cycle-climate models have been performed and compared. For the SRES A2 scenario, and based on a range of model results, the projected increase in atmospheric CO_2 concentration over the 21st century is *likely* between 10 and 25% higher than projections without this feedback, adding more than 1°C to projected mean warming by 2100 for higher emission SRES scenarios. Correspondingly, the reduced CO_2 uptake caused by this effect reduces the CO_2 emissions that are consistent with a target stabilisation level. However, there are still significant uncertainties due, for example, to limitations in the understanding of the dynamics of land ecosystems and soils. {7.3, 10.4}

Increasing atmospheric CO_2 concentrations lead directly to increasing acidification of the surface ocean. Projections based on SRES scenarios give reductions in pH of between 0.14 and 0.35 units in the 21st century (depending on scenario), extending the present decrease of 0.1 units from pre-industrial times. Ocean acidification would lead to dissolution of shallow-water carbonate sediments. Southern Ocean surface waters are projected to exhibit undersaturation with regard to calcium carbonate ($CaCO_3$) for CO_2 concentrations higher than 600 ppm, a level exceeded during the second half of the 21st century in most of the SRES scenarios. Low-latitude regions and the deep ocean will be affected as well. These changes could affect marine organisms that form their exoskeletons out of $CaCO_3$, but the net effect on the biological cycling of carbon in the oceans is not well understood. {Box 7.3, 10.4}

Committed climate change due to past emissions varies considerably for different forcing agents because of differing lifetimes in the Earth's atmosphere (see Box TS.9). The committed climate change due to past emissions takes account of both (i) the time lags in the responses of the climate system to changes in radiative forcing; and (ii) the time scales over which different forcing agents persist in the atmosphere after their emission because of their differing lifetimes.

Typically the committed climate change due to past emissions includes an initial period of further increase in temperature, for the reasons discussed above, followed by a long-term decrease as radiative forcing decreases. Some greenhouse gases have relatively short atmospheric lifetimes (decades or less), such as CH_4 and carbon monoxide, while others such as N_2O have lifetimes of the order of a century, and some have lifetimes of millennia, such as SF_6 and PFCs. Atmospheric concentrations of CO_2 do not decay with a single well-defined lifetime if emissions are stopped. Removal of CO_2 emitted to the atmosphere occurs over multiple time scales, but some CO_2 will stay in the atmosphere for many thousands of years, so that emissions lead to a very long commitment to climate change. The slow long-term buffering of the ocean, including $CaCO_3$-sediment feedback, requires 30,000 to 35,000 years for atmospheric CO_2 concentrations to reach equilibrium. Using coupled carbon cycle components, EMICs show that the committed climate change due to past CO_2 emissions persists for more than 1000 years, so that even over these very long time scales, temperature and sea level do not return to pre-industrial values. An indication of the long time scales of committed climate change is obtained by prescribing anthropogenic CO_2 emissions following a path towards stabilisation at 750 ppm, but arbitrarily setting emissions to zero at year 2100. In this test case, it takes about 100 to 400 years in the different models for the atmospheric CO_2 concentration to drop from the maximum (ranges between 650 to 700 ppm) to below the level of two times the pre-industrial CO_2 concentration (about 560 ppm), owing to a continuous but slow transfer of carbon from the atmosphere and terrestrial reservoirs to the ocean (see Figure TS.31). {7.3, 10.7}

Future concentrations of many non-CO_2 greenhouse gases and their precursors are expected to be coupled to future climate change. Insufficient understanding of the causes of recent variations in the CH_4 growth rate suggests large uncertainties in future projections for this gas in particular. Emissions of CH_4 from wetlands are *likely* to increase in a warmer and wetter climate and to decrease in a warmer and drier climate. Observations also suggest increases in CH_4 released from northern peatlands that are experiencing permafrost melt, although the large-scale magnitude of this effect is not well quantified. Changes in temperature, humidity and clouds could also affect biogenic emissions of ozone precursors, such as volatile organic compounds. Climate change is also expected to affect tropospheric ozone through changes in chemistry and transport. Climate change could induce changes in OH through changes in humidity, and could alter stratospheric ozone concentrations and hence solar ultraviolet radiation in the troposphere. {7.4, 4.7}

CLIMATE CHANGE COMMITMENT
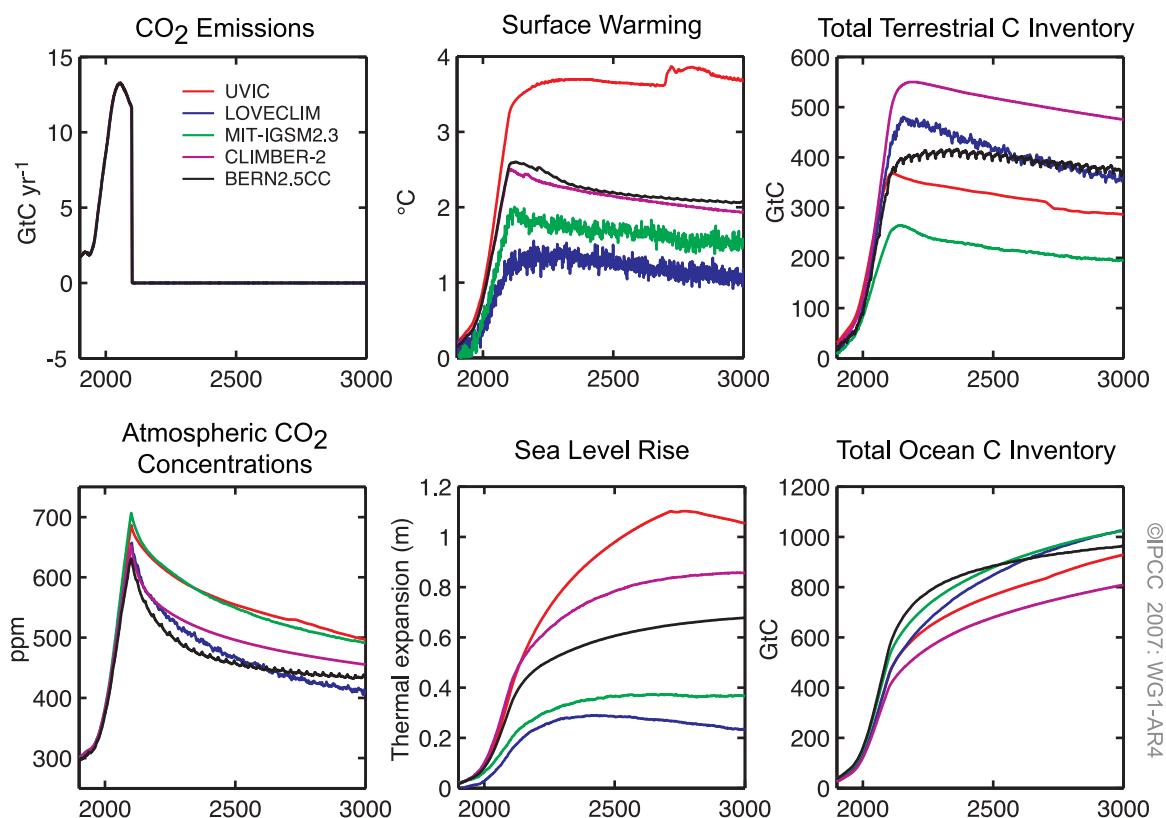
Figure TS.31. *Calculation of climate change commitment due to past emissions for five different EMICs and an idealised scenario where emissions follow a pathway leading to stabilisation of atmospheric CO_2 at 750 ppm, but before reaching this target, emissions are reduced to zero instantly at year 2100. (Left) CO_2 emissions and atmospheric CO_2 concentrations; (centre) surface warming and sea level rise due to thermal expansion; (right) change in total terrestrial and oceanic carbon inventory since the pre-industrial era. {Figure 10.35}*

Future emissions of many aerosols and their precursors are expected to be affected by climate change. Estimates of future changes in dust emissions under several climate and land use scenarios suggest that the effects of climate change are more important in controlling future dust emissions than changes in land use. Results from one study suggest that meteorology and climate have a greater influence on future Asian dust emissions and associated Asian dust storm occurrences than desertification. The biogenic emission of volatile organic compounds, a significant source of secondary organic aerosols, is known to be highly sensitive to (and increase with) temperature. However, aerosol yields decrease with temperature and the effects of changing precipitation and physiological adaptation are uncertain. Thus, change in biogenic secondary organic aerosol production in a warmer climate could be considerably lower than the response of biogenic volatile organic carbon emissions. Climate change may affect fluxes from the ocean of dimethyl sulphide (which is a precursor for some sulphate aerosols) and sea salt aerosols, however, the effects on temperature and precipitation remain very uncertain. {7.5}

While the warming effect of CO_2 represents a commitment over many centuries, aerosols are removed from the atmosphere over time scales of only a few days, so that the negative radiative forcing due to aerosols could change rapidly in response to any changes in emissions of aerosols or aerosol precursors. Because sulphate aerosols are *very likely* exerting a substantial negative radiative forcing at present, future net forcing is very sensitive to changes in sulphate emissions. One study suggests that the hypothetical removal from the atmosphere of the entire current burden of anthropogenic sulphate aerosol particles would produce a rapid increase in global mean temperature of about 0.8°C within a decade or two. Changes in aerosols are also likely to influence precipitation. Thus, the effect of environmental strategies aimed at mitigating climate change requires consideration of changes in both greenhouse gas and aerosol emissions.

Changes in aerosol emissions may result from measures implemented to improve air quality which may therefore have consequences for climate change. {Box 7.4, 7.6, 10.7}

Climate change would modify a number of chemical and physical processes that control air quality and the net effects are *likely* to vary from one region to another. Climate change can affect air quality by modifying the rates at which pollutants are dispersed, the rate at which aerosols and soluble species are removed from the atmosphere, the general chemical environment for pollutant generation and the strength of emissions from the biosphere, fires and dust. Climate change is also expected to decrease the global ozone background. Overall, the net effect of climate change on air quality is highly uncertain. {Box 7.4}

TS.5.5   Implications of Climate Processes and their Time Scales for Long-Term Projections

The commitments to climate change after stabilisation of radiative forcing are expected to be about 0.5 to 0.6°C, mostly within the following century. The multi-model average when stabilising concentrations of greenhouse gases and aerosols at year 2000 values after a 20th-century climate simulation, and running an additional 100 years, is about 0.6°C of warming (relative to 1980–1999) at year 2100 (see Figure TS.32). If the B1 or A1B scenarios were to characterise 21st-century emissions followed by stabilisation at those levels, the additional warming after stabilisation is similar, about 0.5°C, mostly in the subsequent hundred years. {10.3, 10.7}

The magnitude of the positive feedback between climate change and the carbon cycle is uncertain. This leads to uncertainty in the trajectory of CO_2 emissions required to achieve a particular stabilization level of atmospheric CO_2 concentration. Based upon current understanding of climate-carbon cycle feedback, model studies suggest that, in order to stabilise CO_2 at 450 ppm, cumulative emissions in the 21st century could be reduced from a model average of approximately 670 [630 to 710] GtC to approximately 490 [375 to 600] GtC. Similarly, to stabilise CO_2 at 1000 ppm, the cumulative emissions could be reduced by this feedback from a model average of

SRES Mean Surface Warming Projections
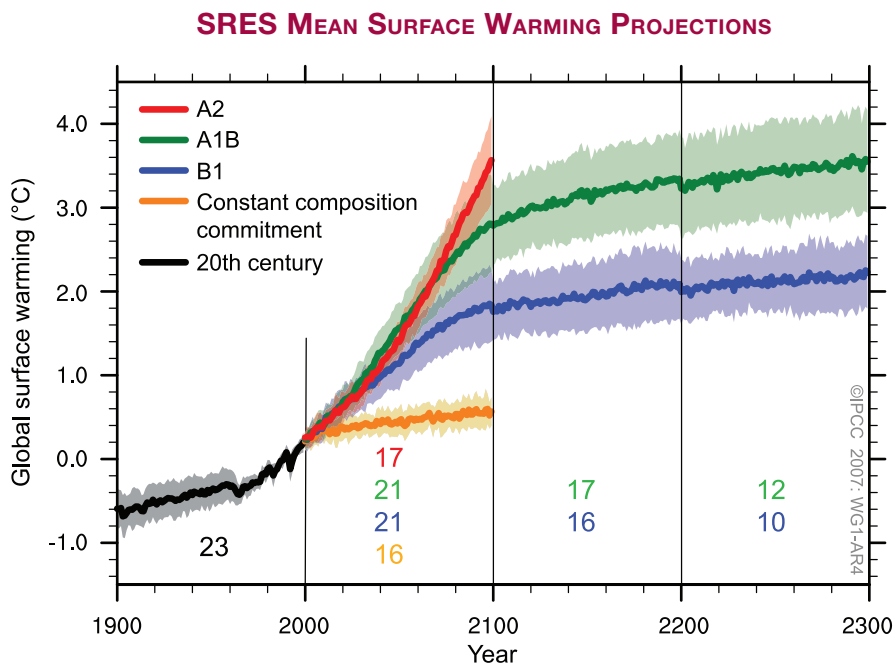
Figure TS.32. *Multi-model means of surface warming (compared to the 1980–1999 base period) for the SRES scenarios A2 (red), A1B (green) and B1 (blue), shown as continuations of the 20th-century simulation. The latter two scenarios are continued beyond the year 2100 with forcing kept constant (committed climate change as it is defined in Box TS.9). An additional experiment, in which the forcing is kept at the year 2000 level is also shown (orange). Linear trends from the corresponding control runs have been removed from these time series. Lines show the multi-model means, shading denotes the ±1 standard deviation range. Discontinuities between different periods have no physical meaning and are caused by the fact that the number of models that have run a given scenario is different for each period and scenario (numbers indicated in figure). For the same reason, uncertainty across scenarios should not be interpreted from this figure (see Section 10.5 for uncertainty estimates). {Figure 10.4}*

approximately 1415 [1340 to 1490] GtC to approximately 1100 [980 to 1250] GtC. {7.3, 10.4}

If radiative forcing were to be stabilised in 2100 at A1B concentrations, thermal expansion alone would lead to 0.3 to 0.8 m of sea level rise by 2300 (relative to 1980–1999) and would continue at decreasing rates for many centuries, due to slow processes that mix heat into the deep ocean. {10.7}

Contraction of the Greenland Ice Sheet is projected to continue to contribute to sea level rise after 2100. For stabilisation at A1B concentrations in 2100, a rate of 0.03 to 0.21 m per century due to thermal expansion is projected. If a global average warming of 1.9°C to 4.6°C relative to pre-industrial temperatures were maintained for millennia, the Greenland Ice Sheet would largely be eliminated except for remnant glaciers in the mountains. This would raise sea level by about 7 m and could be irreversible. These temperatures are comparable to those inferred for the last interglacial period 125,000 years ago, when palaeoclimatic information suggests reductions of polar ice extent and 4 to 6 m of sea level rise. {6.4, 10.7}

Dynamical processes not included in current models but suggested by recent observations could increase the vulnerability of the ice sheets to warming, increasing future sea level rise. Understanding of these processes is limited and there is no consensus on their likely magnitude. {4.6, 10.7}

Current global model studies project that the Antarctic Ice Sheet will remain too cold for widespread surface melting and will gain in mass due to increased snowfall. However, net loss of ice mass could occur if dynamical ice discharge dominates the ice sheet mass balance. {10.7}

While no models run for this assessment suggest an abrupt MOC shutdown during the 21st century, some models of reduced complexity suggest MOC shutdown as a possible long-term response to sufficiently strong warming. However, the likelihood of this occurring cannot be evaluated with confidence. The few available simulations with models of different complexity rather suggest a centennial-scale slowdown. Recovery of the MOC is *likely* if the radiative forcing is stabilised but would take several centuries. Systematic model comparison studies have helped establish some key processes that are responsible for variations between models in the response of the ocean to climate change (especially ocean heat uptake). {8.7, FAQ 10.2, 10.3}

TS.6 Robust Findings and Key Uncertainties

TS.6.1 Changes in Human and Natural Drivers of Climate

Robust Findings:

Current atmospheric concentrations of CO_2 and CH_4, and their associated positive radiative forcing, far exceed those determined from ice core measurements spanning the last 650,000 years. {6.4}

Fossil fuel use, agriculture and land use have been the dominant cause of increases in greenhouse gases over the last 250 years. {2.3, 7.3, 7.4}

Annual emissions of CO_2 from fossil fuel burning, cement production and gas flaring increased from a mean of 6.4 ± 0.4 GtC yr^{-1} in the 1990s to 7.2 ± 0.3 GtC yr^{-1} for 2000 to 2005. {7.3}

The sustained rate of increase in radiative forcing from CO_2, CH_4 and N_2O over the past 40 years is larger than at any time during at least the past 2000 years. {6.4}

Natural processes of CO_2 uptake by the oceans and terrestrial biosphere remove about 50 to 60% of anthropogenic emissions (i.e., fossil CO_2 emissions and land use change flux). Uptake by the oceans and the terrestrial biosphere are similar in magnitude over recent decades but that by the terrestrial biosphere is more variable. {7.3}

It is *virtually certain* that anthropogenic aerosols produce a net negative radiative forcing (cooling influence) with a greater magnitude in the NH than in the SH. {2.9, 9.2}

From new estimates of the combined anthropogenic forcing due to greenhouse gases, aerosols and land surface changes, it is *extremely likely* that human activities have exerted a substantial net warming influence on climate since 1750. {2.9}

Solar irradiance contributions to global average radiative forcing are considerably smaller than the contribution of increases in greenhouse gases over the industrial period. {2.5, 2.7}

Key Uncertainties:

The full range of processes leading to modification of cloud properties by aerosols is not well understood and the magnitudes of associated indirect radiative effects are poorly determined. {2.4, 7.5}

The causes of, and radiative forcing due to stratospheric water vapour changes are not well quantified. {2.3}

The geographical distribution and time evolution of the radiative forcing due to changes in aerosols during the 20th century are not well characterised. {2.4}

The causes of recent changes in the growth rate of atmospheric CH_4 are not well understood. {7.4}

The roles of different factors increasing tropospheric ozone concentrations since pre-industrial times are not well characterised. {2.3}

Land surface properties and land-atmosphere interactions that lead to radiative forcing are not well quantified. {2.5}

Knowledge of the contribution of past solar changes to radiative forcing on the time scale of centuries is not based upon direct measurements and is hence strongly dependent upon physical understanding. {2.7}

TS.6.2   Observations of Changes in Climate

TS.6.2.1   Atmosphere and Surface

Robust Findings:

Global mean surface temperatures continue to rise. Eleven of the last 12 years rank among the 12 warmest years on record since 1850. {3.2}

Rates of surface warming increased in the mid-1970s and the global land surface has been warming at about double the rate of ocean surface warming since then. {3.2}

Changes in surface temperature extremes are consistent with warming of the climate. {3.8}

Estimates of mid- and lower-tropospheric temperature trends have substantially improved. Lower-tropospheric temperatures have slightly greater warming rates than the surface from 1958 to 2005. {3.4}

Long-term trends from 1900 to 2005 have been observed in precipitation amount in many large regions. {3.3}

Increases have occurred in the number of heavy precipitation events. {3.8}

Droughts have become more common, especially in the tropics and subtropics, since the 1970s. {3.3}

Tropospheric water vapour has increased, at least since the 1980s. {3.4}

Key Uncertainties:

Radiosonde records are much less complete spatially than surface records and evidence suggests a number of radiosonde records are unreliable, especially in the tropics. It is likely that all records of tropospheric temperature trends still contain residual errors. {3.4}

While changes in large-scale atmospheric circulation are apparent, the quality of analyses is best only after 1979, making analysis of, and discrimination between, change and variability difficult. {3.5, 3.6}

Surface and satellite observations disagree on total and low-level cloud changes over the ocean. {3.4}

Multi-decadal changes in DTR are not well understood, in part because of limited observations of changes in cloudiness and aerosols. {3.2}

Difficulties in the measurement of precipitation remain an area of concern in quantifying trends in global and regional precipitation. {3.3}

Records of soil moisture and streamflow are often very short, and are available for only a few regions, which impedes complete analyses of changes in droughts. {3.3}

The availability of observational data restricts the types of extremes that can be analysed. The rarer the event, the more difficult it is to identify long-term changes because there are fewer cases available. {3.8}

Information on hurricane frequency and intensity is limited prior to the satellite era. There are questions about the interpretation of the satellite record. {3.8}

There is insufficient evidence to determine whether trends exist in tornadoes, hail, lightning and dust storms at small spatial scales. {3.8}

TS.6.2.2   Snow, Ice and Frozen Ground

Robust Findings:

The amount of ice on the Earth is decreasing. There has been widespread retreat of mountain glaciers since the end of the 19th century. The rate of mass loss from glaciers and the Greenland Ice Sheet is increasing. {4.5, 4.6}

The extent of NH snow cover has declined. Seasonal river and lake ice duration has decreased over the past 150 years. {4.2, 4.3}

Since 1978, annual mean arctic sea ice extent has been declining and summer minimum arctic ice extent has decreased. {4.4}

Ice thinning occurred in the Antarctic Peninsula and Amundsen shelf ice during the 1990s. Tributary glaciers have accelerated and complete breakup of the Larsen B Ice Shelf occurred in 2002. {4.6}

Temperature at the top of the permafrost layer has increased by up to 3°C since the 1980s in the Arctic. The maximum extent of seasonally frozen ground has decreased by about 7% in the NH since 1900, and its maximum depth has decreased by about 0.3 m in Eurasia since the mid-20th century. {4.7}

Key Uncertainties:

There is no global compilation of *in situ* snow data prior to 1960. Well-calibrated snow water equivalent data are not available for the satellite era. {4.2}

There are insufficient data to draw any conclusions about trends in the thickness of antarctic sea ice. {4.4}

Uncertainties in estimates of glacier mass loss arise from limited global inventory data, incomplete area-volume relationships and imbalance in geographic coverage. {4.5}

Mass balance estimates for ice shelves and ice sheets, especially for Antarctica, are limited by calibration and validation of changes detected by satellite altimetry and gravity measurements. {4.6}

Limited knowledge of basal processes and of ice shelf dynamics leads to large uncertainties in the understanding of ice flow processes and ice sheet stability. {4.6}

TS.6.2.3 Oceans and Sea Level

Robust Findings:

The global temperature (or heat content) of the oceans has increased since 1955. {5.2}

Large-scale regionally coherent trends in salinity have been observed over recent decades with freshening in subpolar regions and increased salinity in the shallower parts of the tropics and subtropics. These trends are consistent with changes in precipitation and inferred larger water transport in the atmosphere from low latitudes to high latitudes and from the Atlantic to the Pacific. {5.2}

Global average sea level rose during the 20th century. There is high confidence that the rate of sea level rise increased between the mid-19th and mid-20th centuries. During 1993 to 2003, sea level rose more rapidly than during 1961 to 2003. {5.5}

Thermal expansion of the ocean and loss of mass from glaciers and ice caps made substantial contributions to the observed sea level rise. {5.5}

The observed rate of sea level rise from 1993 to 2003 is consistent with the sum of observed contributions from thermal expansion and loss of land ice. {5.5}

The rate of sea level change over recent decades has not been geographically uniform. {5.5}

As a result of uptake of anthropogenic CO_2 since 1750, the acidity of the surface ocean has increased. {5.4, 7.3}

Key Uncertainties:

Limitations in ocean sampling imply that decadal variability in global heat content, salinity and sea level changes can only be evaluated with moderate confidence. {5.2, 5.5}

There is low confidence in observations of trends in the MOC. {Box 5.1}

Global average sea level rise from 1961 to 2003 appears to be larger than can be explained by thermal expansion and land ice melting. {5.5}

TS.6.2.4   Palaeoclimate

Robust Findings:

During the last interglacial, about 125,000 years ago, global sea level was *likely* 4 to 6 m higher than present, due primarily to retreat of polar ice. {6.4}

A number of past abrupt climate changes were *very likely* linked to changes in Atlantic Ocean circulation and affected the climate broadly across the NH. {6.4}

It is *very unlikely* that the Earth would naturally enter another ice age for at least 30,000 years. {6.4}

Biogeochemical and biogeophysical feedbacks have amplified climatic changes in the past. {6.4}

It is *very likely* that average NH temperatures during the second half of the 20th century were warmer than in any other 50-year period in the last 500 years and *likely* that this was also the warmest 50-year period in the past 1300 years. {6.6}

Palaeoclimate records indicate with high confidence that droughts lasting decades or longer were a recurrent feature of climate in several regions over the last 2000 years. {6.6}

Key Uncertainties:

Mechanisms of onset and evolution of past abrupt climate change and associated climate thresholds are not well understood. This limits confidence in the ability of climate models to simulate realistic abrupt change. {6.4}

The degree to which ice sheets retreated in the past, the rates of such change and the processes involved are not well known. {6.4}

Knowledge of climate variability over more than the last few hundred years in the SH and tropics is limited by the lack of palaeoclimatic records. {6.6}

Differing amplitudes and variability observed in available millennial-length NH temperature reconstructions, as well as the relation of these differences to choice of proxy data and statistical calibration methods, still need to be reconciled. {6.6}

The lack of extensive networks of proxy data for temperature in the last 20 years limits understanding of how such proxies respond to rapid global warming and of the influence of other environmental changes. {6.6}

TS.6.3   Understanding and Attributing Climate Change

Robust Findings:

Greenhouse gas forcing has *very likely* caused most of the observed global warming over the last 50 years. Greenhouse gas forcing alone during the past half century would *likely* have resulted in greater than the observed warming if there had not been an offsetting cooling effect from aerosol and other forcings. {9.4}

It is *extremely unlikely* (<5%) that the global pattern of warming during the past half century can be explained without external forcing, and *very unlikely* that it is due to known natural external causes alone. The warming occurred in both the ocean and the atmosphere and took place at a time when natural external forcing factors would *likely* have produced cooling. {9.4, 9.7}

It is *likely* that anthropogenic forcing has contributed to the general warming observed in the upper several hundred metres of the ocean during the latter half of the 20th century. Anthropogenic forcing, resulting in thermal expansion from ocean warming and glacier mass loss, has *very likely* contributed to sea level rise during the latter half of the 20th century. {9.5}

A substantial fraction of the reconstructed NH inter-decadal temperature variability of the past seven centuries is *very likely* attributable to natural external forcing (volcanic eruptions and solar variability). {9.3}

Key Uncertainties:

Confidence in attributing some climate change phenomena to anthropogenic influences is currently limited by uncertainties in radiative forcing, as well as uncertainties in feedbacks and in observations. {9.4, 9.5}

Attribution at scales smaller than continental and over time scales of less than 50 years is limited by larger climate variability on smaller scales, by uncertainties in the small-scale details of external forcing and the response simulated by models, as well as uncertainties in simulation of internal variability on small scales, including in relation to modes of variability. {9.4}

There is less confidence in understanding of forced changes in precipitation and surface pressure than there is of temperature. {9.5}

The range of attribution statements is limited by the absence of formal detection and attribution studies, or their very limited number, for some phenomena (e.g., some types of extreme events). {9.5}

Incomplete global data sets for extremes analysis and model uncertainties still restrict the regions and types of detection studies of extremes that can be performed. {9.4, 9.5}

Despite improved understanding, uncertainties in model-simulated internal climate variability limit some aspects of attribution studies. For example, there are apparent discrepancies between estimates of ocean heat content variability from models and observations. {5.2, 9.5}

Lack of studies quantifying the contributions of anthropogenic forcing to ocean heat content increase or glacier melting together with the open part of the sea level budget for 1961 to 2003 are among the uncertainties in quantifying the anthropogenic contribution to sea level rise. {9.5}

TS.6.4   Projections of Future Changes in Climate

TS.6.4.1   Model Evaluation

Robust Findings:

Climate models are based on well-established physical principles and have been demonstrated to reproduce observed features of recent climate and past climate changes. There is considerable confidence that AOGCMs provide credible quantitative estimates of future climate change, particularly at continental scales and above. Confidence in these estimates is higher for some climate variables (e.g., temperature) than for others (e.g., precipitation). {FAQ 8.1}

Confidence in models has increased due to:
- improvements in the simulation of many aspects of present climate, including important modes of climate variability and extreme hot and cold spells;
- improved model resolution, computational methods and parametrizations and inclusion of additional processes;
- more comprehensive diagnostic tests, including tests of model ability to forecast on time scales from days to a year when initialised with observed conditions; and
- enhanced scrutiny of models and expanded diagnostic analysis of model behaviour facilitated by internationally coordinated efforts to collect and disseminate output from model experiments performed under common conditions. {8.4}

Key Uncertainties:

A proven set of model metrics comparing simulations with observations, that might be used to narrow the range of plausible climate projections, has yet to be developed. {8.2}

Most models continue to have difficulty controlling climate drift, particularly in the deep ocean. This drift must be accounted for when assessing change in many oceanic variables. {8.2}

Models differ considerably in their estimates of the strength of different feedbacks in the climate system. {8.6}

Problems remain in the simulation of some modes of variability, notably the Madden-Julian Oscillation, recurrent atmospheric blocking and extreme precipitation. {8.4}

Systematic biases have been found in most models' simulations of the Southern Ocean that are linked to uncertainty in transient climate response. {8.3}

Climate models remain limited by the spatial resolution that can be achieved with present computer resources, by the need for more extensive ensemble runs and by the need to include some additional processes. {8.1–8.5}

TS.6.4.2   Equilibrium and Transient Climate Sensitivity

Robust Findings:

Equilibrium climate sensitivity is *likely* to be in the range 2°C to 4.5°C with a most likely value of about 3°C, based upon multiple observational and modelling constraints. It is *very unlikely* to be less than 1.5°C. {8.6, 9.6, Box 10.2}

The transient climate response is better constrained than the equilibrium climate sensitivity. It is *very likely* larger than 1°C and *very unlikely* greater than 3°C. {10.5}

There is a good understanding of the origin of differences in equilibrium climate sensitivity found in different models. Cloud feedbacks are the primary source of inter-model differences in equilibrium climate sensitivity, with low cloud being the largest contributor. {8.6}

New observational and modelling evidence strongly supports a combined water vapour-lapse rate feedback of a strength comparable to that found in AOGCMs. {8.6}

Key Uncertainties:

Large uncertainties remain about how clouds might respond to global climate change. {8.6}

TS.6.4.3 Global Projections

Robust Findings:

Even if concentrations of radiative forcing agents were to be stabilised, further committed warming and related climate changes would be expected to occur, largely because of time lags associated with processes in the oceans. {10.7}

Near-term warming projections are little affected by different scenario assumptions or different model sensitivities, and are consistent with that observed for the past few decades. The multi-model mean warming, averaged over 2011 to 2030 relative to 1980 to 1999 for all AOGCMs considered here, lies in a narrow range of 0.64°C to 0.69°C for the three different SRES emission scenarios B1, A1B and A2. {10.3}

Geographic patterns of projected warming show the greatest temperature increases at high northern latitudes and over land, with less warming over the southern oceans and North Atlantic. {10.3}

Changes in precipitation show robust large-scale patterns: precipitation generally increases in the tropical precipitation maxima, decreases in the subtropics and increases at high latitudes as a consequence of a general intensification of the global hydrological cycle. {10.3}

As the climate warms, snow cover and sea ice extent decrease; glaciers and ice caps lose mass and contribute to sea level rise. Sea ice extent decreases in the 21st century in both the Arctic and Antarctic. Snow cover reduction is accelerated in the Arctic by positive feedbacks and widespread increases in thaw depth occur over much of the permafrost regions. {10.3}

Based on current simulations, it is *very likely* that the Atlantic Ocean MOC will slow down by 2100. However, it is *very unlikely* that the MOC will undergo a large abrupt transition during the course of the 21st century. {10.3}

Heat waves become more frequent and longer lasting in a future warmer climate. Decreases in frost days are projected to occur almost everywhere in the mid- and high latitudes, with an increase in growing season length. There is a tendency for summer drying of the mid-continental areas during summer, indicating a greater risk of droughts in those regions. {10.3, FAQ 10.1}

Future warming would tend to reduce the capacity of the Earth system (land and ocean) to absorb anthropogenic CO_2. As a result, an increasingly large fraction of anthropogenic CO_2 would stay in the atmosphere under a warmer climate. This feedback requires reductions in the cumulative emissions consistent with stabilisation at a given atmospheric CO_2 level compared to the hypothetical case of no such feedback. The higher the stabilisation scenario, the larger the amount of climate change and the larger the required reductions. {7.3, 10.4}

Key Uncertainties:

The likelihood of a large abrupt change in the MOC beyond the end of the 21st century cannot yet be assessed reliably. For low and medium emission scenarios with atmospheric greenhouse gas concentrations stabilised beyond 2100, the MOC recovers from initial weakening within one to several centuries. A permanent reduction in the MOC cannot be excluded if the forcing is strong and long enough. {10.7}

The model projections for extremes of precipitation show larger ranges in amplitude and geographical locations than for temperature. {10.3, 11.1}

The response of some major modes of climate variability such as ENSO still differs from model to model, which may be associated with differences in the spatial and temporal representation of present-day conditions. {10.3}

The robustness of many model responses of tropical cyclones to climate change is still limited by the resolution of typical climate models. {10.3}

Changes in key processes that drive some global and regional climate changes are poorly known (e.g., ENSO, NAO, blocking, MOC, land surface feedbacks, tropical cyclone distribution). {11.2–11.9}

The magnitude of future carbon cycle feedbacks is still poorly determined. {7.3, 10.4}

TS.6.4.4   Sea Level

Robust Findings:

Sea level will continue to rise in the 21st century because of thermal expansion and loss of land ice. Sea level rise was not geographically uniform in the past and will not be in the future. {10.6}

Projected warming due to emission of greenhouse gases during the 21st century will continue to contribute to sea level rise for many centuries. {10.7}

Sea level rise due to thermal expansion and loss of mass from ice sheets would continue for centuries or millennia even if radiative forcing were to be stabilised. {10.7}

Key Uncertainties:

Models do not yet exist that address key processes that could contribute to large rapid dynamical changes in the Antarctic and Greenland Ice Sheets that could increase the discharge of ice into the ocean. {10.6}

The sensitivity of ice sheet surface mass balance (melting and precipitation) to global climate change is not well constrained by observations and has a large spread in models. There is consequently a large uncertainty in the magnitude of global warming that, if sustained, would lead to the elimination of the Greenland Ice Sheet. {10.7}

TS.6.4.5   Regional Projections

Robust Findings:

Temperatures averaged over all habitable continents and over many sub-continental land regions will *very likely* rise at greater than the global average rate in the next 50 years and by an amount substantially in excess of natural variability. {10.3, 11.2–11.9}

Precipitation is *likely* to increase in most subpolar and polar regions. The increase is considered especially robust, and *very likely* to occur, in annual precipitation in most of northern Europe, Canada, the northeast USA and the Arctic, and in winter precipitation in northern Asia and the Tibetan Plateau. {11.2–11.9}

Precipitation is *likely* to decrease in many subtropical regions, especially at the poleward margins of the subtropics. The decrease is considered especially robust, and *very likely* to occur, in annual precipitation in European and African regions bordering the Mediterranean and in winter rainfall in south-western Australia. {11.2–11.9}

Extremes of daily precipitation are *likely* to increase in many regions. The increase is considered as *very likely* in northern Europe, south Asia, East Asia, Australia and New Zealand – this list in part reflecting uneven geographic coverage in existing published research. {11.2–11.9}

Key Uncertainties:

In some regions there has been only very limited study of key aspects of regional climate change, particularly with regard to extreme events. {11.2–11.9}

Atmosphere-Ocean General Circulation Models show no consistency in simulated regional precipitation change in some key regions (e.g., northern South America, northern Australia and the Sahel). {10.3, 11.2–11.9}

In many regions where fine spatial scales in climate are generated by topography, there is insufficient information on how climate change will be expressed at these scales. {11.2–11.9}